SPE
Society of Petroleum Engineers

SPE 22921

Application of a General Material Balance for High-Pressure Gas Reservoirs

M.J. Fetkovich and D.E. Reese, Phillips Petroleum Co., and C.H. Whitson, Consultant
SPE Members

This paper was prepared for presentation at the 66th Annual Technical Conference and Exhibition of the Society of Petroleum Engineers held in Dallas, TX, October 6-9, 1991.

Abstract

This paper presents the derivation of a general gas material balance that has particular application to high pressure gas reservoirs. The material balance is valid for both normal-pressure and over-pressured (geo-pressured) reservoirs. Its main application is to calculate original gas in place and assist in calculating remaining recoverable reserves from pressure-production data.

The form of the material balance equation is

$$(p/z)[1-\bar{c}_e(p)(p_i-p)] = (p/z)_i(1-G_p/G) \quad \ldots\ldots\ldots\ldots\ldots (1)$$

which includes a pressure-dependent cumulative effective compressibility term $\bar{c}_e(p)$ that is defined in terms of the following reservoir parameters: (1) pore compressibility, (2) water compressibility, (3) gas solubility, and (4) total water associated with the gas reservoir volume. "Associated" water includes connate water, water within interbedded shales and non-pay reservoir rock, and any limited aquifer volume. $\bar{c}_e$ physically represents the cumulative change in hydrocarbon pore volume caused by compressibility effects and encroaching water.

High pressure gas reservoirs typically have curved p/z-G_p plots (concave downward). Incorrect extrapolation of early data may result in serious overestimation of original gas in place and remaining recoverable reserves. The proposed form of the gas material balance equation provides a method to linearize the p/z-G_p plot and thereby predict the true original gas in place. A method is suggested to determine initial gas in place by analyzing the behavior of cumulative effective compressibility backcalculated from pressure-production data. The $\bar{c}_e(p)$ function determined by this procedure, or estimated from logs and geological maps (when sufficient production data is not available), is then used to forecast pressure-cumulative behavior.

For most reservoirs $\bar{c}_e$ is fairly constant through most of depletion. The magnitude of $\bar{c}_e(p)$ at initial pressure usually ranges from 15 to $100(10^{-6})$ psi^{-1}, depending mostly on the volume of water associated with the gas reservoir. As defined in this paper, all components of $\bar{c}_e$ represent cumulative volume changes; i.e., instantaneous water and rock compressibilities are *not* used directly.

We show that the effect of pore collapse on high pressure gas reservoirs is generally positive, providing additional pressure support. There is *not* a clear discontinuity in the behavior of p/z-G_p where pore collapse occurs, and pore collapse tends to flatten or increase p/z-G_p at lower pressures.

$\bar{c}_e$ may increase significantly at lower pressures because of gas solubility effects. An example is given for a large gas reservoir with high-CO_2 content that requires an increasing $\bar{c}_e$ term at lower pressures to linearize the p/z-G_p plot; the increasing $\bar{c}_e$ behavior is substantiated by calculations based on gas solubility effects.

The proposed gas material balance is applicable (and should be applied) to any high pressure gas reservoir with an appreciable volume of associated water. Numerous field examples are provided showing the application of the material balance equation to high pressure gas reservoirs.

Introduction

High pressure gas reservoirs experiencing depletion drive typically have downward curving p/z-G_p behavior. Incorrect extrapolation of early depletion data may result in serious over estimation of original gas in place and remaining reserves. Bruns et al.[1] work in 1965 was a result of a field study conducted on a large moderately overpressured gas reservoir in the Texas Gulf Coast area. Investments were made, and never needed, based on linear extrapolation of the early field p/z-G_p performance to an apparent original gas in place that was later found to be overstated by about 200 Bscf. Fig. 5 in Ref. 1 (Run 20) shows the concave downward curvature typical for the pressure response of a conventional limited external aquifer system that simulated the reservoir's response.

This type of "limited" aquifer behavior where pressure in the reservoir and aquifer are virtually equal led to the derivation in 1969 of a general material balance for high pressure gas reservoirs. The derivation includes pressure-dependent rock and water compressibility (with gas evolving from solution). All water and rock volumes associated with the reservoir and available for expansion, including a limited aquifer volume, were included in a cumulative effective compressibility term $\bar{c}_e(p)$. Rock and water compressibilities were defined to account for cumulative changes in pore volume to be multiplied by the cumulative pressure drop (p_i-p); instantaneous compressibilities are not used at all. The final form of the material balance is similar to that published by Ramogast and Farshad[2], except

References and illustrations at end of paper.

that Ref. 2 considered $\bar{c}_e$ as a constant. The 1969 derivation as presented in this paper defines a cumulative effective compressibility $\bar{c}_e(p)$ as a function of pressure expressed in terms of reservoir properties and volumes.

Literature Review

Harville and Hawkins[3] and Hammerlindl[4] attribute the concave downward shape of p/z-G_p curves obtained in abnormally pressured gas reservoirs entirely to pore collapse and formation compaction. No definition of pore collapse is given in Ref. 3, but a plot of backcalculated pore volume change indicated a system compressibility change from $28(10^{-6})$ psi^{-1} at initial pressure to about $6(10^{-6})$ psi^{-1} at low pressures. This magnitude of pore volume change implies associated water volume. The decreasing "system" compressibility is expected for an overpressured reservoir with pressure dependent pore volume compressibility, and based on results presented in this paper pore collapse is *not* a necessary condition for such behavior.

The Anderson "L" reservoir performance presented by Duggan[5] shows curved p/z-G_p field behavior which was primarily attributed to shale water influx with no evidence of reservoir pore compaction. The water influx drive mechanism was supported by the fact that several wells watered out. Wallace[6], in a 1969 paper, also concluded that shale water influx is an important drive mechanism in abnormally pressured gas reservoirs. Bass[7] discounts shale water influx, and attributes curved p/z-G_p behavior to peripheral water influx from a limited aquifer and formation compaction treated with a constant pore volume compressibility c_f. For a limited aquifer Bass defines a term F_p as the ratio of peripheral water pore volume to the pore volume of gas-bearing rock.

Roach[8] and Ramagost and Farshad[2] both utilize the term p/z[1-$c_e(p_i-p)$] for geopressured and abnormally pressured gas reservoirs. Both authors consider c_e a constant and they consider only the Anderson "L" example.

Bernard[9] does not accept the rock collapse theory as the cause for overpressured p/z-G_p behavior, concluding that water influx is the basic drive mechanism. He also uses p/z[1-c(p_i-p)] where c is a "catch-all" approximation for treating the effects of rock and water compressibility, a small steady-state acting aquifer, and steady state shale water influx. He further states that the term c is virtually impossible to quantify in terms of reservoir properties.

Begland and Whitehead[10], Prasad and Rogers[11], and Wang and Teasdale[12] all present studies of overpressured gas reservoirs based on computer models. Refs. 10 and 11 treat c_f and c_w as functions of pressure, including the effect of solution gas in the water. External water sources are also included in Refs. 11 and 12. The differential forms of the material balance used in these references correctly apply instantaneous compressibility in a history matching approach to determine initial gas in place. A direct plot of (p/z)[1-$\bar{c}_e(p_i-p)$] versus G_p was not made because the $\bar{c}_e$ term had not been defined.

Poston and Chen[13] analyzed several abnormally pressured gas reservoirs, and recognized that calculated values of $c_e > 30(10^{-6})$ psi^{-1} required to linearize the material balance equation reflected the influence of water influx.

Bourgoyne[14] demonstrates that reasonable values of shale permeability and compressibilities treated as a function of pressure can be used to match abnormal gas reservoir performance behavior. He points out, however, that determining k and c_f of the shale necessary for modelling this behavior is virtually impossible.

Ambastha[15] uses Bourgoyne's general material balance equation to develop a graphical matching technique based on a constant effective compressibility c_e. The example considered shows a lack of uniqueness in determining initial gas in place.

General Material Balance

The general form of the gas material balance derived in Appendix A is:

$$\frac{p}{z}\left[1-\bar{c}_e(p)(p_i-p)\right] = (p/z)_i - \frac{(p/z)_i}{G}\left[G_p - G_{inj} + W_pR_{sw} + \frac{5.615}{B_g}(W_pB_w - W_{inj}B_w - W_e)\right] \quad (2)$$

which reduces to Eq. 1 when water terms and gas injection can be neglected. The cumulative effective compressibility term $\bar{c}_e(p)$ is pressure dependent consisting of a cumulative pore volume compressibility $\bar{c}_f(p)$, cumulative total water compressibility $\bar{c}_{tw}(p)$, and the total pore and water volumes associated (i.e. in pressure communication) with the gas reservoir,

$$\bar{c}_e(p) = \frac{S_{wi}\bar{c}_{tw}(p)+\bar{c}_f(p)+M[\bar{c}_{tw}(p)+\bar{c}_f(p)]}{1-S_{wi}} \quad \ldots\ldots\ldots\ldots (3)$$

The formation and total water compressibility terms $\bar{c}_f$ and $\bar{c}_{tw}$ account for cumulative changes in pore volume from initial pressure to the current pressure.

The interbedded non-pay volume and limited aquifer contributions to pressure support are quantified in terms of the M ratio,

$$M = \frac{V_{pNNP}\,(\text{NON-NET PAY}) + V_{pAQ}\,(\text{LIMITED AQUIFER})}{V_{pR}\,(\text{NET PAY RESERVOIR})} \quad (4)$$

An important aspect of the material balance for high-pressure gas reservoirs is that the gas in solution in the connate and associated water provide both pressure support and additional gas available for production. The level of pressure support provided by the evolved solution gas depends on the level of depletion, and it is shown that this support is significant below about 1500 psia. The solution gas available for production also depends on the level of depletion, i.e. how much of the original solution gas has evolved [$R_{sw}(p_i)$-$R_{sw}(p)$] and the quantity of this gas that is mobile.

The term G is used for the *initial free gas in place*, and it is this quantity that will be determined from the material balance plot given by Eq. 1 when extrapolated to (p/z)[1-$\bar{c}_e(p_i-p)$]=0. This condition is reached at a pressure when $\bar{c}_e(p)(p_i-p)=0$, and not when p=0, i.e. additional gas may be produced after G_p reaches original free gas in place G. At pressures where G_p exceeds G the corrected p/z term (p/z)[1-$\bar{c}_e(p_i-p)$] becomes negative. If pressure could be brought to standard conditions ($p=p_{sc}$) the total gas produced would be G plus the total solution gas in place G_s, $G_p(@p_{sc})=G+G_s$.

The effect of connate water saturation S_{wi} and M are important to the magnitude of $\bar{c}_e$. With typical values of $\bar{c}_f=c_{fi}=4(10^{-6})$ psi^{-1} and $\bar{c}_{tw}=c_{wi}=3(10^{-6})$ psi^{-1} for a high-pressured Gulf Coast sandstone reservoir the cumulative effective compressibility is initially $\bar{c}_e=7.5(10^{-6})$ psi^{-1} for $S_{wi}=35\%$ and M=0; and $\bar{c}_e=15(10^{-6})$ for $S_{wi}=35\%$ and M=1. Fig. 1 shows the percentage of true original free gas in place that would be overestimated by extrapolating early p/z-G_p data, indicating that the overestimation is greater for larger initial pressure and higher $\bar{c}_e$ values at initial conditions. For an initial pressure of 10,000 psia and a $\bar{c}_e=10(10^{-6})$ psi^{-1} the extrapolation of early data gives an estimate of G that is about 25 percent higher than the true original free gas in place. The sections below discuss the calculation of $\bar{c}_f(p)$ and $\bar{c}_{tw}(p)$ functions.

Cumulative Pore Volume Compressibility $\bar{c}_f$. The material balance presented in this paper uses a *cumulative* pore volume compressibility $\bar{c}_f$ defined as

$$\bar{c}_f(p) = \frac{1}{V_{pi}}\left[\frac{V_{pi}-V_p(p)}{p_i-p}\right] \quad \ldots\ldots\ldots\ldots\ldots\ldots (5)$$

The term in brackets is the slope of the chord from the initial condition (p_i,V_{p_i}) to any lower pressure (p,V_p), as shown in Fig. 2. This implies that $\bar{c}_f$ is a function of both pressure and the initial condition. The instantaneous pore volume compressibility c_f is defined as

$$c_f(p) = \frac{1}{V_p}\frac{\partial V_p}{\partial p} \quad \ldots\ldots\ldots\ldots\ldots\ldots\ldots\ldots\ldots\ldots \quad (6)$$

and is *only* a function of pressure. At initial pressure the two pore volume compressibilities are equal: $\bar{c}_f(p_i)=c_f(p_i)$. The instantaneous compressibility function $c_f(p)$ should be used in reservoir simulation and differential forms of the material balance, while the cumulative compressibility function $\bar{c}_f(p)$ should be used with forms of the material balance that apply the cumulative pressure drop (p_i-p), i.e. p/z vs G_p plots.

The pressure dependence of $\bar{c}_f$ is best determined by special core analysis under appropriate reservoir conditions. Table 1 summarizes the calculation of $\bar{c}_f$ as a function of pressure using laboratory data for a Gulf Coast sandstone. Fig. 3 shows how c_f and $\bar{c}_f$ vary as a function of pressure for this overpressured reservoir rock.

In the absence of pore collapse $\bar{c}_f$ is always greater than or equal to c_f. The cumulative pore volume compressibility remains higher than the instantaneous compressibility because of an averaging effect that reduces the pressure dependence of $\bar{c}_f$ compared with c_f. An important consequence of this behavior is that a rock exhibiting large pore volume change because of a high level of overpressure (and consequently with a high initial c_f value dropping rapidly to a "normal" value) will initially have and maintain a high cumulative compressibility $\bar{c}_f$ as shown in Fig. 3.

Pore collapse is defined as the condition when a rock's instantaneous pore volume compressibility starts to increase at decreasing reservoir pressure. Pore collapse provides greater pressure support when collapse occurs at a high pressure. However, pore collapse is not reflected by the $\bar{c}_e(p)$ function and will not therefore be seen on the p/z-G_p plot at the pressure when pore collapse occurs. In fact pore collapse may not be identifiable at all on the cumulative compressibility term. For example, the Gulf Coast sandstone in Fig. 3 exhibits pore collapse at 4000 psia (about 5000 psi less than initial pressure p_i). Despite the increase in c_f from 4 to $25(10^{-6})$ psi^{-1} in the pressure range 4000 to 1000 psia, the change in $\bar{c}_f$ over the same pressure range is almost insignificant. Fig. 4 shows a North Sea Chalk sample from a reservoir with initial pressure of 7000 psia exhibiting pore collapse at 6000 psia. Here the effect of pore collapse is greater, causing $\bar{c}_f$ to increase from 6 to $20(10^{-6})$ psi^{-1} in the pressure range from 6000 to 2000 psia. *In general, however, pore collapse in and of itself does not have a significant effect on the p/z-G_p plot.*

In the absence of laboratory data, pore volume compressibilities can be estimated from correlations presented by Hall[16] and by Von Gonten and Choudhary[17]. Hall's correlation (his Fig. 2) gives instantaneous pore volume compressibility as a function of porosity, i.e. there is no pressure dependence. The Hall correlation is probably adequate for normal pressured reservoirs. Von Gonten develops correlations for instantaneous pore volume compressibility c_f as a function of net overburden pressure (p_o), where p_o equals the overburden gradient times depth minus reservoir pressure.

Table 2 gives example values of initial pore volume compressibility $c_f(p_i)$ for overpressured and normal pressured reservoir conditions. Typically there are not large differences in c_f values for these two conditions.

Cumulative Total Water Compressibility $\bar{c}_{tw}$. The pressure support provided by water is made up of two components. First the water expansion with decreasing pressure, and second the release of solution gas and its expansion. The total or composite compressibility effect is expressed as

$$\bar{c}_{tw}(p) = \frac{1}{B_{tw}(p_i)}\frac{B_{tw}(p)-B_{tw}(p_i)}{p_i-p} \quad \ldots\ldots\ldots\ldots\ldots\ldots\ldots \quad (7)$$

in terms of the total water formation volume factor B_{tw},

$$B_{tw}(p) = B_w(p) + \frac{[R_{swi}-R_{sw}(p)]B_g(p)}{5.615} \quad \ldots\ldots\ldots\ldots\ldots\ldots \quad (8)$$

Fig. 5 shows typical behavior for B_w and B_{tw} as a function of pressure; the figure also shows the behavior of $\bar{c}_{tw}(p)$ where it is seen that little increase occurs before a pressure of about 1500 psia, and that at pressures below 1000 psia there is a significant increase in $\bar{c}_{tw}$ with a limiting relationship $\bar{c}_{tw} \propto 1/p$ at low pressures,

$$\bar{c}_{tw}(p\to 0) = \left[\frac{1}{5.615}\frac{Tp_{sc}}{T_{sc}}\frac{R_{swi}}{p_iB_{twi}}\right]\frac{1}{p} \quad \ldots\ldots\ldots\ldots\ldots\ldots \quad (9)$$

Specifically at standard conditions (p_{sc}), $\bar{c}_{tw}$ is given by

$$\bar{c}_{tw}(p_{sc}) = \left[\frac{1}{5.615}\frac{T}{T_{sc}}\frac{R_{swi}}{p_iB_{wi}} - \frac{1}{p_i}\right] \quad \ldots\ldots\ldots\ldots\ldots\ldots \quad (10)$$

To calculate $\bar{c}_{tw}$, values of B_w, R_{sw}, and B_g are tabulated with pressure as shown in Table 3. These properties can be obtained from correlations at pressures less than about 10,000 psia and 300°F. At more extreme conditions of pressure and temperature, and for gases with high concentrations of nonhydrocarbons CO_2, N_2, and H_2S, we have used the Peng-Robinson[18] equation of state with volume translation, and using binary interaction coefficients that are dependent on both temperature and salinity[19].

Another approach for high pressures is simply to extrapolate B_w linearly and R_{sw} with a flattening curvature towards a constant value. Nonhydrocarbons can be treated by evaluating R_{sw} of each component separately at its partial pressure, and summing the values for all soluble components

$$[R_{sw}(p)]_{TOTAL} = \sum_j [R_{sw}(y_jp)]_j \quad \ldots\ldots\ldots\ldots\ldots\ldots \quad (11)$$

y_j is the reservoir gas mole fraction of component j. Typically the only components with appreciable solubility are methane, CO_2, and H_2S.

Associated Water Volume Ratio M. The total compressibility effect on the gas material balance depends on the magnitudes of rock and total water compressibilities *and* on the total pore and water volumes in pressure communication with the gas reservoir (including connate water and the pore volume within the net pay).

Associated water and pore volumes external to the net pay include non-net pay (NNP) such as interbedded shales and dirty sands, plus external water volume found in limited aquifers. Including these water volumes in reservoir simulation is referred to as using a "gross" model. In the proposed material balance equations this associated volume is expressed as a ratio relative to the pore volume of the net-pay reservoir,

$$M = M_{NNP} + M_{AQ} \quad \ldots\ldots\ldots\ldots\ldots\ldots\ldots\ldots \quad (12)$$

where

$$M_{NNP} = \frac{V_{pNNP}(\text{INTERBEDDED NONNET PAY})}{V_{pR}(\text{NET PAY})} \quad \ldots\ldots \quad (13)$$

$$M_{AQ} = \frac{V_{pAQ}\,(\text{AQUIFER})}{V_{pR}\,(\text{NET PAY})} \quad \ldots\ldots\ldots\ldots\ldots\ldots \quad (14)$$

In the simplest case when $M=0$ there will be pressure support only from connate water and the net-pay pore volume. This is equivalent in simulation to building a net model. The cumulative effective compressibility term $\bar{c}_e$ will then be expected to have values ranging from 7 to $15(10^{-6})$ psi^{-1} for normal-pressure reservoirs, where the larger values will generally result from high connate water saturation. Even larger values can be obtained in some overpressured reservoirs (see Table 2).

Net-pay compressibility effects alone can cause noticeable curvature in the p/z-G_p plot with potential overestimation of initial free gas in place (G) (see Fig. 1).

M_{NNP}. The non-net pay water volume ratio M_{NNP} is comprised of interbedded reservoir pore volume, including shales and poor quality rock, that are assumed to be completely filled with water. With this definition M_{NNP} can be written in terms of the net-to-gross ratio NGR defined as

$$NGR = \frac{h_R}{h_R+h_{NNP}} = \frac{h_R}{h_{GROSS}} \quad \ldots\ldots\ldots\ldots\ldots\ldots \quad (15)$$

Accounting for different porosities in the net pay and non-net pay M_{NNP} is given by

$$M_{NNP} = \frac{(\overline{\phi h A})_{NNP}}{(\overline{\phi h A})_R} = \frac{\phi_{NNP}}{\phi_R}\left[\frac{1-NGR}{NGR}\right] \quad \ldots\ldots\ldots\ldots \quad (16)$$

Properties and thicknesses of the net pay and non-net pay are readily available from log analysis.

If the non-net pay pore volume is known to have an initial gas saturation, albeit immobile, the material balance is readily modified to account for this fact; the term $M_{NNP}(\bar{c}_f+\bar{c}_{tw})$ is replaced by $M_{NNP}[\bar{c}_f+S_{wi,NNP}\bar{c}_{tw}]$ and the initial gas volume is included in the total original free gas in place G.

M_{AQ}. Aquifers with sufficient permeability and limited areal extent can be treated as part of the total cumulative compressibility term. The water volume ratio of the aquifer M_{AQ} can be determined using geological maps and well control to define areal extent, and electric logs to define the gas-water contact. In general, M_{AQ} is defined as

$$M_{AQ} = \frac{(\overline{\phi h A})_{AQ}}{(\overline{\phi h A})_R} \quad \ldots\ldots\ldots\ldots\ldots\ldots\ldots\ldots \quad (17)$$

and for a radial aquifer geometry quantified in terms of the aquifer-to-reservoir radius r_{AQ}/r_R, the aquifer volume ratio can be expressed

$$M_{AQ} = \frac{(\overline{\phi h})_{AQ}}{(\overline{\phi h})_R}\left[(r_{AQ}/r_R)^2 - 1\right] \quad \ldots\ldots\ldots\ldots\ldots \quad (18)$$

Bruns et al.[1] show that limited aquifers with r_{AQ}/r_R ratios up to 5 have the same p/z-G_p behavior for permeabilities 100 md and higher. This implies that the transient effects in the aquifer have negligible effect on reservoir performance and the aquifer can be treated as part of the cumulative effective compressibility term. Values of M_{AQ} used in the definition of $\bar{c}_e$ may be as high as 25 [$M_{AQ}=(r_{AQ}/r_R)^2-1$] in reservoirs with moderate permeability. With higher permeabilities limited aquifers can include r_{AQ}/r_R ratios greater than 5 and still be treated as part of the cumulative effective compressibility term.

When the aquifer is sufficiently large and requires treatment with either superposition or the Schilthius infinite aquifer model, the $\bar{c}_e$ term should still be used but it will only contain the effect of net pay and non-net pay volumes, i.e. $M=M_{NNP}$.

Cumulative Effective Compressibility $\bar{c}_e$. Total cumulative effective compressibility represents *all* available pressure support from rock and water. The equation for $\bar{c}_e$ is

$$\bar{c}_e(p) = \frac{S_{wi}\bar{c}_{tw}(p)+\bar{c}_f(p)+M[\bar{c}_{tw}(p)+\bar{c}_f(p)]}{1-S_{wi}} \quad \ldots\ldots\ldots\ldots \quad (19)$$

For a specific reservoir a family of $\bar{c}_e(p)$ curves can be generated for several M values. These curves will have specific characteristics depending on the pressure dependence of rock and water compressibilities. The $\bar{c}_{tw}(p)$ curves are relatively constant at high pressure, increasing slightly as pressure decreases, then rising sharply at low pressure around 1000 psia. Typically a constant pore volume compressibility c_f can be assumed and the $\bar{c}_e(p)$ curves will then have the same character as the $\bar{c}_{tw}(p)$ curve. Fig. 6 illustrates an example of $\bar{c}_e(p)$ curves at various M ratios for a typical Gulf Coast reservoir with p_i=9000 psia, T=200°F, γ_g=0.7 (air=1), and a constant $\bar{c}_f=3.2(10^{-6})$ psi^{-1}.

For overpressured reservoirs exhibiting a pressure-dependent $\bar{c}_f(p)$, the family of $\bar{c}_e(p)$ curves *at high pressures* will tend to decrease with depletion. In the absence of pore collapse $\bar{c}_f(p)$ decreases to a constant value at lower pressure and the $\bar{c}_e(p)$ curves at lower pressure are dominated by the increasing $\bar{c}_{tw}(p)$ function. If pore collapse occurs, but not early in depletion, the pore collapse is almost insignificant because (a) the $\bar{c}_f(p)$ function does not start increasing until low pressures because it represents a cumulative pore volume change, and (b) when the $\bar{c}_f(p)$ function finally starts to increase it will be masked by the $\bar{c}_{tw}(p)$ function which is increasing as 1/p. Fig. 7 illustrates this point for a Gulf Coast overpressured reservoir with p_i=9000 psia, T=300°F, and γ_g=0.71 (air=1). Although pore collapse occurs at 4000 psia (Fig. 3), $\bar{c}_f$ does not start increasing until 2000 psia. The increase is insignificant relative to the increase in $\bar{c}_{tw}(p)$ at lower pressures.

The next example is a North Sea chalk (Fig. 4) that shows pore collapse at a pressure only 1000 psi below initial pressure of 7000 psia. The $\bar{c}_f(p)$ function increases almost simultaneously with instantaneous c_f, and the effect of $\bar{c}_f(p)$ on $\bar{c}_e(p)$ is shown in Fig. 8. Although $\bar{c}_f(p)$ has an impact on $\bar{c}_e(p)$ at moderate and high pressures for this example, the $\bar{c}_{tw}(p)$ function still dominates the behavior of $\bar{c}_e(p)$ at pressures less than 1500 psia.

Estimating Gas-In-Place. A method is proposed for estimating the initial (free) gas in place G based on historical pressure-cumulative data. The procedure also determines the water volume ratio M and the $\bar{c}_e(p)$ function. First, a plot of p/z versus cumulative gas production G_p should have the characteristic concave downward shape of a high-pressure reservoir influenced by associated water and pore volume compressibility.

A range of values for G should then be assumed, with the largest value based on an extrapolation of the early depletion data and the lowest value being somewhat larger than the current G_p. For an assumed value of G, calculate for each measured p/z and G_p data the $\bar{c}_e$ value from the rearranged material balance equation (Eq. 1),

$$(\bar{c}_e)_{BACKCALCULATED} = \left[1-\frac{(p/z)_i}{(p/z)}\left(1-\frac{G_p}{G}\right)\right]\frac{1}{(p_i-p)} \quad \ldots\ldots \quad (20)$$

At this point, a plot can be made of backcalculated $\bar{c}_e$ as a function of pressure given the assumed G. Using reservoir rock and water properties, a family of $\bar{c}_e(p)$ curves at various M values can be generated to match against the backcalculated $\bar{c}_e$ values. The data should

honor the shape and magnitude of one $\bar{c}_e(p)$ curve, where this match yields G, the M value, and a $\bar{c}_e(p)$ function that can be used to forecast future p/z-G_p behavior. This procedure gives a sound physical significance to the estimation of G as opposed to a pure statistical best-fit that may lead to unrealistic solutions. The Field Examples section discusses criteria for matching field data, and the expected behavior of $\bar{c}_e(p)$.

Characteristics of p/z-G_p Plots for High-Pressure Reservoirs

Pore volume reduction, water expansion, and solution gas evolution, expressed in terms of $\bar{c}_e(p)$ in the general material balance equation, provide pressure support for *all* reservoirs during depletion. The reservoir does not have to be overpressured or geopressured. The term $\bar{c}_e(p)(p_i-p)$ determines whether the conventional p/z-G_p plot yields a straight line. For most low-pressure reservoirs this term is small and is often neglected because a straight-line p/z-G_p plot is obtained. Reservoirs undergoing depletion with initial pressure exceeding 5000 psia are automatically candidates for being treated with the complete material balance equation.

Fig. 9 presents three generated p/z-G_p curves for a Gulf Coast overpressured sandstone reservoir using M=0 (i.e. $\bar{c}_e(p)=[\bar{c}_f(p)+S_{wi}\bar{c}_{tw}(p)]/(1-S_{wi})$. Curve A accounts for pore volume reduction including pore collapse at about 4000 psia. Curve B uses the same $\bar{c}_f(p)$ function as Curve A down to 4000 psia (where pore collapse occurs) and thereafter uses a constant instantaneous compressibility of $4(10^{-6})$ psi^{-1}. p/z-G_p plots for A and B are almost identical, showing only a slight separation at pressures less than 3500 psia. This clearly shows the limited effect of pore collapse on the p/z-G_p plot when collapse occurs late in depletion. Curve C assumes, *unrealistically*, that the initial pore volume compressibility of $13(10^{-6})$ psi^{-1} remains constant throughout depletion. The difference between the two p/z-G_p curves A and C is a result of the actual decrease in pore volume compressibility. Including an external water volume quantified with M=2 produces more curvature in the p/z-G_p plots, but the separation between curves with and without pore collapse is still very small (not shown).

Another example relates to a North Sea chalk reservoir where pore collapse occurs just below initial pressure. Fig. 10 presents generated p/z-G_p plots for M=0 with pore collapse (curve A) and with no pore collapse (curve B). The effect of pore collapse is more significant than in the previous example because it occurs at a relatively high pressure.

Field Examples

Ellenburger Gas Reservoir. This field example is for a normal pressured (0.5 psi/ft) 1600-foot thick, dry gas reservoir with initial reservoir pressure of 6675 psia at 200°F. Average porosity is about 5.0% with connate water saturation in the pay of about 35%. Permeability is high because of an extensive microfracture system that results in a high degree of interwell pressure communication and almost instantaneous pressure buildup to static conditions. Initial CO_2 concentration was about 28 mol-%, and a gradual increase in CO_2 concentration to 31 mol-% has been observed. The reservoir has produced about 3.1 Tscf and currently has an average fieldwide bottomhole pressure of approximately 1000 psia. The p/z-G_p plot shows a characteristic concave downward behavior, with an initial gas in place estimate of more than 4.4 Tscf using early data (Fig. 11). The p/z-G_p data at low pressures has started flattening.

The procedure outlined earlier for determining initial free gas in place G was used for this reservoir. Fig. 12 shows a plot of backcalculated $\bar{c}_e$ versus pressure for a range of G from 3.0 Tscf to 3.6 Tscf. Another plot of $\bar{c}_e(p)$ was generated for several values of M using $S_{wi}=0.35$, $\bar{c}_f=6.5(10^{-6})$ psi^{-1} (from Hall[16]), and $\bar{c}_{tw}(p)$ calculated from equation of state results. Fig. 13 shows the best-fit of data on the $\bar{c}_e(p)$ curve for M=3.3, corresponding to an initial free gas in place G=3.15 Tscf.

The total water volume including connate and associated waters is given by

$$W = \frac{1}{5.615}\frac{GB_{gi}}{B_{twi}}\frac{(S_{wi}+M)}{(1-S_{wi})} \quad \ldots\ldots\ldots\ldots\ldots\ldots\ldots (21)$$

which yields $8.45(10^9)$ STB. The initial solution gas in place G_s is equal to W times the initial solution gas-water ratio R_{swi},

$$G_s = W R_{swi} \quad \ldots\ldots\ldots\ldots\ldots\ldots\ldots\ldots\ldots\ldots (22)$$

Because of the high CO_2 concentration in this reservoir the solution gas-water ratio (R_{swi}=67.5 scf/STB) is about three times larger than for hydrocarbon gas systems. This yields a solution gas in place of G_s=0.55 Tscf and a total initial gas in place of G+G_s=3.70 Tscf. Fig. 11 shows the p/z-G_p forecast using the M value determined from the match to calculate the $\bar{c}_e(p)$ function from S_{wi}, M, $\bar{c}_f$, and $\bar{c}_{tw}(p)$. Also shown on this figure is the plot of $(p/z)[1-\bar{c}_e(p)(p_i-p)]$ versus G_p for historical performance data and for the forecast, where it is seen that the current cumulative gas produced equals the original free gas in place.

The associated water volume given by M=3.3 consists of non-net pay and an external limited aquifer. Log analysis indicates a net-to-gross ratio NGR=0.5, ϕ_R=0.05, and ϕ_{NNP}=0.03, yielding M_{NNP}=0.6. External water is known to exist but has not been mapped due to lack of well control. The calculated aquifer water volume ratio M_{AQ}=2.7 (3.3-0.6), or an equivalent r_{AQ}/r_R=1.9, seems reasonable for a limited aquifer.

Anderson "L". This reservoir has been studied by several authors and it is perhaps the best recognized example of a high-pressure gas reservoir with concave downward p/z-G_p behavior (Fig. 14). The reservoir was abandoned after producing 55 Bscf, but pressure tests of public record were discontinued after 40 Bscf had been produced.

Different analyses by other authors have indicated original free gas in place between 65 to 75 Bscf. Fig. 15 shows backcalculated $\bar{c}_e$ versus pressure for values of G equal to 65, 72, and 90 Bscf. The 72 Bscf volume is chosen based on a best-fit match with the $\bar{c}_e(p)$ function calculated using M=2.25, S_{wi}=0.35, $\bar{c}_f=3.2(10^{-6})$ psi^{-1}, and a $\bar{c}_{tw}(p)$ function from equation of state results. Although the first four data do not fall on the slightly-increasing $\bar{c}_e(p)$ curve, data at pressures below this value do follow the trend down to the last pressure data near 3000 psia.

The 90 Bscf estimate produces unrealistically low $\bar{c}_e$ values, lower than would be calculated using the net reservoir pore volume and connate water compressibilities. The lowest estimate of 65 Bscf gives a shape for $\bar{c}_e(p)$ that cannot be accounted for using normal $\bar{c}_f(p)$ and $\bar{c}_{tw}(p)$ functions.

The forecasted p/z-G_p performance (Fig. 14) is calculated using the match determined above. Total gas in place of 76 Bscf which includes 72 Bscf of original free gas plus 4 Bscf of solution gas.

Cajun Field. This reservoir was originally reported by Stelly and Farshad[20] and recently analyzed by Ambastha[15]. Initial pressure is 11450 psia at 13,300 ft (0.86 psi/ft). Connate water saturation is reported as 22%. Production data is reported to a pressure of 6850 psia and a cumulative of 145 Bscf.

Using the p/z-G_p data shown in Fig. 16, backcalculated values of $\bar{c}_e$ are shown in Fig. 17. The range of values for G are the same as considered by Ambastha: 410 to 760 Bscf. The 760 Bscf estimate yields unacceptably low $\bar{c}_e$ values, less than $2(10^{-6})$ psi^{-1}. Values lower than 565 Bscf produce $\bar{c}_e(p)$ functions that increase more steeply than would be expected from $\bar{c}_{tw}(p)$ behavior. The expected magnitude and shape of cumulative effective compressibility is exhibited by the backcalculated $\bar{c}_e$ values for an assumed G of 650 Bscf. This

corresponds to M=0.2 using S_{wi}=0.22, $\bar{c}_f$=4(10^{-6}) psi^{-1}, and $\bar{c}_{tw}$(p) from correlations.

Gulf Coast Reservoir C. This example is taken from Bernard[9] (his Fig. 1) and represents a high-pressure, overpressured gas reservoir taken to a low abandonment pressure. The p/z-G_p plot (Fig. 18) shows significant concave downward character with an extrapolation of early data giving an initial free gas in place of 380 Bscf. Depletion from p_i=11500 psia to about 1200 psia produced 180 Bscf, verifying that the early-data extrapolation of 380 Bscf was incorrect.

Fig. 19 shows backcalculated $\bar{c}_e$(p) for values of G from 160 to 240 Bscf. The only curve that produces an approximately constant $\bar{c}_e$ at high pressures is G=160 Bscf, a value 30 Bscf less than the volume already produced. The curve for G=240 Bscf has a downward sloping $\bar{c}_e$(p) that becomes negative, also an unrealistic solution. The G=200 Bscf curve has a downward sloping $\bar{c}_e$(p) function that can be explained by a pressure-dependent pore volume compressibility. A highly overpressured formation can readily have a pressure-dependent $\bar{c}_f$(p) function, i.e. one that decreases with depletion.

Reservoir data was not presented by Bernard[9] for this field example, but making some assumptions about typical Gulf Coast reservoir properties we matched the $\bar{c}_e$(p) backcalculated behavior using G=185 Bscf, and a $\bar{c}_f$(p) function that decreased linearly by a factor of about 2 from initial conditions to abandonment pressure. The backcalculated $\bar{c}_e$(p) behavior at 2000 psia started increasing, indicating that pore collapse could have occurred earlier in depletion.

Duck Lake Field. Cason[21] presents production performance data from the Discorbis 1 reservoir in the Duck Lake field of southern Louisiana. This high-pressure gas reservoir was waterflooded for more than 10 years after first being depleted to about 1000 psia. Fig. 20 shows the p/z-cumulative plot for data prior to the waterflooding project, showing typical concave downward curvature.

Cason reports an initial gas in place of 680 Bscf using traditional water influx analysis. Based on the high reservoir permeability (k=1,750 md) we established that the reservoir performance could be analyzed with the general material balance where the external aquifer was treated as part of the $\bar{c}_e$ term. Using G=680 Bscf, $\bar{c}_e$(p) was backcalculated from the general material balance as shown in Fig. 21. The $\bar{c}_e$(p) behavior is flat throughout depletion. This behavior should be compared with the dashed line representing the expected $\bar{c}_e$(p) behavior based on Eq. 3 using a constant $\bar{c}_f$=3.4(10^{-6}) psi^{-1}, M=4.8, and an appropriate $\bar{c}_{tw}$(p) function. The dashed curve has significant increase in $\bar{c}_e$(p) already at 2000 psia, and the more-or-less constant $\bar{c}_e$(p) behavior backcalculated from production data can not be readily explained. It is expected, however, that conventional water influx analysis which assumes constant water and pore volume compressibility will yield an estimate of initial gas in place that reflects a constant $\bar{c}_e$ when backcalculated from the general gas material balance.

Using a smaller estimate of G=625 Bscf yields backcalculated $\bar{c}_e$(p) behavior that is very similar to $\bar{c}_e$(p) calculated from Eq. 3 using a constant $\bar{c}_f$=3.4(10^{-6}) psi^{-1}, M=6.5, and $\bar{c}_{tw}$(p) function. Cumulative production at abandonment was about 650 Bscf, indicating that about 25 Bscf of the total produced gas came from solution. Based on G=625 Bscf, R_{swi}=20.6 scf/STB, S_{wi}=0.18, and M=6.5 the initial *solution* gas in place is G_s=65 Bscf.

Conclusions

1. A general form of the material balance equation for gas reservoirs has been presented. This equation has particular application to high-pressure reservoirs. A cumulative effective compressibility term $\bar{c}_e$(p) has been defined in terms of pressure-dependent pore volume and total water cumulative compressibilities, $\bar{c}_f$(p) and $\bar{c}_{tw}$(p), and the total volume of water associated with the net pay reservoir expressed as a ratio M.

2. The general material balance equation applies to *all* high-pressure reservoirs, both normal pressured and abnormally pressured (overpressured and geopressured).

3. The effect of a limited aquifer can be included as part of the M term for most depletion-type reservoirs. Using the water volume ratio M in the cumulative effective compressibility term, together with normal values of $\bar{c}_f$ and $\bar{c}_{tw}$, explains the "large" $\bar{c}_e$ values commonly reported for high-pressure gas reservoirs when linearizing the material balance equation. In fact, large values of $\bar{c}_e$ backcalculated from field performance data indicate that associated water influx is a dominant drive mechanism.

4. Only *cumulative* compressibilities ($\bar{c}_f$ and $\bar{c}_{tw}$) can be used in the general gas material balance equation because they are applied against the cumulative pressure drop (p_i-p) in p/z-G_p plots. A method is given for calculating cumulative total water and pore volume compressibility $\bar{c}_{tw}$(p) and $\bar{c}_f$(p).

5. A method is proposed for estimating the original free gas in place from production data. This method uses backcalculated cumulative effective compressibility $\bar{c}_e$ which is plotted versus pressure and compared with expected $\bar{c}_e$(p) behavior calculated from rock and water properties for a range of values of the associated water volume ratio M.

6. In lieu of laboratory data for pore volume compaction we recommend Hall's[16] correlation for normal-pressured reservoirs, and Von Gonten's[17] correlation for abnormally-pressured reservoirs.

7. Pore collapse in and of itself does not contribute significantly to pressure support in overpressured gas reservoirs. In fact, pore collapse has little effect unless it occurs early in depletion at a relatively high pressure. The effect of pore collapse, if present, is a positive effect and tends to flatten the p/z-G_p curve, *not bending the curve downward* as has been implied by others.

8. Gas found initially in solution in the connate and associated water is an important component of pressure support late in depletion (below 1500 psia) and may contribute additional producible volumes of gas. Typically the solution gas in place G_s represents 2 to 10 percent of the original free gas in place, the value depending primarily on total water volume $(M+S_{wi})/(1-S_{wi})$ and the initial solution gas-water ratio R_{swi}. Gas reservoirs with high CO_2 concentration (>20 mol-%) can have even higher solution gas in place, G_s.

Nomenclature

A	=	area, ft^2 [m^2]
B	=	formation volume factor, reservoir per standard volume
c	=	instantaneous compressibility, 1/psi [1/kPa]
$\bar{c}$	=	cumulative compressibility, 1/psi [1/kPa]
G	=	original free gas-in-place, Bscf [std m^3]
G_p	=	cumulative gas production, Bscf [std m^3]
G_s	=	initial solution gas in place, Bscf [std m^3]
G_x	=	early overestimate of G, Bscf [std m^3]
G_{inj}	=	cumulative gas injection, Bscf [std ^{3}]
h	=	thickness, ft [m]
M	=	volume ratio, dimensionless
NGR	=	net-to-gross ratio, dimensionless
p	=	reservoir pressure, psia [kPa]
p_i	=	initial reservoir pressure, psia [kPa]
p_o	=	net overburden pressure, psia [kPa]
r_R	=	radius of reservoir, ft [m]
r_{AQ}	=	radius of aquifer, ft [m]
R_{sw}	=	solution gas water ratio, SCF/STB [std m^3/m^3]
S_{wi}	=	initial water saturation, fraction
T	=	reservoir temperature, °R [K]

V	=	volume, ft³ [m³]
V_p	=	pore volume, cm³ and ft³ [m³]
V_b	=	bulk volume, cm³ [m³]
W	=	total water in place, bbl [m³]
W_e	=	cumulative water influx, bbl [m³]
W_{inj}	=	cumulative water injection, bbl [m³]
W_p	=	cumulative water production, bbl [m³]
z	=	gas compressibility factor, dimensionless
ϕ	=	porosity, fraction

Subscripts

A	=	associated water
AQ	=	limited aquifer
e	=	effective
f	=	pore volume ("formation")
g	=	gas
GROSS	=	gross interval thickness
i	=	initial
inj	=	injection
NNP	=	non-net pay
R	=	reservoir
sc	=	standard conditions
tw	=	total water
w	=	water

Acknowledgements

We thank the management of Phillips Petroleum Company for permission to publish this paper. We also acknowledge Fred Kent for work done on the Ellenburger example.

References

1. Bruns, J.R., Fetkovich, M.J., and Meitzen, V.C.: "The Effect of Water Influx on p/z-Cumulative Gas Production Curves," *JPT* (March 1965) 287-91.
2. Ramagost, B. P. and Farshad, F. F.: "p/z Abnormal Pressured Gas Reservoirs," paper 10125 presented at the 56th Annual Meeting of SPE of AIME, San Antonio, TX, (Oct. 5-7, 1981).
3. Harville, D. W. and Hawkins, M. F. Jr.: "Rock Compressibility and Failure as Reservoir Mechanisms in Geopressured Gas Reservoirs," *JPT* (Dec. 1969)1528-30.
4. Hammerlindl, D. J.: "Predicting Gas Reserves in Abnormally Pressured Reservoirs," paper SPE 3479 presented at the 46th Annual Meeting of SPE of AIME, New Orleans, LA, (Oct. 3-6, 1971).
5. Duggan, J. O.: "The Anderson "L" - An Abnormally Pressured Gas Reservoir in South Texas," *JPT* (Feb. 1971)132-138.
6. Wallace, W.E.: "Water Production from Abnormally Pressured Gas Reservoirs in Louisiana," *JPT* (Aug., 1968) 969-982.
7. Bass, D.M.: "Analysis of Abnormally Pressured Gas Reservoirs with Partial Water Influx," paper SPE 3850 presented at the 1972 Abnormal Subsurface Pressure Symposium, May 15-16.
8. Roach, R. H.: "Analyzing Geopressured Reservoirs - A Material Balance Technique," paper SPE 9968 (1981).
9. Bernard, W. J.: "Gulf Coast Geopressured Gas Reservoirs: Drive Mechanism and Performance Prediction," paper SPE 14362 presented at the 60th Annual Meeting of SPE of AIME, Las Vegas, NV, (Sept. 22-25, 1985).
10. Begland, T. F. and Whitehead, W. R.: "Depletion Performance of Volumetric High Pressured Gas Reservoirs," SPE Reservoir Engineering (Aug. 1989) 279-282. SPE 15523 first presented at the SPE Annual Meeting (Oct. 5-8, 1986) New Orleans, LA.
11. Prasad, R. K. and Rogers, L. A.: "Superpressured Ga Reservoirs: Case Studies and a Generalized Tank Model," paper SPE 16861 presented at the 62nd Annual Meeting of SPE of AIME, Dallas, TX, (Sept. 27-30, 1987).
12. Wang, B. and Teasdale, T.S.: "GASWAT-PC: A Microcomputer Program for Gas Material Balance With Water Influx," paper SPE 16484 presented at the 1987 Petroleum Industry Applications of Microcomputers held in Del Lago on Lake Conroe, Montgomery Texas, June 23-26, 1987.
13. Poston, S. W. and Chen, H. Y.: "Case History Studies: Abnormal Pressured Gas Reservoirs," paper SPE 18857.
14. Bourgoyne, A.T. Jr.: "Shale Water as a Pressure Support Mechanism in Gas Reservoirs Having Abnormal Formation Pressure," *J.Pet.Science*, 3(1990)305-319.
15. Ambastha, A. K.: "Analysis of Material Balance Equations for Gas Reservoirs," Paper No. CIM/SPE 90-36, June 10-13, 1990.
16. Hall, H.N.: "Compressibility of Reservoir Rocks," Trans AIME (1953)198,309-311.
17. Von Gonten, W. D. and Choudhary, B. K.: "The Effect of Pressure and Temperature on Pore-Volume Compressibility," paper SPE 2526 presented at the Annual Meeting of SPE of AIME, Denver, CO (Sept. 28-Oct. 1, 1969).
18. Peng, D.-Y. and Robinson, D.B.: "A New Two-Constant Equation of State," *Ind.Eng.Chem.Fund.*, No. 1 (1976) 59-64.
19. Soreide, I. and Whitson, C.H.: "Mutual Solubilities of Petroleum Reservoir Fluids Including Brine From a Cubic Equation of State," paper submitted for publication in *Fluid Phase Equilibria* (April 10, 1990).
20. Stelly, O.V. and Farshad, F.F.: "Predicting Gas In Place In Abnormal Reservoirs," *Pet.Eng.*(June 1981) 104-110.
21. Cason, L. D. Jr.: "Waterflooding Increases Gas Recovery," *J.Pet.Tech.* (Oct. 1989)1102-1106.

Appendix A _ Derivation of General Gas Material Balance

The derivation that follows is based on the following assumptions:

1. Any pressure change caused by production or injection into the reservoir will be felt immediately throughout the total system including:

a. *Net Pay Reservoir* ("R").

b. *Non-Net Pay* ("NNP") including interbedded shales and poor quality rock assumed to be 100% water saturated.

c. *Limited Aquifer* ("AQ"), when present, also assumed to be water saturated.

The non-net pay and aquifer volumes are referred to as "associated" water volumes and both contribute to water influx during depletion.

2. Simple modifications to the material balance equations can be made to generalize for non-net pay that has an initial free gas saturation.

3. All water in the system is initially saturated with solution gas.

Fig. 22 shows a schematic of the reservoir/associated water system.

Practically, the assumption of equal pressure throughout the system is reasonable, and any transients effects caused by a large aquifer may be treated by a conventional water influx term (W_e) as shown below.

For the sake of brevity we have chosen to omit explicit reference to pressure dependence - i.e. $\bar{c}_e$, $\bar{c}_f$, and $\bar{c}_{tw}$ should actually read $\bar{c}_e(p)$, $\bar{c}_f(p)$, and $\bar{c}_{tw}(p)$.

Derivation. The volumetric balance at any pressure states that the total pore volume ($V_{pR}+V_{pA}$) equals the net reservoir pore volume occupied by gas and water ($V_{gR}+V_{wR}$) plus the associated (non-net pay and aquifer) pore volume which also is occupied by gas and water ($V_{gA}+V_{wA}$):

$$(V_{pR}+V_{pA}) = (V_{gR}+V_{wR}) + (V_{gA}+V_{wA}) \quad \ldots\ldots\ldots\ldots (A1)$$

The net-pay reservoir pore volume V_{pR} is given by the initial volume V_{pRi} less the change in pore volume ΔV_{pR},

$$V_{pR} = V_{pRi}-\Delta V_{pR} \quad \ldots\ldots\ldots\ldots\ldots\ldots\ldots\ldots (A2)$$

$$V_{pRi} = V_{gRi} + V_{wRi}$$

$$V_{pRi} = GB_{gi} + \frac{GB_{gi}}{1-S_{wi}} S_{wi} \quad \ldots\ldots\ldots\ldots\ldots\ldots\ldots\ldots (A3)$$

$$\Delta V_{pR} = \frac{GB_{gi}}{1-S_{wi}} \bar{c}_f (p_i-p) \;\; ; \;\; \bar{c}_f = (\bar{c}_f)_R \quad \ldots\ldots\ldots\ldots (A4)$$

yielding

$$V_{pR} = GB_{gi} + \frac{GB_{gi}}{1-S_{wi}} S_{wi} - \frac{GB_{gi}}{1-S_{wi}} \bar{c}_f (p_i-p) \quad \ldots\ldots\ldots (A5)$$

Pore volume of the associated rock is given by the initial pore volume less the change in pore volume,

$$V_{pA} = V_{pAi} - \Delta V_{pA} \quad \ldots\ldots\ldots\ldots\ldots\ldots\ldots\ldots (A6)$$

$$V_{pAi} = \frac{GB_{gi}}{1-S_{wi}} M \quad \ldots\ldots\ldots\ldots\ldots\ldots\ldots\ldots (A7)$$

$$\Delta V_{pA} = \frac{GB_{gi}}{1-S_{wi}} M \bar{c}_f (p_i-p) \;\; ; \;\; \bar{c}_f = (\bar{c}_f)_A \quad \ldots\ldots\ldots\ldots (A8)$$

yielding

$$V_{pA} = \frac{GB_{gi}}{1-S_{wi}} M - \frac{GB_{gi}}{1-S_{wi}} M \bar{c}_f (p_i-p) \quad \ldots\ldots\ldots\ldots (A9)$$

The net reservoir gas volume is given by the sum of unproduced free gas, gas released from solution, and any injected gas,

$$V_{gR} = (V_{gR})_{\substack{\text{Unproduced}\\ \text{Free Gas}}} + (V_{gR})_{\substack{\text{Released}\\ \text{From Solution}}} + (V_{gR})_{\text{Injected}} \quad \ldots\ldots (A10)$$

$$(V_{gR})_{\substack{\text{Unproduced}\\ \text{Free Gas}}} = [G-(G_p-W_pR_{sw})]B_g \quad \ldots\ldots\ldots\ldots (A11)$$

$$(V_{gR})_{\substack{\text{Released}\\ \text{From Solution}}} = \frac{GB_{gi}}{1-S_{wi}} \frac{S_{wi}}{B_{wi}} (R_{swi}-R_{sw}) B_g \frac{1}{5.615} \quad \ldots\ldots (A12)$$

$$(V_{gR})_{\text{Injected}} = G_{inj} B_g \quad \ldots\ldots\ldots\ldots\ldots\ldots\ldots (A13)$$

resulting in

$$V_{gR} = [G-(G_p-W_pR_{sw})]B_g + \frac{GB_{gi}}{1-S_{wi}} \frac{S_{wi}}{B_{wi}} (R_{swi}-R_{sw}) \frac{B_g}{5.615} + G_{inj} B_g \quad \ldots\ldots\ldots\ldots (A14)$$

PVT properties B_g and R_{sw} are evaluated at current reservoir pressure. G_p for a gas condensate is the wet gas volume calculated by adding separator gas to liquid condensate converted to an equivalent surface gas volume. Also, the two-phase Z-factor must be used to calculated B_g for gas condensate reservoirs. Strictly speaking the cumulative water production term W_p represents "free" water production and not the water condensed out of solution from the produced gas wellstream.

The gas volume in the associated pore volume is a function of the amount of gas that has come out of solution,

$$V_{gA} = \frac{GB_{gi}}{1-S_{wi}} M \frac{1}{B_{wi}} (R_{swi}-R_{sw}) B_g \frac{1}{5.615} \quad \ldots\ldots\ldots\ldots (A15)$$

The water volume in the net-pay reservoir equals the unproduced initial water plus injected water plus water encroachment from an external aquifer,

$$V_{wR} = (V_{wR})_{\text{Unproduced}} + (V_{wR})_{\text{Injected}} + [(V_{wR})_{\text{Encroachment}}] \quad \ldots\ldots (A16)$$

$$(V_{wR})_{\text{Unproduced}} = \frac{GB_{gi}}{1-S_{wi}} \frac{S_{wi}}{B_{wi}} B_w - W_pB_w \frac{1}{5.615} \quad \ldots\ldots\ldots (A17)$$

$$(V_{wR})_{\text{Injected}} = 5.615\, W_{inj} B_w \quad \ldots\ldots\ldots\ldots\ldots\ldots (A18)$$

$$(V_{wR})_{\text{Encroachment}} = 5.615\, W_e \quad \ldots\ldots\ldots\ldots\ldots\ldots (A19)$$

yielding

$$V_{wR} = \frac{GB_{gi}}{1-S_{wi}} \frac{S_{wi}}{B_{wi}} B_w + 5.615(W_{inj}B_w+W_e-W_pB_w) \quad \ldots\ldots (A20)$$

The aquifer encroachment term W_e represents any external water volume that is not already included in the "M" term. Later in the derivation we show the conditions required so that water encroachment (treated rigorously by the method of superposition) can be included as part of the M term used in the cumulative effective compressibility $\bar{c}_e$.

The water volume in the associated pore volume is given by simple expansion,

$$V_{wA} = \frac{GB_{gi}}{1-S_{wi}} M \frac{1}{B_{wi}} B_w \quad \ldots\ldots\ldots\ldots\ldots\ldots\ldots (A21)$$

Combining terms gives

$$GB_{gi} + \frac{GB_{gi}}{1-S_{wi}} S_{wi} - \frac{GB_{gi}}{1-S_{wi}} \bar{c}_f (p_i-p) + \frac{GB_{gi}}{1-S_{wi}} M - \frac{GB_{gi}}{1-S_{wi}} M \bar{c}_f (p_i-p)$$

$$= GB_g - (G_p-W_pR_{sw})B_g + G_{inj}B_g + \frac{GB_{gi}}{1-S_{wi}} \frac{S_{wi}}{B_{wi}} \frac{(R_{swi}-R_{sw})B_g}{5.615}$$

$$+ \frac{GB_{gi}}{1-S_{wi}} M \frac{1}{B_{wi}} \frac{(R_{swi}-R_{sw})B_g}{5.615} + \frac{GB_{gi}}{1-S_{wi}} \frac{S_{wi}}{B_{wi}} B_w$$

$$+ 5.615(W_{inj}B_w+W_e-W_pB_w) + \frac{GB_{gi}}{1-S_{wi}} M \frac{1}{B_{wi}} B_w \quad (A22)$$

Changing signs and grouping terms yields

$$G(B_g-B_{gi}) + \frac{GB_{gi}}{1-S_{wi}}\left\{S_{wi}\left[\frac{B_w+\frac{(R_{swi}-R_{sw})B_g}{5.615}}{B_{wi}} - \frac{B_{wi}}{B_{wi}}\right] + \bar{c}_f(p_i-p)\right.$$
$$\left. +M\left[\frac{B_w+\frac{(R_{swi}-R_{sw})B_g}{5.615}}{B_{wi}} - \frac{B_{wi}}{B_{wi}}\right] + M\,\bar{c}_f(p_i-p)\right\} \quad (A23)$$
$$= (G_p-W_pR_{sw}-G_{inj})B_g + 5.615\left(W_p-W_{inj}-\frac{W_e}{B_w}\right)B_w$$

Defining the total water-gas formation volume factor B_{tw},

$$B_{tw} \equiv B_w + \frac{(R_{swi}-R_{sw})B_g}{5.615} \quad \ldots\ldots\ldots\ldots\ldots\ldots \quad (A24)$$

and noting that $B_{twi}=B_{wi}$ gives

$$G(B_g-B_{gi}) + \frac{GB_{gi}}{1-S_{wi}}\left[S_{wi}\left(\frac{B_{tw}-B_{twi}}{B_{twi}}\right)+\bar{c}_f(p_i-p)\right.$$
$$\left. + M\left(\frac{B_{tw}-B_{twi}}{B_{twi}}\right) + M\,\bar{c}_f(p_i-p)\right] \quad \ldots\ldots (A25)$$
$$= (G_p-W_pR_{sw}-G_{inj})B_g + 5.615\left(W_p-W_{inj}-\frac{W_e}{B_w}\right)B_w$$

Defining the cumulative total water-gas compressibility $\bar{c}_{tw}$,

$$\bar{c}_{tw} \equiv \frac{(B_{tw}-B_{twi})}{B_{twi}}\frac{1}{(p_i-p)} \quad \ldots\ldots\ldots\ldots\ldots\ldots \quad (A26)$$

gives

$$G(B_g-B_{gi}) + GB_{gi}\left[\frac{S_{wi}\bar{c}_{tw}+\bar{c}_f}{1-S_{wi}}(p_i-p)\right.$$
$$\left. + \frac{M(\bar{c}_{tw}+\bar{c}_f)}{1-S_{wi}}(p_i-p)\right] \quad \ldots\ldots (A27)$$
$$= (G_p-W_pR_{sw}-G_{inj})B_g+5.615\left(W_p-W_{inj}-\frac{W_e}{B_w}\right)B_w$$

Defining an cumulative effective compressibility $\bar{c}_e$

$$\bar{c}_e \equiv \frac{S_{wi}\bar{c}_{tw} + \bar{c}_f + M(\bar{c}_{tw}+\bar{c}_f)}{1-S_{wi}} \quad \ldots\ldots\ldots\ldots\ldots\ldots \quad (A28)$$

gives

$$G(B_g-B_{gi}) + GB_{gi}[\bar{c}_e(p_i-p)]$$
$$= B_g\left[G_p - G_{inj} + W_pR_{sw} + \frac{5.615}{B_g}(W_pB_w - W_{inj}B_w - W_e)\right] \quad (A29)$$

Dividing through by GB_{gi} and expressing $B_g=(p_{sc}/T_{sc})(zT/p)$ gives the final form of the material balance

$$(p/z)\left[1-\bar{c}_e(p_i-p)\right] =$$
$$(p/z)_i\left\{1-\frac{1}{G}\left[G_p - G_{inj} + W_pR_{sw} + \frac{5.615}{B_g}(W_pB_w - W_{inj}B_w - W_e)\right]\right\} \quad (A30)$$

The p/z-cumulative plot including all terms would consider $(p/z)[1-\bar{c}_e(p_i-p)]$ versus the entire production/injection term Q

$$(p/z)[1-\bar{c}_e(p_i-p)] = (p/z)_i - \frac{(p/z)_i}{G}Q \quad \ldots\ldots\ldots\ldots \quad (A31)$$

with

$$Q = G_p - G_{inj} + W_pR_{sw} + \frac{5.615}{B_g}(W_pB_w - W_{inj}B_w - W_e) \quad \ldots (A32)$$

where the intercept is given by $(p/z)_i$ and the slope equals $(p/z)_i/G$. Setting $G_{inj}=W_{inj}=W_p=W_e=0$ gives the common form of the gas material balance,

$$(p/z)\left[1-\bar{c}_e(p_i-p)\right] = (p/z)_i\left[1-\frac{G_p}{G}\right] \quad \ldots\ldots\ldots\ldots \quad (A33)$$

Treating Limited Aquifers in $\bar{c}_e$ Term. The material balance thus far has considered any associated water volume expressed in terms of the M parameter. In fact M may include a limited aquifer with up to 25 times the reservoir pore volume for a system permeability greater than about 100 md, and even larger aquifer volumes for higher permeabilities. The condition that determines when a limited aquifer can be treated as part of the $\bar{c}_e$ term is outlined below. We start with the general material balance equation including a water encroachment term W_e and a $\bar{c}_e$ term that considers only non-net pay.

$$(p/z)\left[1-\bar{c}_e(p_i-p)\right] = (p/z)_i\left[1-\frac{G_p}{G}+5.615\frac{W_e}{GB_g}\right] \quad \ldots\ldots (A34)$$

$$\bar{c}_e = \frac{S_{wi}\bar{c}_{tw} + \bar{c}_f + \frac{V_{pNNP}}{V_{pR}}(\bar{c}_{tw}+\bar{c}_f)}{1-S_{wi}} \quad \ldots\ldots\ldots\ldots\ldots\ldots \quad (A35)$$

The water encroachment term calculated by superposition is expressed,

$$W_e = B\sum_j Q_D(\Delta t_j)_D\,\Delta p_j \quad \ldots\ldots\ldots\ldots\ldots\ldots \quad (A36)$$

where $Q_D(t_D)$ is the dimensionless cumulative influx given as a function of dimensionless time t_D and aquifer-to-reservoir radius $r_D=r_{AQ}/r_R$. Δp_j is given by p_j-p_{j-1} (in the limit for small time steps), and $\Delta t_j=t-t_{j-1}$. Assuming that permeability is reasonably high and the ratio r_{AQ}/r_R is not

too large, Q_D for the smallest time step will approach the limiting value Q_D^{∞}, and the summation can be closely approximated by

$$\sum_j Q_D(\Delta t_j)_D \Delta p_j = Q_D^{\infty}(p_i - p) \quad \ldots\ldots\ldots\ldots\ldots\ldots \quad (A37)$$

giving a simple expression for W_e which is independent of time and only dependent on reservoir pressure,

$$W_e = B\, Q_D^{\infty}(p_i - p) \quad ; \; W_e(\text{bbl}) \quad \ldots\ldots\ldots\ldots\ldots\ldots \quad (A38)$$

$$B = \frac{2\pi}{5.615}\phi r_R^2 h(\bar{c}_{tw} + \bar{c}_f) \quad \ldots\ldots\ldots\ldots\ldots\ldots \quad (A39)$$

$$Q_D^{\infty} = \frac{1}{2}\left[\left(\frac{r_{AQ}}{r_R}\right)^2 - 1\right]$$

Expressing W_e in terms of aquifer pore volume V_{pAQ},

$$W_e = \pi\left(r_{AQ}^2 - r_R^2\right)\phi h(\bar{c}_{tw} + \bar{c}_f)(p_i - p) \quad ; \quad W_e(\text{ft}^3) \quad \ldots\ldots\ldots \quad (A40)$$

$$= V_{pAQ}(\bar{c}_{tw} + \bar{c}_f)(p_i - p)$$

The material balance equation can then be written:

$$(p/z)\left[1 - \bar{c}_e(p_i - p)\right] = (p/z)_i\left[1 - \frac{G_p}{G}\right] + (p/z)_i \frac{W_e}{GB_g} 5.615 \quad \ldots \quad (A41)$$

and simplified in a form where the $\bar{c}_e$ term includes the aquifer contribution to pressure support,

$$(p/z)_i \frac{W_e}{GB_g} = (p/z)_i \frac{W_e}{G} \frac{T_{sc}}{P_{sc} T}(p/z)$$

$$(p/z)_i \frac{W_e}{GB_g} = (p/z)\frac{W_e}{GB_{gi}} \quad ; \; GB_{gi} = V_{pR}(1 - S_{wi}) \quad \ldots\ldots\ldots \quad (A42)$$

$$(p/z)_i \frac{W_e}{GB_g} = (p/z)\frac{V_{pAQ}(\bar{c}_{tw} + \bar{c}_f)(p_i - p)}{V_{pR}(1 - S_{wi})}$$

Rearranging we arrive at the general form of the material balance (without water production and gas/water injection terms):

$$(p/z)\left[1 - \bar{c}_e(p_i - p)\right] = (p/z)_i\left[1 - \frac{G_p}{G}\right] \quad \ldots\ldots\ldots\ldots\ldots \quad (A43)$$

where

$$\bar{c}_e = \frac{S_{wi}\bar{c}_w + \bar{c}_f + \left[\frac{V_{pNNp}}{V_{pR}} + \frac{V_{pAQ}}{V_{pR}}\right](\bar{c}_w + \bar{c}_f)}{1 - S_{wi}} \quad \ldots\ldots\ldots \quad (A44)$$

$$M \equiv \frac{V_{pNNP} + V_{pAQ}}{V_{pR}} = \frac{V_{pA}}{V_{pR}} \quad \ldots\ldots\ldots\ldots\ldots\ldots \quad (A45)$$

$$\bar{c}_e = \frac{S_{wi}\bar{c}_{tw} + \bar{c}_f + M(\bar{c}_{tw} + \bar{c}_f)}{(1 - S_{wi})} \quad \ldots\ldots\ldots\ldots\ldots\ldots \quad (A46)$$

TABLE 1 - CALCULATION OF PORE VOLUME COMPRESSIBILITY FROM LABORATORY DATA								
Reported Laboratory Data					Calculations for p_i=9800 psia			
p_e (psia)	V_p (cm^3)	V_b (cm^3)	ϕ (%)	c_f	p (psia)	p_i-p (psi)	V_{pi}-V_p (cm^3)	$\bar{c}_f$ Eq. 5
200.0	3.420	20.530	16.70	16.50	9800	0	0.000	16.50
1000.0	3.379	20.489	16.49	13.70	9000	800	0.041	14.99
2000.0	3.337	20.447	16.32	11.40	8000	1800	0.083	13.48
3000.0	3.303	20.413	16.18	9.10	7000	2800	0.117	12.22
4000.0	3.276	20.386	16.07	6.90	6000	3800	0.144	11.08
5000.0	3.257	20.367	15.99	5.00	5000	4800	0.163	9.93
6000.0	3.243	20.353	15.93	3.80	4000	5800	0.177	8.92
7000.0	3.230	20.340	15.88	4.10	3000	6800	0.190	8.17
8000.0	3.213	20.323	15.81	7.30	2000	7800	0.207	7.76
9000.0	3.177	20.287	15.70	16.80	1000	8800	0.243	8.07
9500.0	3.144	20.254	15.50	25.80	500	9300	0.276	8.68
All compressibilities in 10^{-4} psi^{-1}.								

TABLE 2 - COMPARISON OF c_f FOR NORMAL PRESSURE AND OVERPRESSURED CONDITIONS			
Sample	Initial Porosity (%)	Normal Pressure c_{fi} (psi^{-1})	Over-Pressured c_{fi} (psi^{-1})
Gulf Coast Sandstones			
Sample 1	13	4.8	6.4
Sample 2	20	4.4	16.5
North Sea Chalk			
Sample 9 (pore collapse)	32	18.3	7.9
Sample 10 (pore collapse)	30	20.1	7.4
Von Gonten			
Sample 9A	11	3.0	6.0
Sample 4A	22	4.6	9.2
Sample 7A	26	5.9	7.2
Sample 3A	28	8.6	10.6
Sample 6A	25	7.8	8.6
Normal Pressured is 0.5 psi/ft x Depth ; *Overpressured* is 0.8 psi/ft x Depth. Depth Used is 10,000 ft.			

TABLE 3A - EXAMPLE CALCULATION OF TOTAL WATER CUMULATIVE COMPRESSIBILITY FOR THE ANDERSON "L" RESERVOIR						
Pressure psia	B_w bbl/STB	R_{sw} scf/STB	Z_g	B_g ft3/scf	B_{tw} bbl/STB	c_{tw} 10^{-6} psi^{-1}
9510	1.0560	31.8	1.4401	0.00282	1.056	2.40
9000	1.0569	31.0	1.3923	0.00288	1.057	2.43
8000	1.0586	29.2	1.2991	0.00303	1.060	2.51
7000	1.0604	27.2	1.2072	0.00322	1.063	2.65
6000	1.0621	25.0	1.1176	0.00347	1.066	2.78
5000	1.0638	22.5	1.0325	0.00385	1.070	2.98
4000	1.0654	19.6	0.9562	0.00446	1.075	3.28
3000	1.0669	16.1	0.8977	0.00558	1.083	3.86
2000	1.0681	11.8	0.8744	0.00815	1.097	5.19
1500	1.0686	9.3	0.8832	0.01098	1.113	6.69
1000	1.0691	6.5	0.9078	0.01693	1.145	9.95
750	1.0692	5.0	0.9258	0.02302	1.179	13.30
500	1.0693	3.3	0.9472	0.03533	1.249	20.24
250	1.0694	1.6	0.9708	0.07242	1.459	41.20
100	1.0694	0.5	0.9835	0.18341	2.092	104.23
14.7	1.0694	0.0	1.0000	1.26860	8.254	717.86
B_w and R_{sw} were calculated from the Peng-Robinson EOS with volume translation using binary interaction parameters that are functions of temperature and salinity (28,000 PPM for this example); the gas Z-factor was calculated from the Standing-Katz correlation.						

TABLE 3B - EXAMPLE CALCULATION OF TOTAL WATER CUMULATIVE COMPRESSIBILITY FOR THE ELLENBURGER RESERVOIR WITH INITIAL 28% CO_2 CONCENTRATION						
Pressure psia	B_w bbl/STB	R_{sw} scf/STB	Z_g	B_g ft3/scf	B_{tw} bbl/STB	c_{tw} 10^{-6} psi^{-1}
6675	1.0761	67.5	1.0464	0.00292	1.076	2.75
6000	1.0765	64.5	0.9962	0.00310	1.078	2.83
5000	1.0768	59.5	0.9262	0.00345	1.082	3.12
4000	1.0770	53.5	0.8732	0.00407	1.087	3.84
3000	1.0767	46.1	0.8493	0.00528	1.097	5.24
2500	1.0764	41.5	0.8513	0.00635	1.106	6.61
2000	1.0758	36.1	0.8638	0.00805	1.121	8.89
1750	1.0754	33.0	0.8742	0.00932	1.133	10.67
1500	1.0749	29.6	0.8872	0.01103	1.149	13.15
1250	1.0743	25.8	0.9028	0.01347	1.174	16.83
1000	1.0735	21.6	0.9208	0.01717	1.214	22.56
750	1.0727	16.9	0.9408	0.02339	1.284	32.53
500	1.0716	11.7	0.9621	0.03588	1.428	52.99
250	1.0704	5.8	0.9833	0.07335	1.876	115.75
100	1.0695	1.9	0.9946	0.18548	3.236	305.33
14.7	1.0689	0.0	1.0000	1.26860	16.319	2126.80
B_w and R_{sw} were calculated from the Peng-Robinson EOS with volume translation using binary interaction parameters that are functions of temperature and salinity (50,000 PPM for this example); the gas Z-factor was calculated from the Standing-Katz correlation.						

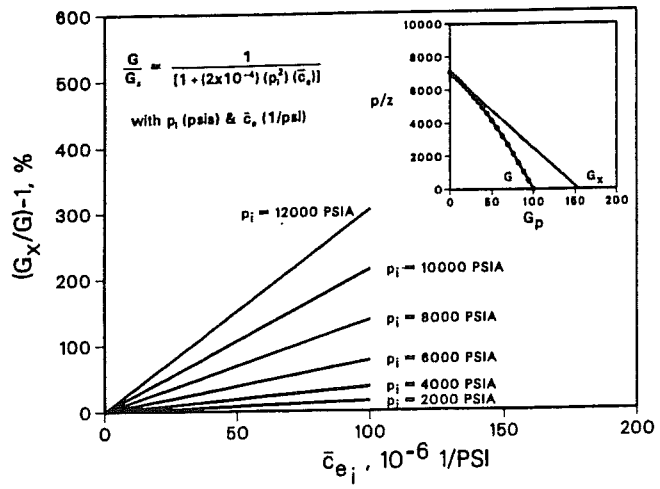

Fig. 1—Effect of p_i and $\bar{c}_e$ on overestimating G.

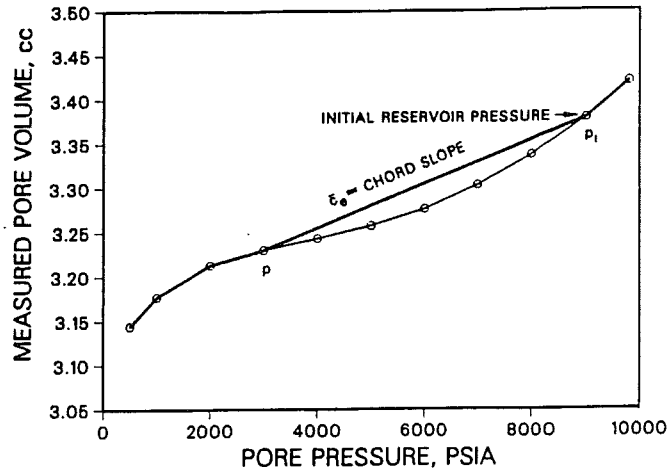

Fig. 2—Cumulative pore volume compressibility as a chord slope.

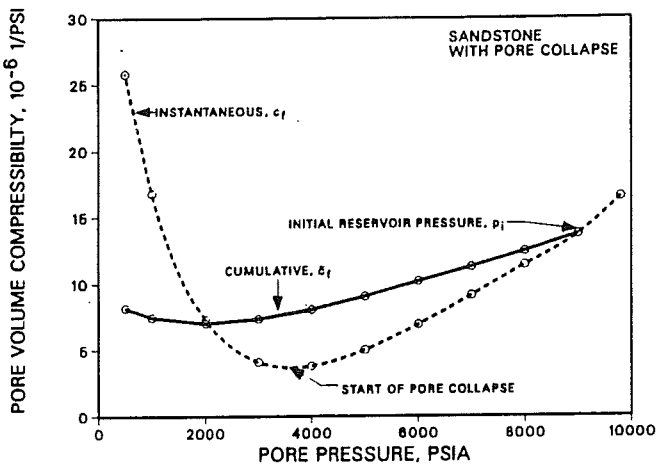

Fig. 3—Cumulative and instantaneous c_f vs. p for a sandstone with pore collapse.

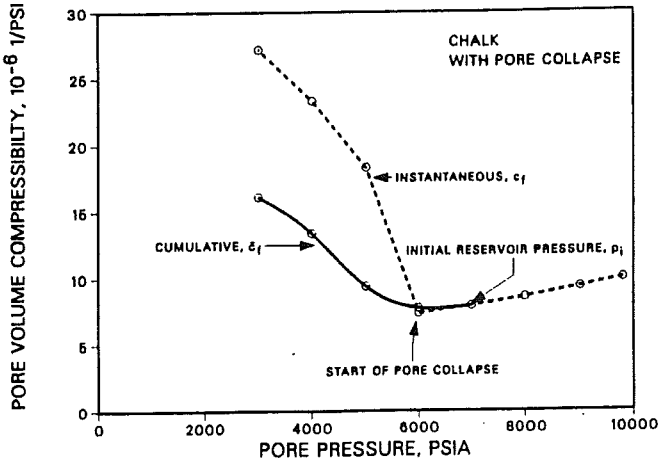

Fig. 4—Cumulative and instantaneous c_f vs. p for a chalk with pore collapse.

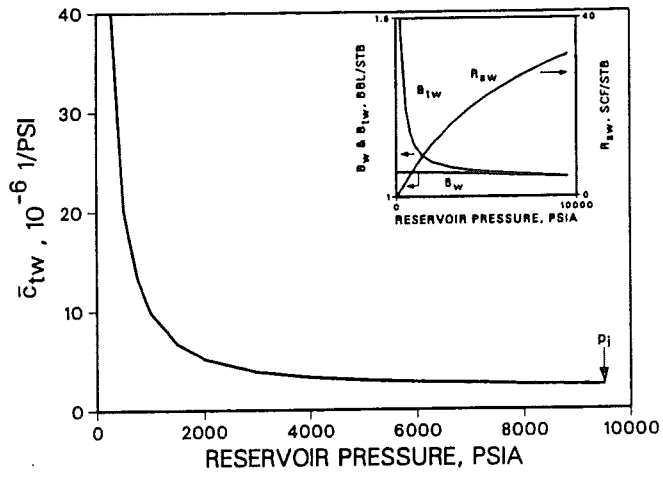

Fig. 5—Cumulative total water compressibility, $\bar{c}_{tw}$ vs. p.

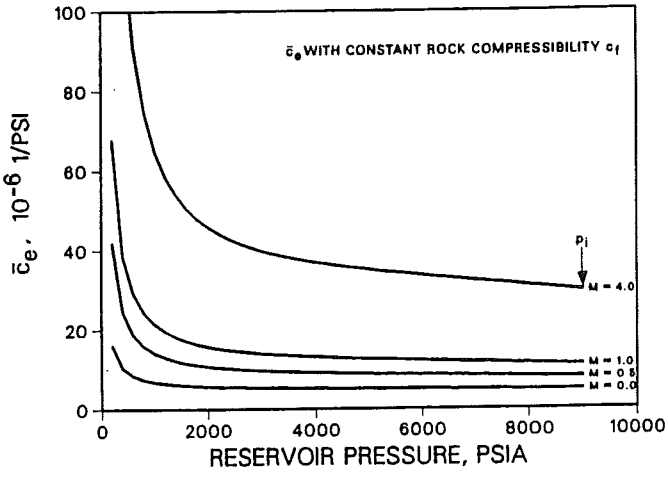

Fig. 6—Cumulative effective compressibility vs. p at various M ratios.

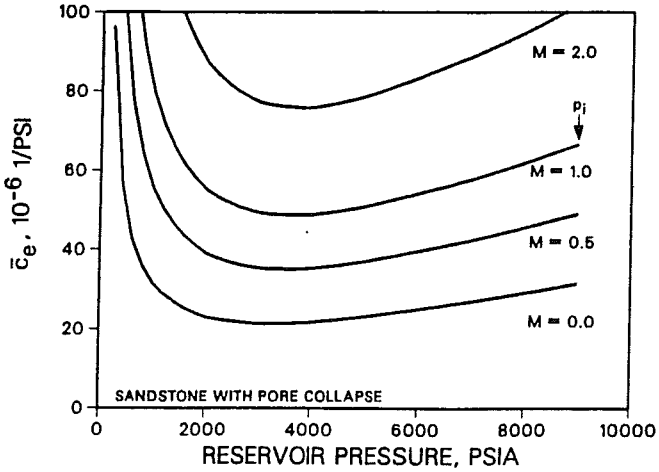

Fig. 7—Cumulative effective compressibility vs. p for a sandstone with pore collapse.

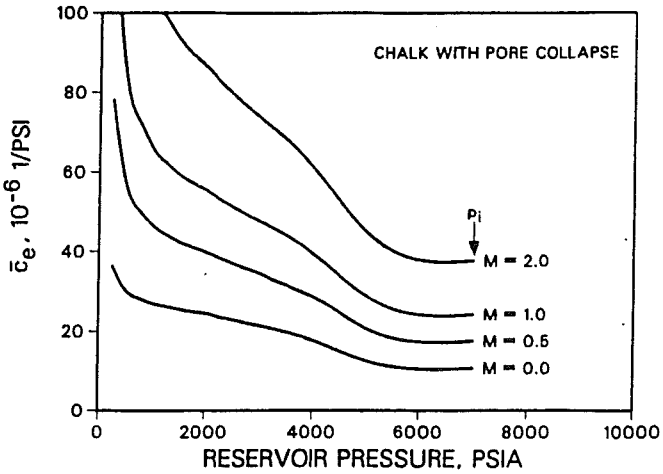

Fig. 8—Cumulative effective compressibility vs. p for a chalk with pore collapse.

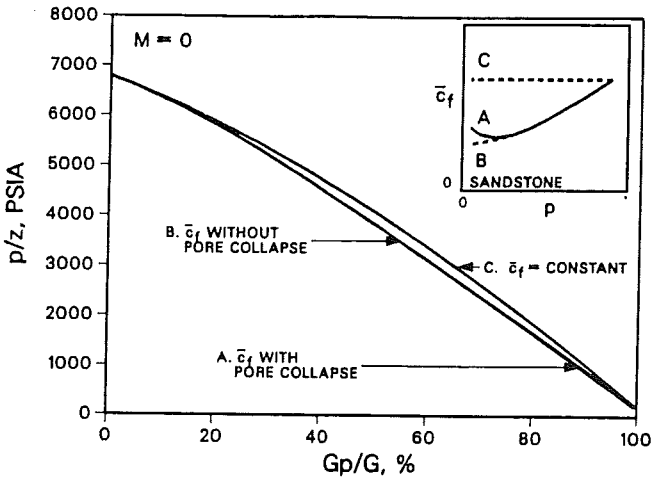

Fig. 9—Effect on p/Z vs. G_p with and without pore collapse, sandstone.

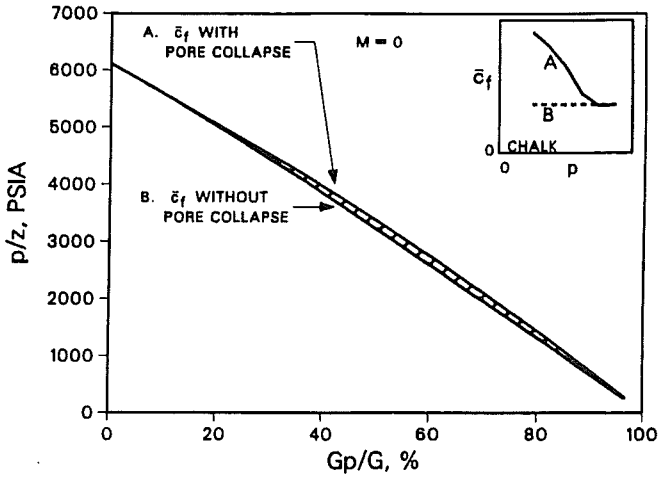

Fig. 10—Effect on p/Z vs. G_p with and without pore collapse, chalk.

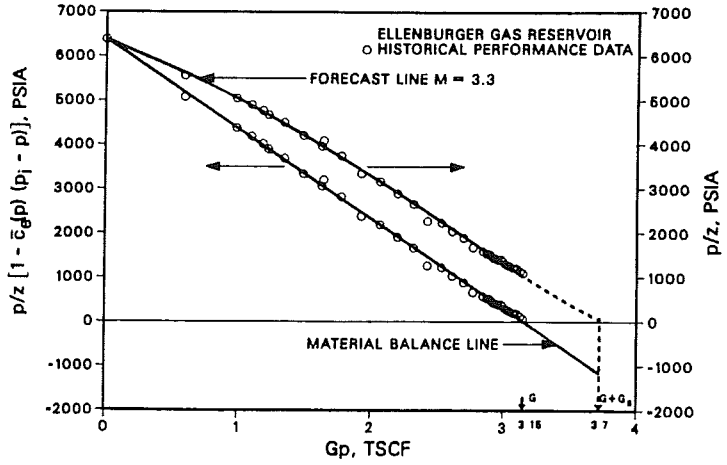

Fig. 11—Pressure vs. cumulative production, Ellenburger gas reservoir.

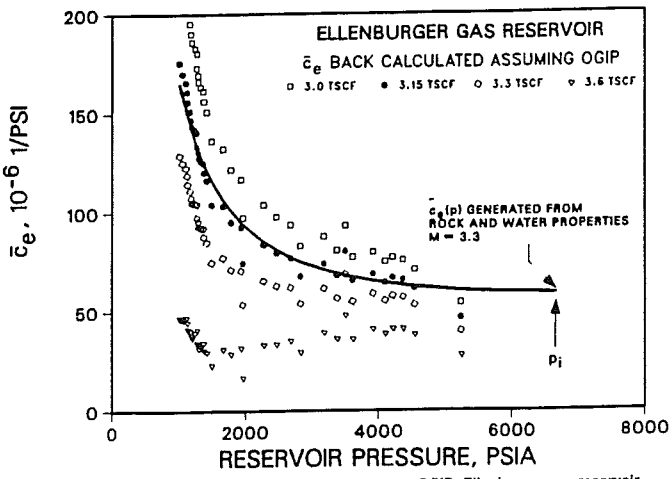

Fig. 12—Backcalculated $\bar{c}_e$ vs. p at various OGIP, Ellenburger gas reservoir.

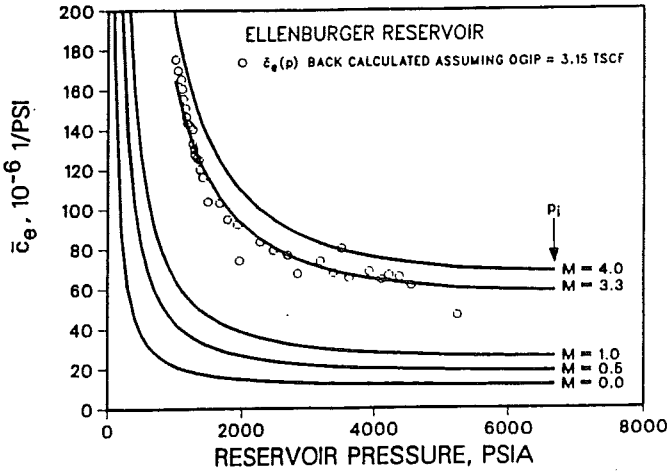

Fig. 13—Matching backcalculated $\bar{c}_e$ to generated $\bar{c}_e$ curves, Ellenburger gas reservoir.

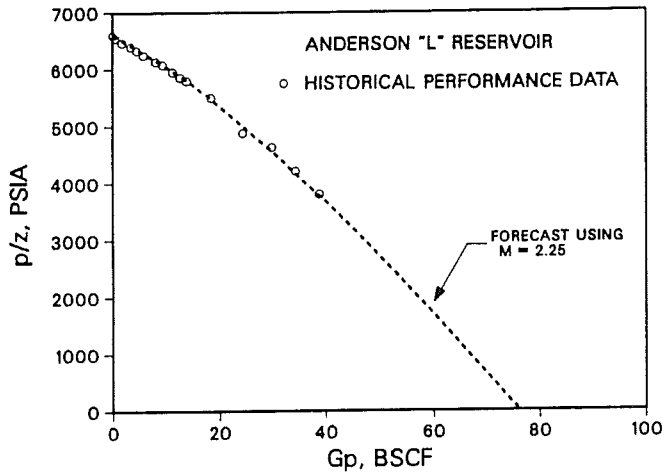

Fig. 14—p/Z vs. cumulative production, Anderson "L" reservoir.

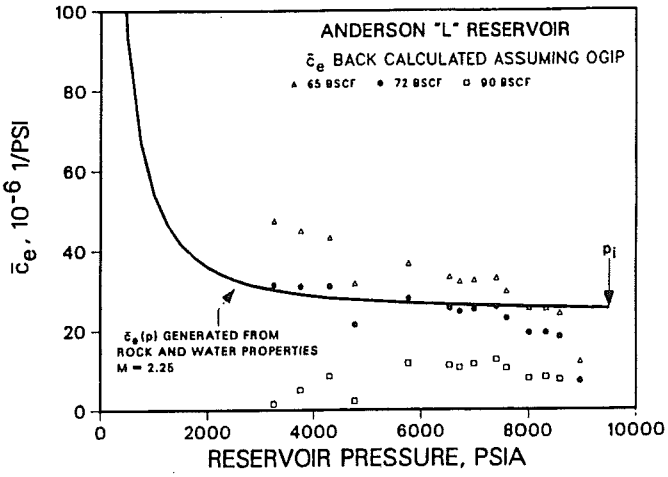

Fig. 15—Backcalculated $\bar{c}_e$ vs. p at various OGIP, Anderson "L" reservoir.

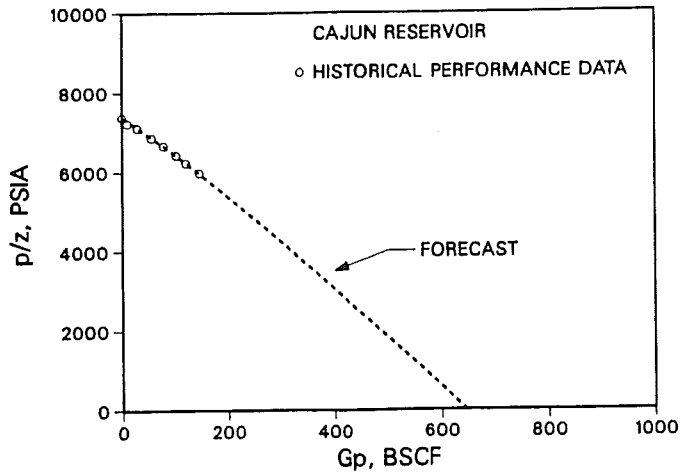

Fig. 16—p/Z vs. cumulative production, Cajun reservoir.

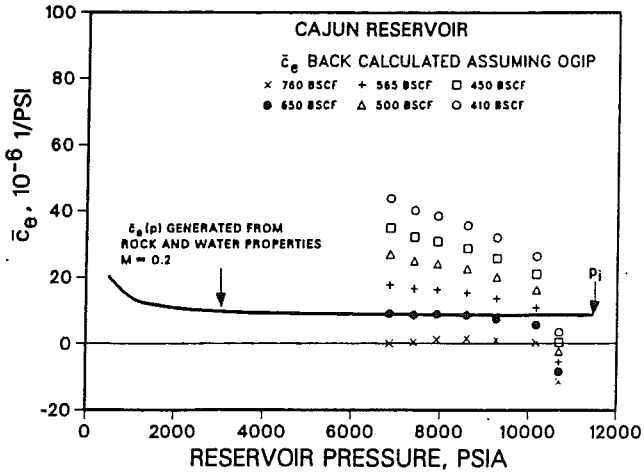

Fig. 17—Backcalculated $\bar{c}_e$ vs. p at various OGIP, Cajun reservoir.

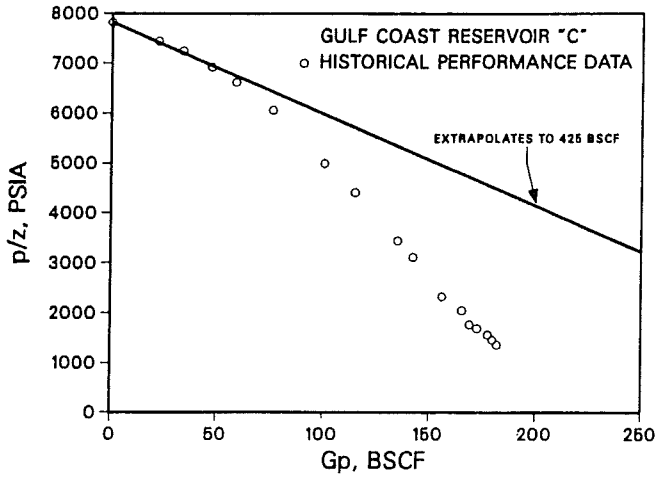

Fig. 18—p/Z vs. cumulative production, Gulf Coast Reservoir "C".

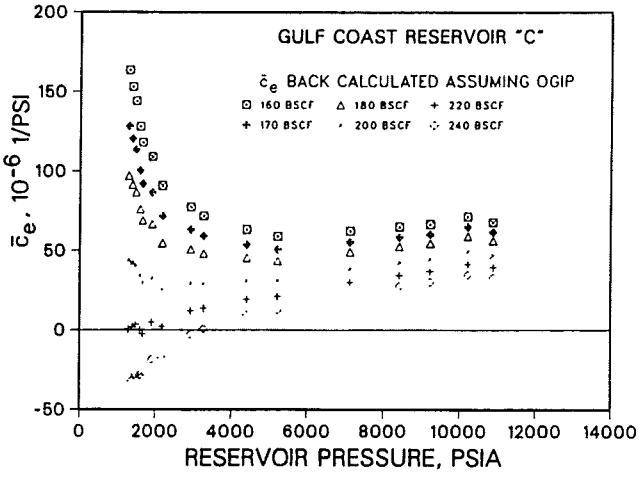

Fig. 19—Backcalculated $\bar{c}_e$ vs. p at various OGIP, Gulf Coast Reservoir "C".

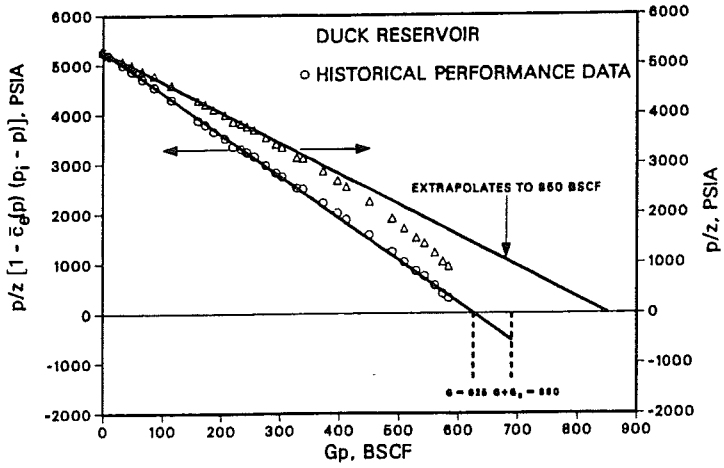

Fig. 20—Pressure vs. cumulative production, Duck reservoir.

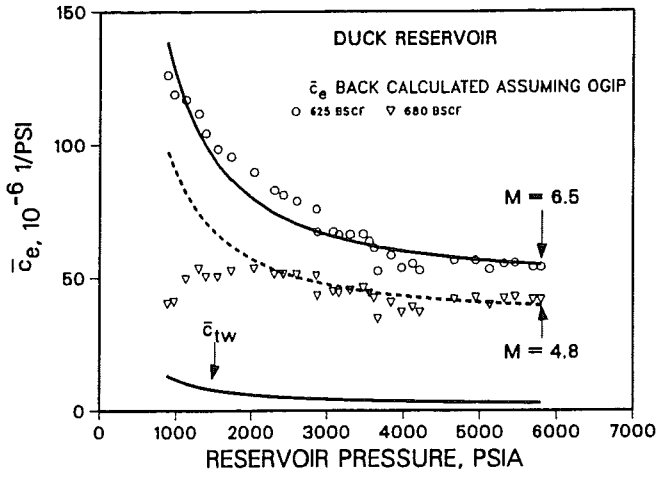

Fig. 21—Backcalculated $\bar{c}_e$ vs. p at various OGIP, Duck reservoir.

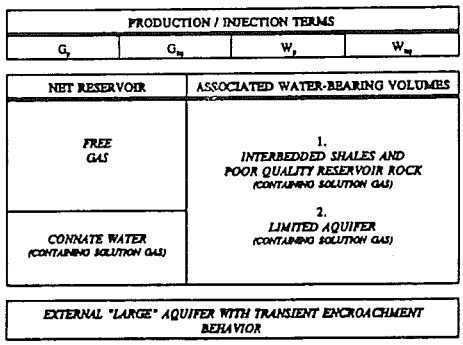

Fig. 22—General material balance schematic.

Analysis of the Kansas Hugoton Infill-Drilling Program

T.F. McCoy, SPE, **M.J. Fetkovich,** SPE, **R.B. Needham,** SPE, and **D.E. Reese,** SPE, Phillips Petroleum Co.

Summary. This paper uses official deliverability tests and production histories to compare the performances of infill wells and companion original wells drilled in the Kansas Hugoton field. In addition, the performance of one of the five Mesa replacement test wells drilled in 1977 in the Kansas Hugoton is reviewed. Pitfalls in the use of official deliverability and wellhead shut-in pressure differences between infill wells and companion original wells to indicate additional gas in place (GIP) are presented. Analysis of the performance of the first 659 infill wells has found no evidence of additional GIP.

Introduction

We examined more than 12 years of performance data from a five-replacement-well program in the Kansas Hugoton and evaluated the results of the Kansas Hugoton infill-drilling program started in 1987. This work focuses on the pressure, deliverability, and rate-vs.-time relationship between two wells on a 640-acre section with respect to any GIP additions made by the second well.

In 1977, Mesa undertook a five-replacement-well test program to determine if increased reserves and improved deliverability could be obtained by drilling an additional well on each of the five 640-acre-spacing units. One aspect of the five-replacement-well study is that the original wells were shut in for nearly 10 years and wellhead observation pressures recorded monthly while the replacement wells were produced. The observed pressures, combined with pressure and flowmeter data taken on each of the four no-crossflow layers in the productive interval, provide a unique look at the performance relationship between two wells on the same 640-acre-spacing unit. We found no evidence that the replacement wells encountered any gas that was not already being drained by the original wells.

This paper also examines the performance data of the first 659 infill wells placed on production in the Kansas Hugoton. In April 1986, the Kansas Corporation Commission (KCC) amended its basic proration order[1] for the Kansas Hugoton gas field to permit a second optional well to be drilled on all basic acreage units larger than 480 acres. The KCC based its decision to allow infill wells on the premise that these wells would recover an additional 3.5 to 5.0 Tscf of gas that could not be recovered by existing wells. Data used in our analysis include the official deliverability test data and monthly allowable and production history for each infill and companion original well. Results indicate that infill wells have not encountered or indicated additional GIP. This conclusion is supported by companion papers on the Guymon-Hugoton field.[2-4]

The performance of the five replacement wells compared with the companion original wells illustrates the rate and pressure-vs.-time relationship of a well pair on 640-acre-spacing units in the Kansas Hugoton. Results obtained from the five-well program provide a more complete understanding of infill-well performance in the Kansas Hugoton and other similar layered no-crossflow reservoirs.

History

The Hugoton field is the largest gas accumulation in the Lower 48 states, covering about 6,500 sq. miles in three states. Approximately two-thirds of the field lies in southwest Kansas on all or portions of nine counties (**Fig. 1**). In Nov. 1989, there were 4,853 producing gas wells in the Kansas Hugoton, including 659 infill wells. Cumulative production from the Kansas Hugoton through Dec. 1989 totaled more than 20 Tscf, with an estimated remaining GIP of about 10 Tscf.

The Kansas Hugoton field was discovered in 1922; most of the wells were drilled in the 1940's and early 1950's on 640-acre units.[5,6] The early wells were completed open hole; later, slotted liners were run over the openhole interval to avoid cave-in problems. By 1938, operators were treating the whole productive interval with HCl. In the late 1940's, many operators found that maximum deliverability could be obtained by setting casing through the pay zones and selectively perforating and acidizing each zone.[7-9] By the early 1960's, the primary method of stimulation was hydraulic fracturing.

Geology

The Lower Permian section across southwestern Kansas and the Oklahoma and Texas panhandles was deposited in cyclical sequences on a shallow marine carbonate ramp.[2,10] Each cycle consists of laterally continuous anhydritic carbonates and fine-grained clastics capped and separated by shaley redbeds and paleosols. The Chase group is the major gas pay within the Hugoton field and is subdivided primarily into carbonate units and interlayered shaly units. The carbonate units, including (from the bot-

intervals with different porosity/permeability relationships.

5. Routine core data have shown that there can be significant variation in porosity/permeability relationships between formations, within what are considered to be uniform sands, between wells in the same area of a field, and between the oil and water zones.

6. Oil-based drilling mud can significantly alter reservoir wettability and affect measurements of relative permeability and ROS.

Nomenclature

k = permeability, md
k_r = relative permeability
k_o = oil effective permeability, md
k_{ro} = oil relative permeability
k_{rw} = water relative permeability
P_c = capillary pressure, psi
S_{wi} = initial (low) water saturation
ϕ = porosity

Acknowledgments

We thank Shell U.K. E&P for participating in several of the special core analysis programs discussed, for providing the core material and reservoir fluids required in laboratory tests, and for granting permission to publish the paper. A special note of thanks to our colleagues at Exxon Production Research Co., who conducted the special core analysis tests described.

References

1. Johnson, H.D. and Stewart, D.J.: "Role of Clastic Sedimentology in the Exploration and Production of Oil and Gas in the North Sea," *Sedimentology: Recent Developments and Applied Aspects*, The Geological Soc./Blackwell, Oxford (1985) 261–73.
2. Archer, J.S.: "Reservoir Definition and Characterization for Analysis and Simulation," *Proc.*, 11th World Pet. Cong., London (1983) **3**, 65–68.
3. Amott, E.: "Observations Relating to the Wettability of Porous Rock," *Trans.*, AIME (1959) **216**, 156–62.
4. Bobek, J.E., Mattax, C.C., and Denekas, M.O.: "Reservoir Rock Wettability—Its Significance and Evaluation," *Trans.*, AIME (1958) **213**, 155–60.
5. Anderson, W.G.: "Wettability Literature Survey—Part 1: Rock/Oil/Brine Interactions and the Effects of Core Handling on Wettability," *JPT* (Oct. 1986) 1125–44.
6. Richardson, J.G., Perkins, F.M., and Osoba, J.S.: "Differences in the Behavior of Fresh and Aged East Texas Woodbine Cores," *Trans.*, AIME (1955) **204**, 86–91.
7. Auman, J.B.: "A Laboratory Evaluation of Core-Preservation Materials," *SPEFE* (March 1989) 53–55.
8. Huppler, J.D.: "Waterflood Relative Permeabilities in Composite Cores," *JPT* (May 1969) 539–40.
9. Braun, E.M. and Blackwell, R.J.: "A Steady-State Technique for Measuring Oil-Water Relative Permeability Curves at Reservoir Conditions," paper SPE 10155 presented at the 1981 SPE Annual Technical Conference and Exhibition, San Antonio, Oct. 5–7.
10. Mungan, N.: "Relative Permeability Measurements Using Reservoir Fluids," *SPEJ* (Oct. 1972) 398–402; *Trans.*, AIME, **253**.
11. Wendel, D.J., Anderson, W.G., and Meyers, J.D.: "Restored-State Core Analysis for the Hutton Reservoir," *SPEFE* (Dec. 1987) 509–17.
12. Anderson, W.G.: Wettability Literature Survey—Part 5: The Effects of Wettability on Relative Permeability," *JPT* (Nov. 1987) 1453–68.
13. Treiber, L.E., Archer, D.L. , and Owens, W.W.: "Laboratory Evaluation of the Wettability of Fifty Oil Producing Reservoirs," *SPEJ* (Dec. 1972) 531–40; *Trans.*, AIME **253**.
14. Hagoort, J.: "Oil Recovery by Gravity Drainage," *SPEJ* (June 1980) 139–50.
15. Hassler, G.L. and Brunner, E.: "Measurement of Capillary Pressures in Small Core Samples," *Trans.*, AIME (1945) **160**, 114–23.
16. Kyte, J.R.: "A Centrifuge Method To Predict Matrix-Block Recovery in Fractured Reservoirs," *SPEJ* (June 1970) 164–70; *Trans.*, AIME, **249**.
17. Stiles, J.H. and McKee, J.W.: "Cormorant: Development of a Complex Field," *SPEFE* (Dec. 1991) 427–36; *Trans.*, AIME, **291**.
18. Stiles, J.H. and Valenti, N.P.: "The Use of Detailed Reservoir Description and Simulation Studies in Investigating Completion Strategies—Cormorant Field, U.K. North Sea," *SPEFE* (March 1990) 23–30.

SI Metric Conversion Factors

ft	× 3.048*	E−01	= m
°F	(°F−32)/1.8		= °C
mile	× 1.609 344*	E+00	= km
psi	× 6.894 757	E+00	= kPa

*Conversion factor is exact.

Provenance

Original SPE manuscript, **The Use of Routine and Special Core Analysis in Characterizing Brent Group Reservoirs, U.K. North Sea**, received for review Oct. 16, 1988. Revised manuscript received March 3, 1992. Paper accepted for publication March 17, 1992. Paper (SPE 18386) first presented at the 1988 SPE European Petroleum Conference held in London, Oct. 16–19.

JPT

Authors

Stiles

Hutfilz

J.H. Stiles Jr., a senior technical adviser, formerly in Esso E&P U.K.'s reservoir engineering group, moved to the USSR Business Development Group at Exxon Co. Intl. in Houston in Aug. 1991. Stiles began his career in the East Texas Div. of Humble Oil & Refining Co. in 1968. He then worked at Esso Standard Libya and Exxon Production Malaysia Inc. He holds a BS degree in petroleum engineering from Texas A&M U. Stiles was a 1990–91 member of the European Forum Series Steering Committee. James M. Hutfilz is a senior engineering associate with Exxon Production Research Co. in Houston. Since joining Exxon in 1975, he has worked in the areas of reservoir simulation, core analysis, and reservoir management. He is currently involved in the application of reservoir simulation to solve reservoir management problems. Hutfilz holds a BS degree from Michigan State U. and a PhD degree from Rice U., both in chemical engineering.

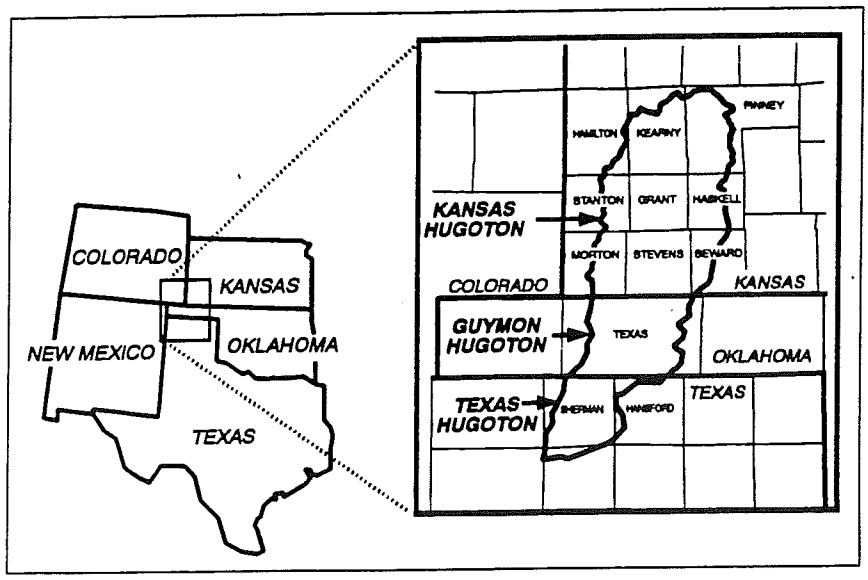

Fig. 1—Kansas Hugoton field location map.

"Results obtained from the five-well program provide a more complete understanding of infill-well performance in the Kansas Hugoton and other similar layered no-crossflow reservoirs."

tom up) the Upper and Lower Fort Riley, Winfield, Krider, and Herington limestones and dolomites, constitute the potential reservoir intervals within the Kansas Hugoton field. These reservoir intervals are separated by sealing shaly units, including the Oketo, Holmesville, Gage, Odell, and Paddock shales. The reservoir and shaly nonreservoir units exhibit characteristic log signatures recognizable throughout the field. Regional north-south and east-west cross sections (**Figs. 2 and 3**), developed from cross sections by Clausing,[11] illustrate the lateral continuity of the reservoir layers and shaly barrier units across the field. Additional information on the geological features in Oklahoma's Guymon-Hugoton field can be found in Ref. 2.

Five-Replacement-Well Study

In 1977, Mesa drilled and completed five replacement wells in the Kansas Hugoton field to determine the performance of replacement wells in relation to original wells.[12,13] Specifically, the operator was interested in determining if increased reserves and deliverability could be achieved with the replacement wells by (1) encountering undrained pay stringers within the Chase group, (2) encountering a higher reservoir pressure in a different part of the 640-acre section, and (3) improving stimulation procedures by selectively perforating and controlling hydraulic fracture treatments. Cross sections generated by the operator indicated laterally continuous producing zones with little discontinuity between wells. From individual-layer pressure and flowmeter data, the operator concluded that the Krider, Winfield, and Upper and Lower Fort Riley zones are separate and distinct producing horizons within the Chase formation, having different reservoir pressures and depleting at different rates. From flowmeter tests, wellbore backflow was found to occur between zones when a well was shut in, further evidence of differential depletion—i.e., a no-crossflow layered reservoir system. The operator found that commingled wellhead shut-in pressures on these wells reflect the pressure in the layer with the lowest reservoir shut-in pressure. One unique aspect of the replacement-well study was that the original wells were shut in for almost 10 years and monthly wellhead shut-in pressures taken and reported to the KCC. The initial wellhead shut-in pressure of the replacement wells averaged 14.4 psi higher than the original wells' 72-hour shut-in pressure at that time. Initial calculated official 72-hour deliverability for the replacement wells averaged 753 Mscf/D/well higher than the latest deliverability of the original wells. No conclusions about any additional GIP were offered in Mesa's original work.[12]

The first of the five replacement wells drilled was the Gano No. A1 located in Sec. 20 T29S R37W in Grant County, KS. Because this was the only replacement well with complete individual-layer pressure buildups and flowmeter test results, its performance is presented in detail.

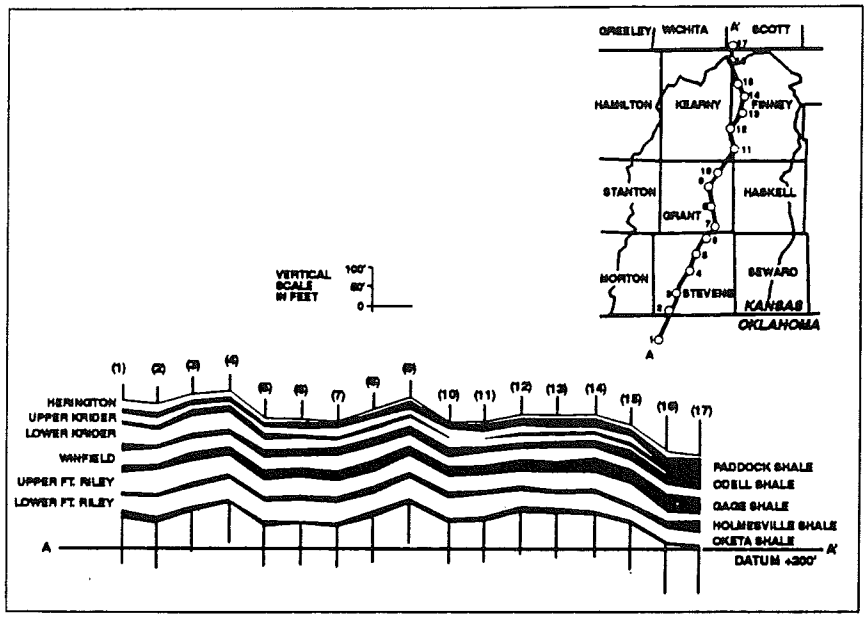

Fig. 2—East-west cross section through the Kansas Hugoton (after Clausing[11]).

Gano No. 1, Original Well. The Gano No. 1 was drilled on Aug. 28, 1951, by Hugoton Producing Co. and completed open hole in the Krider, Winfield, and Upper and Lower Fort Riley layers with a slotted liner. The entire openhole interval was acidized. Initial wellhead shut-in pressure was 434 psia with an absolute open-flow potential (AOFP) of 33,000 Mscf/D. In 1969, Mesa purchased the Gano No. 1 and restimulated the well in 1970 with 150,000 lbm of sand and 150,000 gals of water, resulting in a four-fold increase in productivity. When the well was shut in as an observation well on April 13, 1977, the cumulative production was about 6 Bscf.

Gano No. A1, Replacement Well. The Gano No. A1 reached a total depth of 2,960

"One unique aspect of the replacement-well study was that the original wells were shut in for almost 10 years and monthly wellhead shut-in pressures taken..."

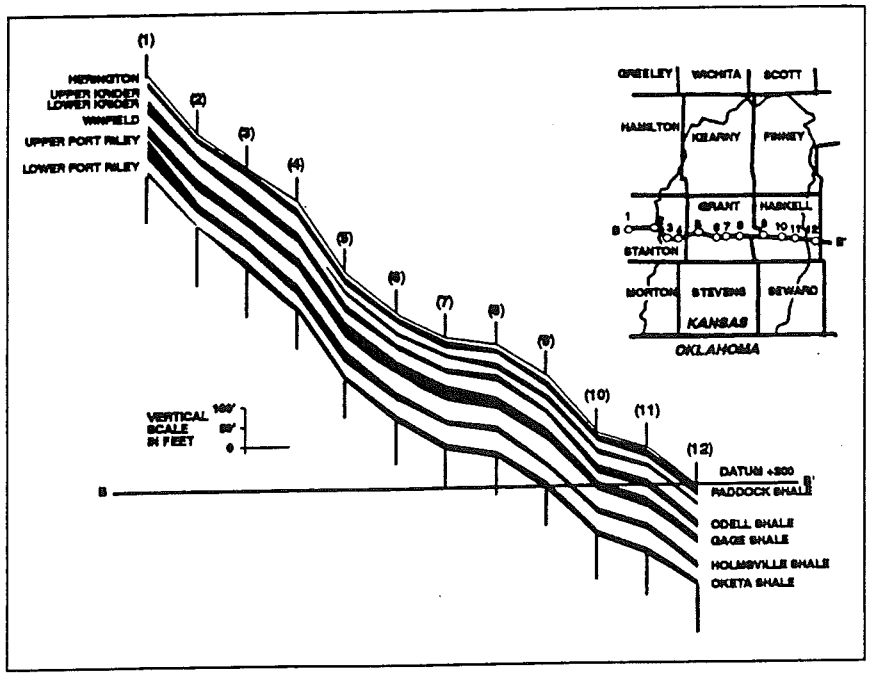

Fig. 3—North-south cross section through the Kansas Hugoton (after Clausing[11]).

ft on April 7, 1977, with 7-in. casing cemented through all the productive intervals. Each layer was separately acidized, flowed to clean up, and then shut in for a pressure-buildup test. After each layer had been individually perforated, acidized, and tested, a final commingled pressure buildup was run. All four layers were then sand fractured with 200,000 gals of gelled water and 200,000 lbm of sand.

Fig. 4 presents permeabilities and bottomhole pressures (BHP's) from the individual-layer pressure-buildup tests and log-calculated porosities for the Gano No. A1. The individual-layer buildup test results clearly indicate that each layer has a different pressure and permeability. The most permeable layer, Krider, has the lowest pressure, 188 psia; the least permeable layer, Lower Fort Riley, has the highest pressure, 284 psia. The greatest amount of depletion has occurred in the more permeable layer(s). The commingled buildup pressure of 190 psia reflects the pressure in the low-pressure, more-permeable Krider layer. During the commingled buildup, the operator indicated[12] that wellbore backflow was occurring from the higher-pressure, lower-permeability layers to the low-pressure, high-permeability layer during the test.

To assess the contribution of flow from each layer and to confirm that wellbore backflow between layers was occurring during shut in, the operator ran a differential temperature log and flowmeter survey on the Gano No. A1. Production was stabilized at 1,200 Mscf/D for 7 days before the survey with a final p_{whf} of 158.4 psia. Fig. 4 shows flow rates from each layer. The Krider contributed 47% of the total flow, while the Lower Fort Riley contributed only 2%. This survey also showed that, during shut in at the surface, the lower two layers, the Upper and Lower Fort Riley, continued to produce gas into the wellbore, backflowing into the upper two layers, the Winfield and the Krider.

Fig. 5 is a plot of p_{whs} vs. G_p with a wellhead backpressure curve and a location plat for the Gano lease. The distance between the two wells on this section is 2,150 ft. The shift to the right in the backpressure curve for the original well (solid circles) corresponds to a sand fracture restimulation performed in 1970. The backpressure curve for the replacement well (open circles) lies slightly to the right of that of the original well after restimulation, indicating only slightly better stimulation results in this

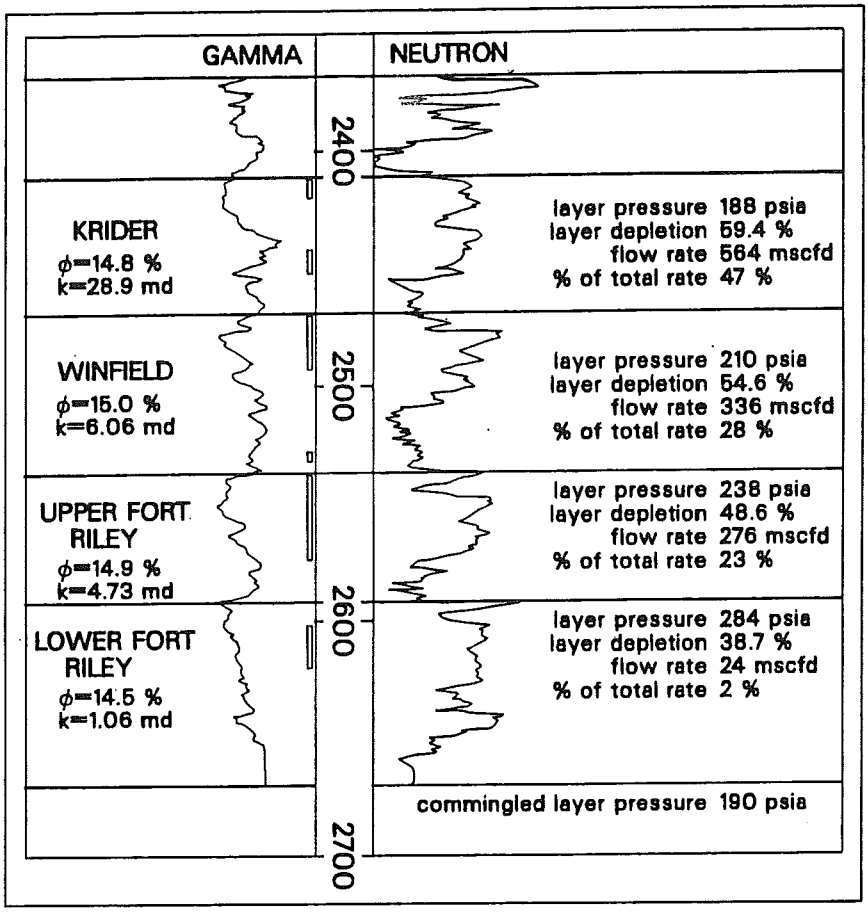

Fig. 4—Type log for the Gano No. A1 with individual-layer pressures and flow rates (after Carnes[12]).

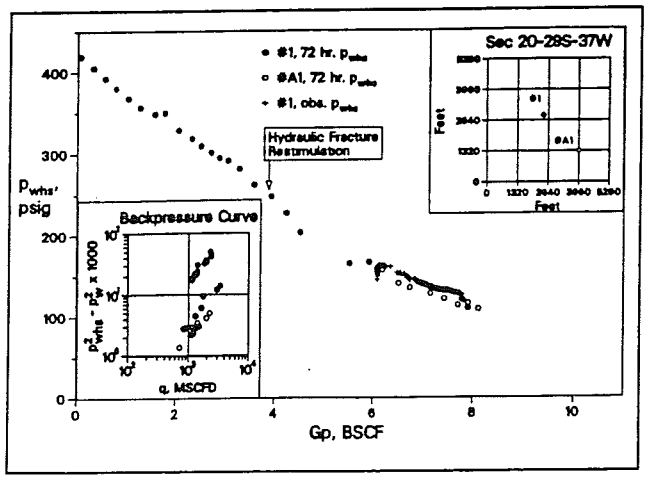

Fig. 5—Wellhead shut-in pressure vs. cumulative production with a wellhead backpressure curve and a location plat for the Gano lease.

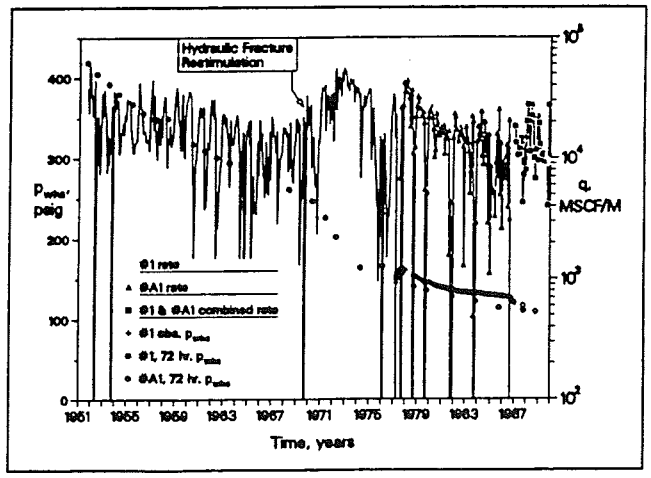

Fig. 6—Wellhead shut-in pressure and monthly rate vs. time for the Gano lease.

replacement well. If the original well had not been restimulated, there would have been an "apparent" dramatic (stimulation or higher-areal-layer pressure-rate contribution) benefit attributed solely to the replacement well or an equivalent infill well. The p_{whs} vs. G_p curve has several apparent slope changes, making it difficult to extrapolate to a GIP properly. The producing rate and/or shut-in duration before the official deliverability test and the no-crossflow layered nature of the reservoir all play important roles in interpreting and evaluating the p_{whs} vs. G_p curve.

The sand fracture restimulation conducted in 1970 on the original well substantially increased the official deliverability, resulting in a much higher allowable for this well. The increased downward slope represented by the p_{whs} points taken after the fracture job appear to indicate a decrease in remaining GIP for this well. The change in slope of the p_{whs} vs. G_p curve after the fracture job in Fig. 5 is primarily caused by the change in the production rate due to the increased allowables resulting from the restimulation and does not reflect a change in the drainage volume for this well.

Another important consideration in evaluating the shape of the p_{whs} vs. G_p curve is the effect of any large rate changes, including extended shut-ins, before the official deliverability test. The production rate was decreased before the 1976 official deliverability test, and the well was shut in during the month immediately before the official test. The effect of rate and "rest period" can be seen more clearly in the rate and pressure vs. time plot of **Fig. 6**. The resulting p_{whs} in 1976 is clearly higher than that of the previous test in 1974. In the Kansas Hugoton, an official deliverability test consists of a 72-hour flow followed by a 72-hour shut-in. The rate and flowing pressure are recorded at the end of the flow period and the p_{whs} at the end of the shut-in. Resting a well before an official deliverability test will allow the 72-hour p_{whs} to build up to a higher pressure than if the well had been producing before the test. The wellbore backflow from the high-pressure layer(s) to the low-pressure layer(s) that occurs during shut-in also causes the well to build up to a higher pressure. (In the Kansas Hugoton, p_{whs} is an important factor in the calculation of allowables. For a given well, the higher the p_{whs}, the higher the allowable.)

Taking into account the expected curvature of the p_{whs} vs. G_p curve in a layered no-crossflow reservoir with contrasting layer properties and the effect of the rate and shut-in periods on the shape of this same curve (see Figs. 5 and 6), we can conclude that the replacement well is producing from the same drainage area as the original well. The p_{whs} for the replacement well falls on the p_{whs} trend started by the original well (Fig. 5).

Observation-Well Pressures. **Fig. 7** is a plot of p_{whs} and monthly rate vs. time since 1977 for the Gano lease. The solid and open circles represent the 72-hour p_{whs} for the original (Gano No. 1) and replacement (Gano No. A1) wells, respectively. The triangles with the dashed line represent the replacement well (Gano No. A1) rates, while the solid line represents the monthly rates for the original well (Gano No. 1). The plus symbol denotes the observation wellhead shut-in pressures taken on the original well (Gano No. 1). The first observation pressure is 144.7 psig and was taken after

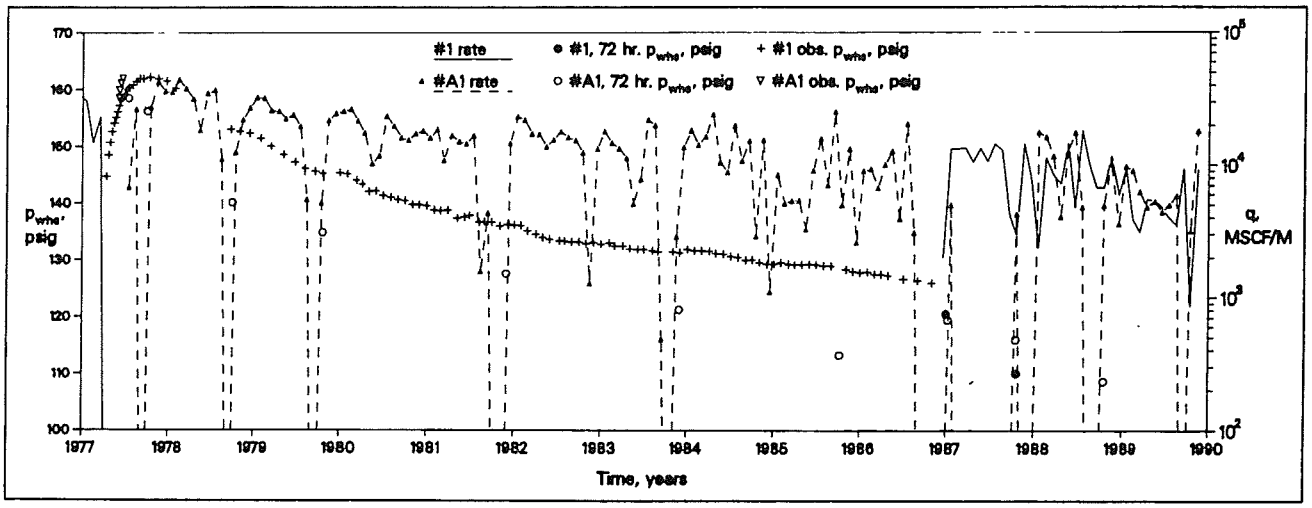

Fig. 7—Wellhead shut-in pressure and monthly rate vs. time since 1977 for the Gano lease.

TABLE 1—EFFECT OF LAYERING ON DEPLETION AND TIME TO ABANDONMENT RATE
(p_i = 463 psia. B_{gi} = 31.98 scf/res ft³. μ_g = 0.01045 cp. T = 550°R. r_w = 0.2539 ft)

Comments	Parameter	Krider	Winfield	Upper Fort Riley	Lower Fort Riley	Total
	k, md	21.8	12.6	5.4	0.53	
	h, ft	34	28	42	26	130
	kh, md-ft	741	353	227	14	1,335
	ϕ	0.148	0.150	0.149	0.128	
	S_w	0.235	0.285	0.312	0.308	
	G_i, MMscf	3,432	2,676	3,840	2,052	12,000
	$\bar{p}$, psia (1977)*	188	210	238	284	
	G_p/G_i	0.610	0.563	0.503	0.402	
	G_r, MMscf	1,284	1,123	1,830	1,178	5,415
One producing well per section, each layer produced separately to an abandonment rate of 10 Mscf	$(q_g)_{max}$, Mscf/D	889	528	436	38	1,795
	t_a, years	60	63	91	108	
	G_p/G_i, fraction	0.96	0.94	0.92	0.69	
One producing well per section, commingled well	t_a, years	162	162	162	162	
	q_{layer}, Mscf/D	0.72	0.90	2.70	5.68	10.0
	G_p/G_i, fraction	0.99	0.98	0.96	0.77	0.94
	$\bar{p}_{layer}$, psia	5	10	20	112	
Two producing wells per section, each layer produced separately to an abandonment rate of 20 Mscf	$(q_g)_{max}$, Mscf/D	1,968	1,169	965	83	3,950
	t_a, years**	43	44	58	67	
	G_p/G_i, fraction	0.96	0.94	0.92	0.71	
Two producing wells per section, commingled production	t_a, years	92	92	92	92	
	q_{layer}, Mscf/D	1.4	1.8	5.3	11.5	20.0
	G_p/G_i, fraction	0.99	0.98	0.96	0.77	0.94
	$\bar{p}_{layer}$, psia	5	10	20	112	

*Pressure distribution of layers at time = 27 years (1977).
**t_a = total producing life, including the first 27 years of commingled production.

the well had been shut in for 1 week. Wellhead shut-in pressures taken on the replacement well (Gano No. A1) for several weeks after the sand fracture, while the well was waiting for an official deliverability test, are denoted by inverted triangles. Note that through time, before the start of production from the replacement well, the observation-well (Gano No. 1) pressure builds up to the pressure of the replacement well (Gano No. A1). This indicates that before any production from the replacement well, the pressure in the most permeable layer is basically the same between these two wells.

Once the replacement well begins to produce, the subsequent 72-hour p_{whs} from the official deliverability tests falls below the observation-well pressures. The difference between the first observation-well pressure on the original well and the first pressure on the replacement well is 10 psi. Approximately 1 year later, at the time of the official deliverability test for the replacement well, the pressure difference between the two wells is 12.9 psi. Although the absolute pressure difference is basically the same, the pressures for the two wells have traded positions. The wellhead shut-in pressure of the original well is now higher than that of the replacement well. This indicates that the pressure difference is simply a reflection of the pressure gradient between the two wells in the most permeable layer when one well is shut in and the other producing. Ref. 14 attempts to confirm this conclusion by use of the steady-state radial flow equation in a bounded system.

Another interesting point in Fig. 7 relates to the effect of resting the original well on the observation-well pressures. In 1978, 1979, 1981, and 1983, the replacement well was "rested" for about 1 month before the official deliverability test. The slope of the observation-well pressures flattens out after each of these rest periods. This subtle change in slope indicates pressure communication between these two wells in the most permeable layer.

In late 1986, Mesa applied for the transfer of allowables from the five replacement wells back to the five original wells that were designated as pressure observation wells. The replacement wells then were shut in until they could be brought back on production as infill wells. The replacement well (Gano No. A1) was shut in during Sept. 1986 and the original well (Gano No. 1) began producing again in Dec. 1986. In Jan. 1988, the replacement well was placed back into production as an infill well. The p_{whs} for both wells at the start of 1987, after several months of no production from either well, are nearly identical. Note in Fig. 7 that the second 1987 p_{whs} for the original well falls back into the pressure trend of the replacement well while it was producing.

An analysis of the Mesa replacement-well program demonstrates that the replacement well and the original well are in pressure communication and the pressure difference between the two wells is caused by the pressure gradient in the most permeable layer. We found no evidence that the replacement well encountered any gas that was not already being drained by the original well. The same conclusion can be drawn from the performance of the other four replacement wells in Mesa's study.[14]

Effect of Layering on Depletion and Abandonment

In this section, we use the simple rate/time and cumulative-time equations of Ref. 15 to illustrate the effect of no crossflow on individual-layer pressure depletion and time to abandonment for the Gano No. A1. Calculations were made assuming equal skins for all layers (−5) and adjusting the permeability for each layer to be in proportion to the rates obtained from the flowmeter survey. Water saturations for each layer are calculated from the layer GIP estimates provided in Ref. 13 with log-derived porosity and thickness and a 640-acre drainage area. **Table 1** gives the calculated depletion times and layer abandonment pressures for the Gano No. 1 assuming wide-open production starting in 1977 at a limiting flowing BHP of 0 psia. The equations used to calculate the time to an abandonment rate and layer pressures at abandonment are summarized in the Appendix. Produced separately, the Krider, Winfield, and Upper and Lower Fort Riley layers take a total of 60, 63, 91, and 108 years, respectively, to reach an abandonment rate of 10 Mscf/D. Commingled production against 0-psia flowing BHP takes 162 years to reach the 10-Mscf/D abandonment rate. The time to an abandonment rate of 10 Mscf/D is almost double the time to the same abandonment rate for the Buf No. 1 well calculations given in Ref. 4. These much longer calculated times are primarily caused by the addition of a fourth productive layer in the Kansas portion of the Hugoton field. The calculated layer abandonment pressures for the Krider, Winfield, and Up-

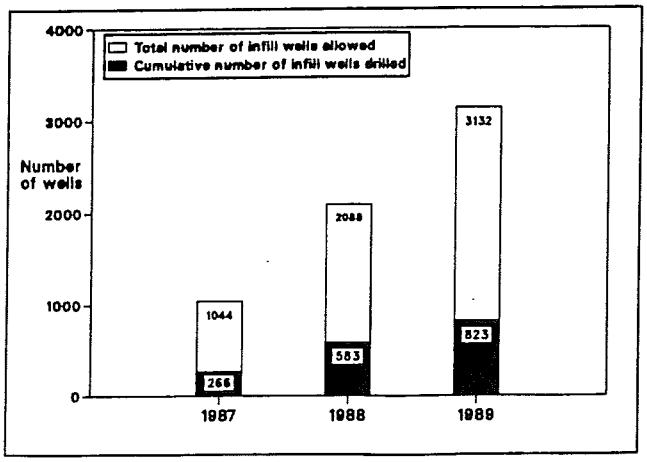

Fig. 8—Actual number of infill wells drilled compared to the total number of wells allowed.

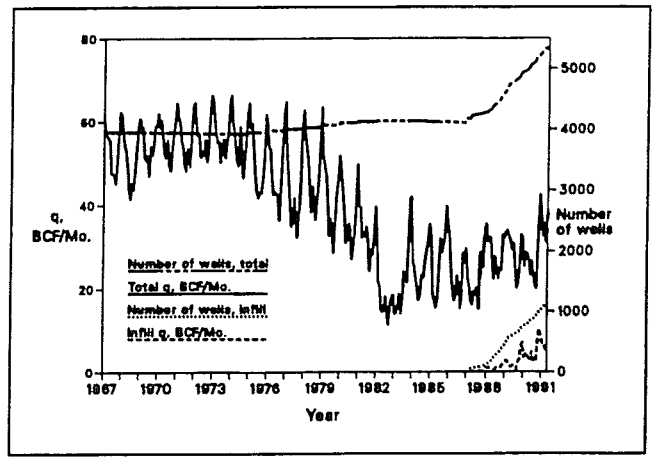

Fig. 9—Historical production and well count for the Kansas Hugoton since 1967.

per Fort Riley are 5, 10, and 20 psia, respectively, while the abandonment pressure for the Lower Fort Riley is 112 psia.

Table 1 also presents the effect of layering on depletion and time to an abandonment rate when there are two wells per section (each well assigned a 320-acre drainage area). The second well is drilled when the layer pressure distribution is identical to that measured in 1977 on the Gano No. A1. The abandonment rate now becomes 20 Mscf/D because there are two wells producing in this section. Both wells are assumed to produce wide open starting in 1977. The remaining time to an abandonment rate of 20 Mscf/D for each layer is reduced by half, while the layer pressure at abandonment does not change compared with the single-well case. The fractional recoveries for the one- and two-well cases are identical at an abandonment rate of 10 Mscf/D per well. The infill well will accelerate production, but the recovery does not change to the same per-well abandonment rate.

Using the method to calculate time to an abandonment rate and layer abandonment pressures, we can conclude for the Kansas Hugoton that a very long producing life can be expected and infill wells produced to the same per-well abandonment rate as the original wells do not add incremental reserves.

Infill Drilling Order

Cities Service Oil & Gas Corp. (now OXY U.S.A.) filed an application with the KCC on July 31, 1984, requesting that an optional well be permitted on each basic proration unit[1] of 640 acres in the Kansas Hugoton. A hearing on the application, in which 110 witnesses testified, began on July 29, 1985, and ended on Dec. 5, 1985.

In April 1986, the KCC amended the proration order for the Kansas Hugoton to permit a second optional well. Starting in 1987, the KCC ordered that the infill drilling be phased in over a 4-year period to avoid a boom/bust race to drill the infill wells. Each operator would be permitted to drill a maximum of one-quarter of its infill locations each year, with any undrilled infill locations carried forward to the next year.

Data Analysis

Infill-Drilling Activity. The infill wells analyzed in this study are the 659 wells that were assigned allowables and listed in the Nov. 1989 monthly Kansas Hugoton field report. Infill drilling in the Kansas Hugoton began in 1987, with 260 wells being spudded in the first year compared with the 1,044 allowed by the KCC. **Fig. 8** compares the actual number of infill wells drilled to the total number of infill wells allowed by year. As of the end of 1989, only 823 infill wells of the 3,132 allowed (26%) had been drilled. The overall infill-drilling activity progressed at a significantly slower pace than was allowed by the KCC.

Fig. 9 presents the Kansas Hugoton monthly production and well count since 1967 for both the infill and original wells. The gas market curtailment is evident in this plot by the rate decline in the early 1980's. The production from the infill wells has not had an appreciable effect on the total production from the field. In fact, the increase in demand for gas from the Kansas Hugoton between 1987 and 1988 had a greater impact on total field production than the infill wells.

Infill Well Initial Wellhead Shut-In Pressures. Fig. 10 presents a cumulative frequency and frequency distribution histogram of the initial shut-in wellhead pressures,

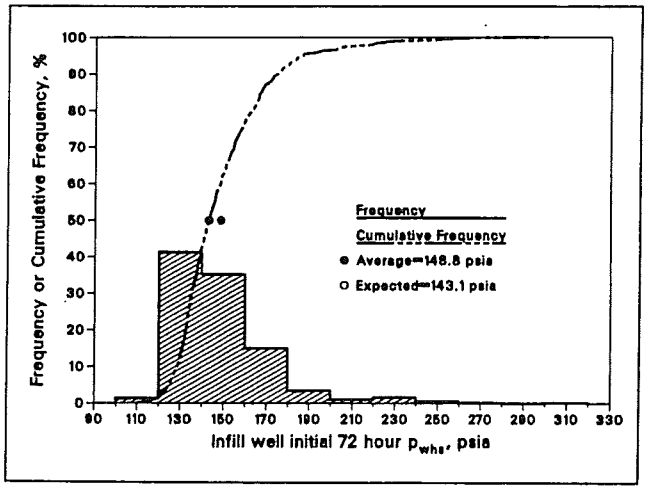

Fig. 10—Infill-well initial wellhead shut-in pressure histogram.

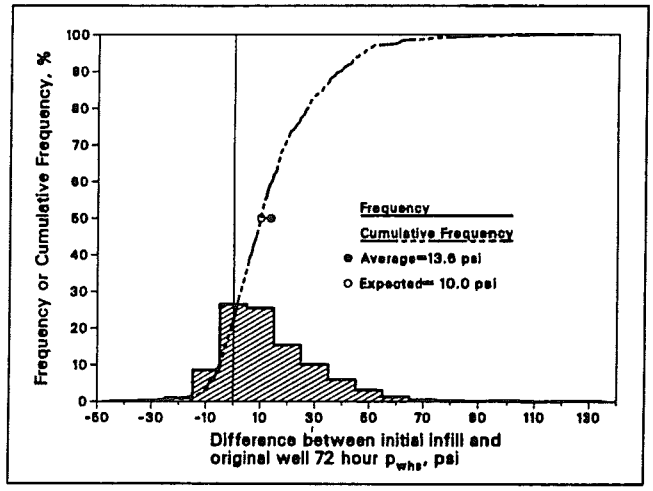

Fig. 11—Histogram of the difference between initial infill and original wellhead shut-in pressures.

"For the Kansas Hugoton, we can conclude that a long producing life can be expected and that infill wells produced to the same abandonment rate as the original wells will not add any incremental reserves."

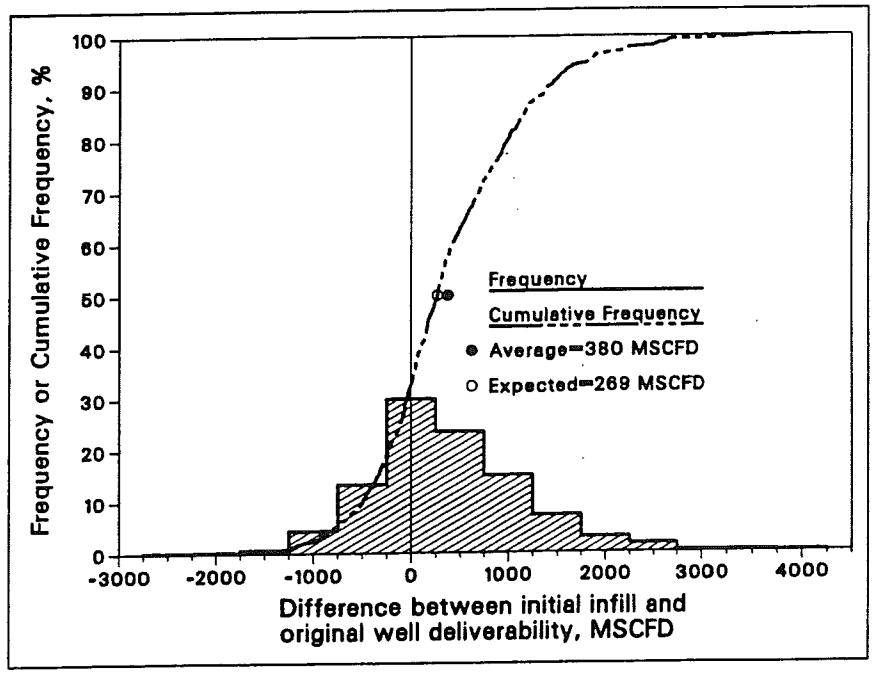

Fig. 12—Histogram of the difference between initial infill- and original-well official deliverability.

p_{iwhs}, encountered by the infill wells between Jan. 1987 and Nov. 1989. The $\bar{p}_{iwhs}$ is 148.8 psia, with an expected value of 143.1 psia. The expected value accounts for skewness in the data. Note the skewness in the upper end of the distribution in Fig. 10. The $\bar{p}_{iwhs}$ of 148.8 psia is significantly lower than the original field discovery pressure of about 450 psia.[1] This average reduction in initial pressure of more than 300 psi in the infill wells drilled in the Kansas Hugoton is evidence that the existing wells have drained gas from the reservoir in the areas of every new infill well.

Infill p_{iwhs} is generally a function of well location and the permeability of the low-pressure layer. The lower pressures are found in the more productive areas of the field and the higher pressures are found on the edges of the field. The fact that no infill well encountered the initial discovery pressure of 450 psia in the Kansas Hugoton indicates lateral continuity of the more permeable productive layers and that the existing wells have drained significant volumes of gas from these layers in the areas of every new infill well.

Difference Between Initial Infill and Original Wellhead Shut-In Pressure. In this section, we compare the difference between the p_{iwhs} of the infill well and the original well p_{whs} or Δp_{iwhs}. The average elapsed time between the initial infill-well official deliverability test and the companion test for the original well was 8½ months. **Fig. 11** presents the cumulative frequency and frequency distribution histogram for Δp_{iwhs}. The average difference is 13.6 psi, with an expected value of 10.0 psi. Almost one-quarter of the infill wells had a p_{iwhs} that was lower than the p_{whs} for the original well, mainly as a result of test time differences. Some of the original wells had been shut in for a significant period of time before their official deliverability tests, while the companion infill wells were being flowed to clean up before their official deliverability tests. This combination of events would cause the p_{iwhs} for the infill well to be lower than the p_{whs} for the companion original well.

Because the p_{whs} typically reflects the pressure of the most permeable layer, the pressure differences are basically a function of the permeability variations in the most permeable layer across the field. Because the p_{iwhs} for the infill wells are much lower than the field discovery pressure, the infill wells must be tapping into the existing drainage area of the original well. For gas to flow within this drainage area to the original well, a pressure drop must exist from the drainage area boundary to the original well.

An infill well drilled anywhere within this drainage area should have a higher p_{iwhs} because of the pressure sink at the original well. Claims have been made that the higher pressures observed in the infill wells compared with those for the original wells indicate that the original wells were not effectively and efficiently draining all the existing gas reserves and that infill drilling has increased ultimate recoverable reserves. The average initial Δp_{whs} of 13.6 psi between the infill and original wells is simply a reflection of the pressure gradient toward the original well in the most permeable layer and reflects no additional GIP found by the infill well.

The fact that in a no-crossflow layered reservoir the 72-hour wellhead shut-in pressure generally reflects the pressure in the low-pressure, high-permeability layer does not diminish its value as a meaningful reservoir parameter. Fetkovich *et al.*[4,15] showed that the 72-hour wellhead shut-in pressure reflects the performance of all layers. The contribution from the other layers is evident in the relationship between the wellhead shut-in pressure and the cumulative production. The 72-hour wellhead shut-in pressures and the cumulative production would be much lower had the other layers not contributed.

Infill-Well Official Deliverability. Initial official deliverabilities observed in the infill wells that were higher than those for the original wells also have been interpreted as a reflection of an increase in GIP. The higher official deliverabilities found in the infill wells, however, cannot be used as a reliable indication that the infill wells are encountering additional GIP. The official deliverability of each well in the Kansas Hugoton is determined by conducting a one-point 72-hour deliverability test. The official deliverability, D, is calculated by

$$D=q[(p_{whs}^2-p_d^2)/(p_{whs}^2-p_w^2)]^{0.85}. \quad \ldots(1)$$

The deliverability standard pressure, p_d, is equal to 70% of $\bar{p}_{whs}$ for all the wells tested in the Kansas Hugoton in the previous year. **Fig. 12** presents the difference in infill- and original-well official deliverabilities used in the determination of well allowables. If the p_{whs} for either the original well or the infill well is less than p_d, then the well has a zero deliverability and is assigned a minimum allowable of 65 Mscf/D. The initial deliverability for the average infill well is 380 Mscf/D higher than for the original well. However, official deliverability is not an accurate measure of the difference between infill- and original-well performance because the field average standard deliverability pressure is involved. For ex-

ample, the initial test for the Wagner 1-2 (infill well), located in Sec. 20 T24S R35W, on April 13, 1988, had a p_{whs} of 93.6 psig and flowed 253 Mscf/D at a flowing pressure, p_{whf}, of 85.4 psig. With the 1987 standard deliverability pressure, p_d, of 102.3 psig, use of Eq. 1 results in an official deliverability of zero for the Wagner 1-2. The official deliverability is simply a measure of relative productive capacities against a standard deliverability pressure and is a number used for assigning allowables. The higher p_{iwhs} at the infill well caused by the pressure sink at the original well becomes a factor in the calculated official deliverability.

We can illustrate the effect of a higher p_{whs} on a calculated official deliverability by using the official test data for a typical infill well as an example. **Fig. 13** is a wellhead backpressure curve for the Nafzinger No. 1 (original well) and the Nafzinger No. 2-2 (infill well) located in Sec. 2 T29S R37W. The initial difference in p_{whs} for these two wells is 16.7 psi, which corresponds to a 92-Mscf/D difference in official deliverability. The official deliverability for each well is marked graphically on the plot: The difference in these official deliverabilities is a result of the 16.7-psi higher p_{iwhs} for the infill well. The Nafzinger No. 2-2 was tested 15 months later on Jan. 10, 1989, with a p_{whs} of 122.9 psig, corresponding to a 16.4-psi wellhead shut-in pressure drop over that period. The average pressure drop for the field during the same period was only 7.4 psi. The subsequent official deliverability calculated from the second test was 288 Mscf/D lower than the first test, while the rate for the second test was only 2 Mscf/D lower than that of the first.

The higher official deliverabilities in the infill wells are generally temporary and are caused by the higher initial wellhead shut-in pressure observed in the infill wells.

A better method to compare well or completion performance between the infill and original wells is to use the AOFP calculation corrected to the 1989 average field p_{whs}. This calculation puts all the wells on the same pressure basis and removes the effect of testing time between original- and infill-well tests. This method presents a better comparison of current well productivities and demonstrates the effectiveness of infill-well completion and stimulation techniques relative to those used on the original wells.

$$q_{AOFP,c}=q[(\bar{p}^2_{whs}-14.4^2)/(p^2_{whs}-p^2_w)]^{0.85}, \quad \ldots\ldots\ldots\ldots\ldots (2)$$

where $q_{AOFP,c}$ is the calculated AOFP at the field $\bar{p}_{whs}$ for 1989 (147.6 psia). With this method, the corrected AOFP for the infill well in Fig. 13 is 1,715 Mscf/D less than the corrected AOFP for the original well. The ratio of the corrected AOFP's for this infill well to that of the original well is about 0.64. This indicates that the stimulation and/or completion procedures for this infill well were not as effective as those of the original well.

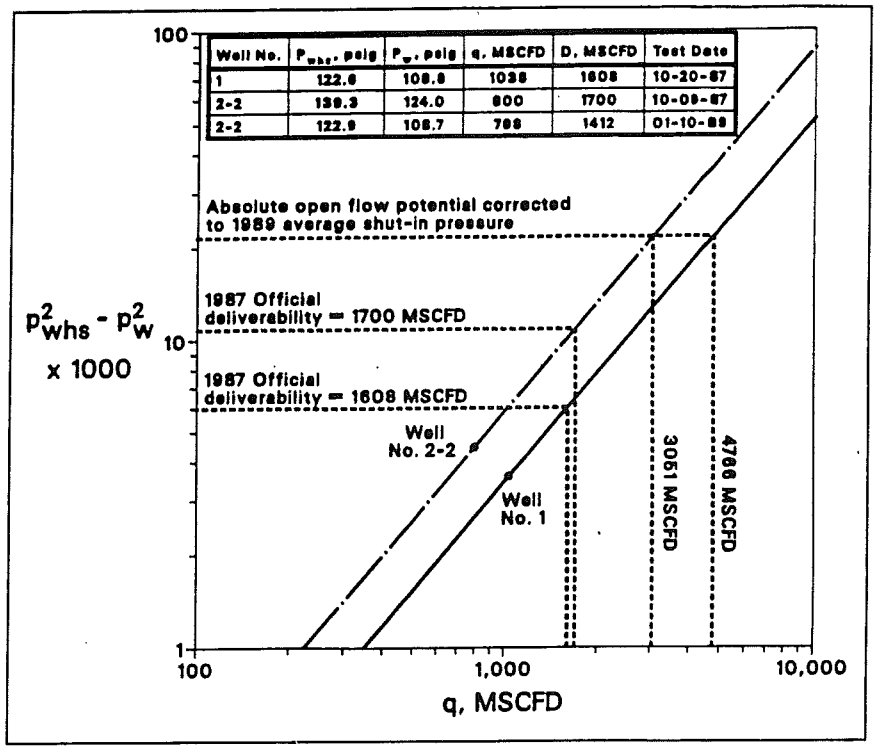

Fig. 13—Wellhead backpressure curve for the Nafzinger No. 1 and No. 2-2.

Corrected AOFP Comparison. The average infill well has a corrected AOFP of 457 Mscf/D less than that of the original well. On average, this indicates poorer stimulation results in the infill wells compared with the original wells. (At the time of the original well stimulation, all layer pressures were equal.) **Fig. 14** compares the corrected AOFP's by use of a ratio of the corrected AOFP's for the infill and original wells. The average ratio is 1.1, with a most probable value of 0.85. This ratio is a direct measure of the difference between the completion performance of a typical infill-well and original-well pair. Fig. 14 indicates that more than 60% of the infill wells have corrected AOFP's that are less than the original well. Because the infill wells were generally stimulated with a water-based treatment, the infill wells may have experienced some degree of cleaning up over time. This possibility was investigated by calculating the ratio of corrected AOFP between the first and second official deliverability tests for the 261 infill wells with more than one test. The average ratio was 1.08 with a most probable ratio of 1.04, indicating an average increase in productivity of 8% between the first and second tests. Although a slight increase in productivity is observed in the infill wells over time because of clean-up effects, this increase has no appreciable effects on the results of this study. Fig. 14 also shows that the performance of some of the infill wells is dramatically better than the companion original well. Investigation of these cases found that either the original well was not properly stimulated or restimulated in the early 1960's or the original well was suffering from mechanical integrity problems. Albeit the calculated official deliverabilities for the infill wells averaged 380 Mscf/D greater than those for the original wells, the corrected AOFP, which represents a better comparison of well performance, averaged 457 Mscf/D less than those of the original wells.

Infill- vs. Original-Well Allowables. Through the beginning of 1989, the presence of the infill well did not add significantly to the volumes of gas allowed to be produced from the infilled proration units. By Nov. 1989, the infill wells accounted for an overall incremental allowable of about 12% from the infilled proration units. Because the infill wells are only allowed to produce a fraction of their capacity, some operators appear to be overproducing their wells, which may accelerate revenue to help defray the cost of the infill well. Once a nonminimum well becomes overproduced by six times its basic monthly allowable, the KCC shuts the well in until the overproduction is worked off. For example, in Jan. 1989, 102 (24.5%) of the 417 infill wells at that time were overproduced to the point where the KCC shut them in, while only 16 (3.8%) of the 417 companion original wells were shut in by the KCC.

Cumulative frequency and frequency distribution plots were generated of the difference between the current allowable for the infilled proration units and the allowable for that proration unit had the infill well never been drilled. Distributions of this difference were generated for each month from May 1987 through Nov. 1989. For the first 11 months of 1989, the average infilled prora-

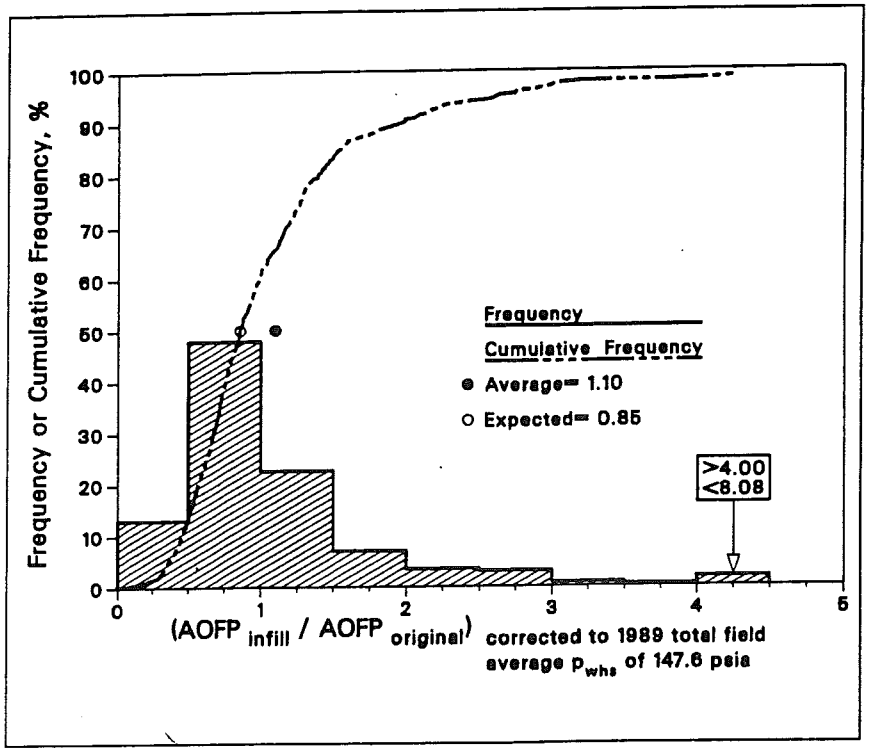

Fig. 14—Histogram of the ratio of corrected AOFP.

tion unit had an increase in allowable of only 36 Mscf/D as a result of the presence of the infill well. For this same period, 35% of the infilled proration units actually lost allowable because of the infill well.

Further information on the performance of the infill wells with respect to the original wells by operator and by county can be found in Ref. 16.

Conclusions

1. An analysis of the Mesa replacement-well program demonstrates that the replacement well and original well are in pressure communication and the pressure difference between each set of original and replacement wells is caused by the pressure gradient in the most permeable layer(s) between the two wells. We found no evidence that the replacement well encountered any gas that was not already being drained by the original well.

2. A simple method can be used to calculate time to an abandonment rate and layer abandonment pressures for a layered, no-crossflow reservoir such as the Kansas Hugoton. These calculations can be made for any number of layers and wells within a drainage area. For the Kansas Hugoton, we can conclude that a long producing life can be expected and that infill wells produced to the same abandonment rate as the original wells will not add any incremental reserves.

3. Our analysis of the infill- and companion original-well performance data in the Kansas Hugoton, showed no evidence that the infill wells found any additional GIP.

4. The infill wells have an average initial wellhead shut-in pressure of 148.8 psia with no infill well encountering the initial discovery pressure of 450 psia. The magnitude of this average reduction in pressure indicates lateral continuity of the more permeable productive layers and that the existing wells have drained significant volumes of gas from these layers in the areas of every new infill well.

5. The average infill well's initial wellhead shut-in pressure is 13.6 psi higher than the average corresponding wellhead shut-in pressure for the original well. This pressure difference does not reflect additional GIP but is a result of the pressure gradient in the most permeable layer(s) toward the original well.

6. The higher initial official deliverabilities found in the infill wells over the original wells cannot be used as an indication that the infill wells are encountering additional GIP. To compare well performance between the infill and corresponding original well better, a calculation may be made of the AOFP corrected to the 1989 field-average shut-in pressure of 147.6 psia. This calculation puts all the wells on the same shut-in-pressure basis. Although the calculated official deliverabilities for the infill wells average 380 Mscf/D greater than that for the original wells, the corrected AOFP's, which represent a better comparison, averaged 476 Mscf/D less than those for the original wells. On average, this indicates poorer stimulation results in the infill wells than in the original wells, possibly because of layer pressure differences.

7. During the first 11 months of 1989, the average infilled proration unit had an increase in allowable of 36 Mscf/D as a result of the presence of the infill well. For the same period, 35% of the infilled proration units actually lost allowable because of the infill well.

8. Through 1989, only 26% of the infill wells allowed by the KCC have been drilled. The overall infill drilling activity has progressed at a significantly slower pace than was permitted by the KCC.

Nomenclature

B_{gi} = gas FVF, scf/res ft^3
D = official deliverability (Eq. 1), Mscf/D
G_i = initial GIP, Bscf
G_p = cumulative gas production, Bscf
G_r = remaining GIP, Bscf
h = thickness, ft
k = effective permeability, md
n = number of layers
p = pressure, psia
$\bar{p}$ = average field shut-in pressure, psia
p_d = deliverability standard pressure, psia
p_w = working wellhead pressure at rate q, psia
q = observed producing rate at end of 72 hours, Mscf/D
$q(t)$ = surface flow rate at time t, Mscf/D
$(q_{gi})_{max}$ = initial surface rate of flow from stabilized curve at p_w=0, Mscf/D
q_a = abandonment flow rate, Mscf/D
$q_{AOFP,c}$ = AOFP at the field $\bar{p}_{whs}$
r_e = external boundary radius, ft
r_w = wellbore radius, ft
s = skin factor, dimensionless
S_w = water saturation, fraction
t_a = time to abandonment rate, years
T = reservoir temperature, °R
z = gas compressibility factor, dimensionless
μ = viscosity, cp
ϕ = porosity, fraction of bulk volume

Subscripts

f = flowing
g = gas
i = initial
n = layer number
s = shut-in
wh = wellhead

Acknowledgments

We thank Phillips Petroleum Co. for permission to publish this paper. We also thank M.L. Fraim for his early efforts on this project. The assistance of J.J. Voelker, C.D. Javine, and S.A. Baughman is also gratefully acknowledged. Special thanks to Kay Patton for outstanding typing of this manuscript.

References

1. Order Docket No. C-164, Kansas Corporation Commission, Topeka (July 18, 1986).

2. Siemers, W.T. and Ahr, W.H.: "Reservoir Facies, Pore Characteristics, and Flow Units—Lower Permian, Chase Group, Guymon-Hugoton Field, Oklahoma," paper SPE 20757 presented at the 1990 SPE Annual Technical Conference and Exhibition, New Orleans, Sept. 23–26.
3. Ebbs, D.J., Works, A.M., and Fetkovich, M.J.: "A Field Case Study of Replacement Well Analysis Guymon-Hugoton Field, Oklahoma," paper SPE 20755 presented at the 1990 SPE Annual Technical Conference and Exhibition, New Orleans, Sept. 23–26.
4. Fetkovich, M.J., Ebbs, D.J., and Voelker, J.J.: "Development of a Multiwell, Multilayer Model To Evaluate Infill Drilling Potential in the Guymon-Hugoton Field," paper SPE 20778 presented at the 1990 SPE Annual Technical Conference and Exhibition, New Orleans, Sept. 23–26.
5. Hemsell, C.C.: "Geology of Hugoton Gas Field of Southwestern Kansas," *AAPG Bulletin* (July 1939) 1054–67.
6. Pippin, L.: "Panhandle Hugoton Field, Texas-Oklahoma-Kansas—The First Fifty Years," Spec. Publication No. 3, Tulsa Geol. Soc., Tulsa (1970) 125–31.
7. Mercier, V.J.: "The Hugoton Gas Area," *Tomorrows Tools Today* (Oct. 1946) 29–32.
8. Le Fever, R.B. and Schaefer, H.: "Productivity of Individual Pay Zones Used For Determining Completion Efficiencies—Hugoton Field, Kansas," *Drill. and Prod. Prac.*, API (1948) 133–47.
9. Keplinger, C.H., Wanemacher, M.M., and Burns, K.R.: "Hugoton—World's Largest Dry-Gas Field is Amazing Development," *Oil & Gas J.* (Jan. 6, 1949) 86–88.
10. Webb, J.C.: "Prefiled Testimony," Docket No. C-164, Kansas Corporation Commission, Topeka (1985) 1–39.
11. Clausing, R.G.: "Prefiled Testimony," Docket No. C-164, Kansas Corporation Commission, Topeka (1985) 1–26.
12. Carnes, L.M. Jr.: "Replacement Well Drilling Results—Hugoton Gas Field," paper presented at the 1979 Kansas U. Heart of America Drilling & Prod. Inst. Meeting, Liberal, KS, Feb. 6–7.
13. Daugherty, M.S.: "Report of Data Collected During Mesa's Five Replacement Well Drilling Program," Mesa Petroleum Co., Amarillo, TX (1977).
14. Fetkovich, M.J., Needham, R.B., and McCoy, T.F.: "Analysis of Kansas Hugoton Infill Drilling, Part II: Twelve Year Performance History of Five Replacement Wells," paper SPE 20779 presented at the 1990 SPE Annual Technical Conference and Exhibition, New Orleans, Sept. 23–26.
15. Fetkovich, M.J. *et al.*: "Depletion Performance of Layered Reservoirs Without Crossflow," *SPEFE* (Sept. 1990) 310–18; *Trans.*, AIME, **289**.
16. McCoy, T.F. *et al.*: "Analysis of Kansas Hugoton Infill Drilling—Part I: Total Field Results," paper SPE 20756 presented at the 1990 SPE Annual Technical Conference and Exhibition, New Orleans, Sept. 23–26.

Appendix—Equation Summary

Rate/time equation:

$$q(t)=\frac{(q_{gi})_{\max}}{\left\{\left[\frac{(q_{gi})_{\max}}{G_i}\right]t+1\right\}^2}. \quad \ldots(A\text{-}1)$$

Rate/time equation for four layers:

$$q(t)=\sum_{n=1}^{4}\frac{(q_{gi})_{\max}}{\left\{\left[\frac{(q_{gi})_{\max}}{G_i}\right]t+1\right\}^2}. \quad \ldots(A\text{-}2)$$

$q_{\max}$ equation, pseudosteady state:

$$(q_{gi})_{\max}=\frac{kh\bar{p}^2}{1424\bar{\mu}\bar{z}T\left[\ln\left(\frac{0.472r_e}{r_w}\right)+s\right]}. \quad \ldots(A\text{-}3)$$

Material-balance equations:

$$G_p/G_i=1-\left(\frac{p/z}{p_i/z_i}\right) \quad \ldots(A\text{-}4)$$

and

$$G_p=\pi r_e^2 B_{gi}\sum_{n=1}^{4}\phi_n(1-S_{wn})\left(\frac{G_p}{G_i}\right)_n. \quad \ldots(A\text{-}5)$$

Time to abandonment rate, q_a:

$$t_a=\frac{\sqrt{\frac{(q_{gi})_{\max}}{q_a}}-1}{\left[\frac{(q_{gi})_{\max}}{G_i}\right]}. \quad \ldots(A\text{-}6)$$

Fractional recovery for each layer at abandonment:

$$(G_p/G_i)_a=1-\frac{1}{\left[\frac{(q_{gi})_{\max}}{G_i}\right]t_a+1}. \quad \ldots(A\text{-}7)$$

SI Metric Conversion Factors

acre	×	4.046 873	E−01	= ha
cp	×	1.0	E−03	= Pa·s
ft	×	3.048*	E−01	= m
ft³	×	2.831 685	E−02	= m³
°R		°R/1.8		= K
gal	×	3.785 412	E−03	= m³
in.	×	2.54*	E+00	= cm
lbm	×	4.535 924	E−01	= kg
md	×	9.869 233	E−04	= μm²
psi	×	6.894 757	E+00	= kPa
sq.mile	×	2.589 988	E+00	= km²

*Conversion factor is exact.

Provenance

Original SPE Manuscript, **Analysis of Kansas Hugoton Infill Drilling: Part II—12-Year Performance History of Five Replacement Wells** received for review Sept. 2, 1990. Revised manuscript received Aug. 30, 1991. Paper accepted for publication Jan. 17, 1992. Paper (SPE 20779) first presented at the 1990 SPE Annual Technical Conference and Exhibition held in New Orleans, Sept. 23–26.

JPT

Authors


McCoy


Fetkovich


Needham


Reese

Thomas F. McCoy is a reservoir engineer at Phillips Petroleum Co. in Bartlesville, OK. His interests include transient well testing, horizontal wells, and rate/time analysis. He holds BS and MS degrees in petroleum engineering from the U. of Tulsa. M.J. Fetkovich is staff director and senior principal reservoir engineer for the Drilling & Production Div. of Phillips Petroleum Co. Fetkovich joined Phillips as a gas well-test engineer in the Texas/Oklahoma panhandles. He became a gas reservoir engineer in Bartlesville in 1957 and reservoir engineering and gas technology specialist in the Computing Dept. 6 years later. Fetkovich joined the E&P Dept. in 1974. He holds a BS degree in petroleum and natural gas engineering from the U. of Pittsburgh and a Dr.Ing. degree in petroleum engineering from the Norwegian Inst. of Technology. A recipient of the 1989 Reservoir Engineering Award, Fetkovich is a member of the 1991–92 Forum Series Committee and a Technical Program Committee for the 1992 Annual Meeting. He was a 1977–78 Distinguished Lecturer. Riley B. Needham is manager of production technology in the E&P Group of Phillips Petroleum Co., responsible for research and service work in oil recovery processes, well completions, reservoir fundamentals and simulation, well stimulation practices, and drilling fluids. He holds BS and PhD degrees in petroleum engineering from the U. of Oklahoma. A 1988–91 SPE Director, Needham has served on the Reprint Series and Engineering Manpower committees and on technical program committees for the 1979 and 1990 Annual Meetings. He was a 1985–86 Distinguished Lecturer and 1973–74 Bartlesville Section chairman. Dave E. Reese is a senior reservoir engineering specialist at Phillips Petroleum Co. His interests are gas reservoir engineering and rate/time analysis. He holds a BS degree in petroleum engineering and an MS degree in petroleum management from the U. of Kansas.

Wilcox Formation Evaluation: Improved Procedures for Tight-Gas-Sand Evaluation

D.J. Lewis, SPE, and **J.D. Perrin,** SPE, BP Exploration Inc.

Summary. Risks in tight-gas-sand evaluation are reduced by defining relationships between pore geometry and critical water saturations. These results are integrated with log interpretation to derive an estimated *kh* that compares favorably with a true *kh* from production tests. These procedures are potentially applicable for evaluating other complex reservoirs.

Introduction

Tight gas sands, such as those common in the Lower Wilcox formation of Texas, are routinely difficult to identify accurately as candidates for testing, completion, or abandonment. Several factors contribute to this difficulty.

1. Porosity and permeability are controlled by complex and variable diagenesis that leads to a poor correlation between porosity and permeability.
2. A dual-porosity system is present, where depositional and diagenetic clays, along with grain and cement dissolution, create isolated macro- and micropores that do not contribute to flow.
3. Pore-lining clays are present and variable, and although they can preserve porosity and permeability by limiting quartz overgrowths, they also can completely fill pore throats. Clay types and their positions within the pore structure are not quantifiable from log responses.
4. Critical water saturation is difficult to establish because the heterogeneity of rock types causes extreme variability in critical water saturations. This leads to some productive rock types having water saturations approximately equal to other rock types that are at residual gas saturation.
5. Wilcox formation water resistivity, R_w, frequently varies from zone to zone and is difficult to determine petrophysically, especially in wells with oil-based mud. Obtaining R_w from porosity logs is difficult because a 100% wet zone is seldom available for the calculation.
6. Completions are difficult and variable because the pore system is fragile and easily damaged by drilling and completion fluids.

Producing Behavior, Theory, and Definitions

Wilcox formation gas production is controlled primarily by the pore geometry and the amount of water present. This production behavior assumes no retrograde condensate dropout in the reservoir and is characterized by two main factors: increasing water saturation significantly decreases effective permeability and relative permeability behavior changes as a function of pore geometry.

Relative permeability behavior changes with the amount of water present in the producing pores. Multiple types of pore geometries can isolate water from main flow paths and reduce the amount of water available to flow.

Understanding the differences between laboratory-measured unstressed and stressed air permeabilities and the actual effective permeability of a reservoir fluid is key to distinguishing nonproductive from productive intervals. In tight-gas-sand formations, permeability must be measured at in-situ conditions, including elevated confining pressure, pore pressure, and water saturation.[1-4]

We define absolute permeability, k_K, as the gas permeability, k_g, of the dry rock ($S_{we}=0$) at in-situ effective stress conditions (overburden minus pore pressure). Effective permeability is the k_g at in-situ conditions. Relative permeability is the ratio of effective to absolute permeability.

Methodology

A comprehensive approach that addressed complex formation characteristics was required to improve evaluation of tight gas sands. To develop the procedures, we established commercial criteria, measured core properties, measured pore geometry from core and cuttings, developed a k_a estimator from pore geometry and a k_K estimator from k_a, defined k_g/k_K type curves, and developed a type-curve estimator from pore geometry.

First, we developed commercial production criteria by examining well production characteristics. The criteria were calculated from pressure buildup data and four-point production tests that provided the minimum *kh* required for both successful nonstimulated and stimulated completions.[5] Second, rock properties were measured from core plugs. We measured unstressed and stressed dry porosity and permeability, as well as mercury-injection capillary pressure and drainage non-steady-state pulse-decay permeability. We took thin-sections from each plug and used image analysis to collect pore geometry and compositional characteristics.

SPE 24872

The Rejuvenation of the 30-Year-Old McAllen Ranch Field: An Application of Cross-Functional Team Management

A.J. Durrani,* B.M. Escovedo,* and Bill Ordemann,* Shell Western E&P Inc.; J.A. Bickley, Shell Oil Co.; and B.J. Tepper* and J.M. Simon,* Shell Western E&P Inc.

*SPE Members

This paper was prepared for presentation at the 67th Annual Technical Conference and Exhibition of the Society of Petroleum Engineers held in Washington, DC, October 4–7, 1992.

ABSTRACT

This case history overview paper describes the process of managing redevelopment of the 30-year old geopressured McAllen Ranch gas field in South Texas by a cross-functional team made up of Petroleum Engineers (reservoir, production, drilling, petrophysical, geological, facilities), Exploration Geophysicists and Geologists, Field Operations personnel, and staff from Land, Permitting, Business/Regulatory Affairs, Tax, and Legal Departments.

Faced with declining production with over 40 percent of the reserves non-contributing and behind pipe, the concept of cross-functional team management was applied in promoting multi-disciplinary cooperation and synergism, and focusing on a common team goal rather than separate objectives for each specialty. The common goal was simply to increase gas production (and associated profitability) from existing and new reserves. Innovation was encouraged by empowering individual decision-making and reducing routine supervision.

INTRODUCTION

By the mid-eighties, McAllen Ranch field gas production had declined to a low of 24 MMcf/D due to reservoir depletion and curtailment. The end of curtailment and subsequent development drilling activity increased the rate up to 80 MMcf/D by early 1988. However, with reduced drilling and natural decline, the rate had fallen again to about 50 MMcf/D by early 1989.

At this time, a cross-functional team was established to evaluate additional investment opportunity and develop a plan to increase production from the non-contributing reserves which were behind pipe. This team looked at all aspects of the field's production and developed a consensus plan which included acquisition, processing and interpretation of a fine grid 3-D seismic survey, development drilling focused in the northern portion of the field (B-area), procedures to obtain regulatory approval to commingle non-contributing reserves in existing wellbores, and enhanced drilling and completion techniques.

This paper describes the interaction and synergism between the various specialties and functions involved in the producing operations at McAllen Ranch, and how the concept of cross-functional team management has led to the rejuvenation of this 30-year old field. It focuses on the process of cross-functional team management rather than just the results achieved.

BACKGROUND

The McAllen Ranch Field, located in Hidalgo County in South Texas, is operated by Shell Western E&P Inc. (SWEPI) on behalf of itself and its working interest partners Fina Oil and Chemical Company and Conoco Inc. Geographical location is shown on Figure 1.

Regional Geologic Setting

The field is located in the expanded Oligocene aged Vicksburg productive trend which covers 4,200 square miles, extending 140 miles northeast from south of the Mexico/Texas border to just west of Corpus Christi Bay. The trend averages 30 miles in width.

Structurally, many of the Vicksburg fields in this area are associated with rollover anticlines which developed as a result

References and illustrations at end of paper.

of the lateral translation of the expanded Vicksburg along a decollement surface located on top of the Eocene age, Jackson Shale. Movement of these sediments has been as much as 20 miles from their point of deposition at the head of the main Vicksburg flexure. Stratigraphically, the primary productive intervals, which were deposited at a sea level high stand, are comprised of alternating coarsening upward deltaic sands and shallow marine shales. Overall, these sand and shale packages are wedge shaped with the thickest and most sand rich portion located at the detachment surface. Typically these wedges then thin and shale out in a basinward direction.

Developmental History

The McAllen Ranch Field, discovered in 1960, is comprised of stacked, deep (14,000 ft.), geopressured, tight (less than .1 md), condensate rich, gas reservoirs with porosities ranging from 12-20 percent. Due to the relatively tight nature of the pay sands, massive hydraulic fracturing is required to sustain commercial production. Gas production in this field peaked in the late 1960's at almost 150 MMcf/D but by 1984 had declined to 24 MMcf/D due to reservoir depletion and curtailment. A field study was conducted in 1985 which identified new well locations (without seismic) and recompletion opportunities.

In 1987, a program was initiated to develop these opportunities. As implementation of this program began, recently acquired 2-D seismic data was incorporated into the existing interpretation. This work combined with revised log correlations indicated an area of significant potential in the northern part of the field (B-area). Subsequently, in 1988, the McAllen Ranch B-16 well was drilled which confirmed this new interpretation. At this point, further development in this structurally complex area was deferred in order to acquire the first ever fine grid Vicksburg 3-D seismic data set across this area. With the deferment of drilling, it became evident that without additional development and/or contribution from behind pipe reserves, the field production would show a steep decline.

CONCEPT OF CROSS-FUNCTIONAL TEAM MANAGEMENT AND DEVELOPMENT OF McALLEN RANCH ASSET MANAGEMENT TEAM

At the initiation of the McAllen Ranch Field cross-functional team effort in early 1989, the Engineering Group of the Production Department was organized along specialty lines, similar to many other major oil and gas upstream organizations. The specialties within the Engineering Group were Drilling, Facilities, Geological, Petrophysical, Production and Reservoir Engineering.

A group of engineers of similar discipline (e.g., drilling engineers) formed a section and reported to a Division Engineer. The various Division Engineers did not always report to the same manager and each had his/her own specific goals and targets. For example, the targets for Reservoir Engineering might have been reserve additions while Production Engineering might have concentrated on production increase via Recompletion & Reconditioning (R&R), and Drilling Engineering on reduced trouble cost. Given the silo nature of the various specialties and the sometimes incompatible goals, the prioritization required to focus on a specific target was difficult to achieve and the results were poor.

Efforts had been made in the past at multi-disciplinary teams by putting together a team of various engineering disciplines under one supervisor (Division Engineer). This concept, although focusing a group on compatible targets, did not provide the overall technical depth required in complex projects since the supervisor may not have had in depth exposure to all the specialties who reported to him. For example, the Division Engineer may have had only a reservoir engineering background and was supervising a geological engineer in a field with complex stratigraphy and structural features. Furthermore, these multi-disciplinary teams were generally limited to engineering specialties and did not include staff from non-engineering functions. Many of these non-engineering functions like Exploration, Operations, etc., are an integral part of the field's ongoing performance. While most of the functions were well integrated vertically, there was little horizontal communication existing between functions.

This lack to cohesion led to the realization that the application of cross-functional team management was critical to the rejuvenation of McAllen Ranch Field.

Asset Management Teams

The concept of cross-functional team management was that staff assigned to a specific field team would be from all functions involved in the operation of the field (i.e., all appropriate specialties of Engineering, Exploration, Operations, Business and Regulatory Affairs, Land, Permitting, Tax, Legal, etc.), and would have compatible and consistent targets. Furthermore, each member of the team would remain in his/her own specialty and thus have the technical backup and review available from his/her peers and supervisor but would not be directed towards "provincial" goals and targets.

Such cross-functional teams were formed for several major South Texas fields and are referred to as Asset Management Teams (originally Surveillance Teams). The specialties and functions that were represented on the asset management team were determined based on the primary activities of a specific field. Not all specialties or functions were required on all teams, and furthermore, the team membership expanded and contracted based on the priority and activity on which the members were focused.

A Management Steering Committee was set up to overview the progress of these teams, and was made up of the Engineering Manager(s), Division Engineers and Operations management (Production Superintendent). Prior to the kick-off of a team, there was a "Field Management Strategy Session" (FMSS) to outline the team's targets and goals including both short-term and long-term plans for the field. "Buy in" by the team and management steering committee members was essential so that there was consensus on the plans for the field and efforts were focused on common goals. A FMSS is held on an annual basis to review the team's efforts and calibrate the goals/targets with actual results. A Field Data Book containing salient facts, targets/goals and work plans was developed for each field and made available to each team member irrespective of specialty or function.

The various specialties (individuals on the team) were empowered to make collective consensus decisions for the team regarding the asset (field). Supervisors (Division Engineers) were encouraged to minimize individual technical reviews in favor of joint review with other specialty supervisors. In this way, individuals could discuss their technical findings and evaluations with their team members without waiting to get their supervisor's approval of their technical conclusions. In the cross-functional team concept, the supervisors of the dividual team members were less of a "boss" and more of an "advisor/nurturer".

To facilitate the efforts of the various asset management teams, an Asset Management Coordinator was selected to advise the teams on the general framework of cross-functional management and to schedule periodic reviews. These periodic reviews were an integral and important part of cross-functional management, and ensured that all members of the team were involved in decision-making and were contributing towards the overall goals. Depending upon the nature of the team's activity, there were 3-4 full team reviews including at least one team review at the field office with participation of key field staff, including lease operators. The team members were encouraged to hold informal update sessions as frequently as needed. Additionally, a Computer Coordinator was identified to assist the team members in computer utilization and technology transfer between the asset teams.

Management Involvement

Significant management involvement and support in many areas was critical if the desired results were to be achieved in a timely manner. The following areas were some of the most important:

- Ensuring appropriate dedication of resources.
- Developing clear goals and focusing staff efforts on their attainment.
- Striving for multi-disciplinary and cross-functional cooperation, and maintaining effective communication at all levels.
- Encouraging innovative thinking and supporting appropriate "risk taking".

The overall effort required a significant dedication of resources including staff, technical tools and funding. Well trained, highly motivated individuals were assigned to the major fields including a mix of those experienced and essentially inexperienced in the areas. The experienced individuals served as coaches and trainers while those that were less experienced approached the work from an unbiased perspective and contributed many new ideas.

These individuals were all provided with state-of-the-art technical tools (personal computers, advanced technical software, access to research, etc.). They were also informed early on that Management would secure necessary funding provided that the opportunities they generated were economically attractive. No strict "budget" was established so that perceived restrictions would not inhibit the identification and development of profitable opportunities.

Staff assigned to the field were given a clear goal, to increase near-term production in a cost-effective manner, and Management assisted them in focusing their efforts on its attainment whenever possible. In addition, they were assisted in establishing priorities on an ongoing basis and then allowed to proceed with minimal supervision. Frequent informal communication and clarification of priorities was then used to ensure that the staff was appropriately empowered but not abandoned.

Management support was also critical in ensuring multi-disciplinary cooperation and maintaining open, informal lines of communication between all those involved in the effort. This required work to prevent "barriers" from forming between groups (example - engineering versus non-engineering) and ensure common goals were developed and maintained.

Finally, the development of an atmosphere where Management encouraged innovative thinking and supported appropriate "risk taking" was an extremely important factor in ensuring that new ideas were brought forward without apprehension of failure.

McAllen Ranch Asset Management Team

In the developing the membership framework of the McAllen Ranch Asset Management Team, we evaluated the major focus of the field activities. These included :

- 3-D seismic survey acquisition and interpretation
- Development drilling
- Commingling (including regulatory approval)
- Field producing operations and remedial well work

To incorporate seismic information from the 3-D survey in overall field activities, a geophysicist was made a member of the team. Due to a high level of anticipated drilling activity, a drilling engineer, a drilling rig foreman, a geological engineer, a petrophysical engineer, a permitting staff member and a landman were also included. The commingling effort and level of anticipated remedial well work required the addition of a reservoir engineer and production engineer. An operations foreman and a facilities engineer were also included to ensure the development and commingling activities would be integrated smoothly into existing field operations. Since the approval of the Texas Railroad Commission was required to commingle the various productive intervals, a regulatory staff member was added. Gas production from various parts of the McAllen Ranch field is qualified for Section 29 Federal Tight Gas Sand Tax Credit and so a tax department staff member and an attorney were also designated as team members. A Team Leader was chosen from the amongst the members of the team.

McAllen Team Goals

'h the challenge of a declining production rate and low wellbore utilization (40 percent of the developed reserves were behind pipe), the following goals for the McAllen Ranch Team were identified :

- Develop a technique to allow accelerated production of existing reserves.
- Add reserves profitably.
- Incorporate 3-D seismic into the planned drilling program.
- Identify potential for commingling similar pay sands and obtain regulatory approval to commingle them.

These became the goals of the team. Team members were encouraged to concentrate on these overall goals rather than on those segments which were specifically applicable to their specialty or function.

McAllen Team Targets

Given the broad but field-specific goals outlined above, the team members came up with the following specific targets to be accomplished within two years (1990-1991):

- Increase total field gas production rate above 100 MMcf/D.
- Reduce non-contributing behind pipe reserves by 50 percent.
- Complete 3-D seismic interpretation and mapping, and identify at least 10 new drilling locations.
- Reduce drilling costs by at least 10 percent.
- Commingle production from all S, T, and U sands in the B-area.

3-D SEISMIC SURVEY - PLANNING AND APPLICATION

Objectives of 3-D Survey

The geological engineer along with the reservoir and petrophysical engineers consulted with the Exploration geophysicist and developed the objectives of acquiring a 3-D survey over the B-area. Two objectives of the 3-D acquisition program were identified. Our first objective was to improve the success rate by "sharp shooting" well locations in this structurally complex area using higher resolution data than existing 2-D seismic could provide. Early in the program it had been determined that accurate identification and location of faults, including those with less than 100 feet of throw, was critical to a successful drilling program. The second objective was to expand our knowledge of the structural evolution and trapping mechanisms associated with these very complex Vicksburg reservoirs.

Acquisition Parameters

Acquired in 1988 over the northern half of McAllen Ranch Field where well control was sparse and the potential considered largest, the survey was designed to image a 22 square mile area with 45-fold multiplicity. To accomplish this, source and receiver lines were run perpendicular to each other on 1200-foot spacing resulting in acquisition of data points every 75 feet. During the acquisition of the survey and the subsequent processing phase, there was close coordination between the seismic crew, the geophysicist, and the geological engineer.

Interpretation and Application

The quality of the 3-D migrated data exceeded expectations and showed a dramatic improvement over even the modern 100-fold 2-D seismic data.[1] Additionally, the 3-D survey confirmed that the area contained numerous small faults not previously identified. Since the pay sands are not massive, but are comprised of multiple stacked pays generally less than 100' in thickness (See Figure 2), even relatively small faults (displacements of under 100 ft) could potentially cut out key productive intervals. Consequently, every well location selected to date in the B-area, since the 3-D survey was acquired, has been the result of a rigorous evaluation by a team comprised of a geophysicist, geological engineer, petrophysical engineer, and reservoir engineer. Validation of the data quality and this team approach is evidenced by the 93 percent (14 of

15) success rate for wells drilled in association with this survey. The one dry hole drilled to date was considered to be a high risk delineation well.

DRILLING OPERATIONS

Daily communication between Geological, Petrophysical, Construction, Reservoir, and Production Engineering was maintained during the entire drilling program. The need for this communication was essential to maintain a continuous drilling program while planning and drilling these complex wells in a relatively short duration of time.

For well planning, the geological engineer was asked not only to provide anticipated formation tops and thicknesses for the objective formations but also tops and thicknesses for formations (usually shale) needed to plan intermediate casing points as well.

Petrophysical and Reservoir Engineering provided a significant aspect of new well planning in predicting pore pressure and fracture gradients so mud weight and casing programs could be optimized. Objective intervals are typically highly geopressured requiring 16-18 ppg muds. However, due to the geologic complexity of the field and the various stages of depletion of some reservoirs, pore pressure reversals and/or substantially depleted intervals are sometimes encountered. Proper placement of the protective casing to achieve a sufficient fracture gradient is critical for minimizing drilling trouble costs, and eliminating the use of protective liners. In this regard, pore pressure and fracture gradient plots were made for all new wells as part of the planning process to determine the optimum mud and casing program. Input from geological engineers and the drilling staff was essential to determine the most appropriate analog for a given well and to obtain actual mudweight and leakoff data which were incorporated in the analysis.

Prespud meetings were held on location between engineering and field personnel (both Shell and outside contractors involved). Ideas and comments from all individuals were actively solicited at these meeting.

Production Engineering involvement was required for each well design. Their input was also needed immediately after the production logging run to provide the drilling rig with their production casing string requirements (i.e., centralizer and flag joint placement, etc.). Communication of the decision of whether or not to make a completion in a timely manner was necessary to eliminate any rig downtime.

Close communication between the drilling engineers and the drilling foreman helped to spawn the redesign of the 8.5-in. PDC bits used during the program.. The steel body PDC bit which had been run in this area doubled the penetration rate of previous bits, but did not have the bit life needed to drill over 100 hours in this harsh environment. The need for a new bit design was passed to the bit manufacturer's engineering staff, who in turn produced a matrix body bit design to specifically meet our requirement. This new bit design not only met our requirement of drilling the entire interval with a single bit, it also doubled the penetration rate of the steel body PDC bit. Additionally, the first bit ever run (which was designated as experimental) drilled the entire 8.5-in. interval in the next three wells. This bit design set a then world record of 19,066 ft for the most footage drilled by a single 8.5-in. bit.

The initial 14 wells drilled in the B-area required an average of 66 days to drill. The 15 redevelopment wells were drilled in an average of only 32 days (50+ percent improvement). Figure 3 shows the time required to drill and case each well. One of the wells drilled during this redevelopment program reached a depth of 14,450 ft in less than 17 days . (This is believed to be the fastest onshore geopressured well ever drilled to this depth.)[2] Teamwork was a key ingredient of this enhancement in drilling performance which has resulted in savings of over $7 million in total drilling costs.

SUBSURFACE ENGINEERING STUDIES

As part of the team effort, subsurface (geological, reservoir and petrophysical) engineers have contributed to the rejuvenation of McAllen Ranch field by completing a number of geologic/reservoir studies to better define reserve potential, optimize well placement and assess recompletion potential . A significant component of these studies was the process of integrating log evaluations for all wells in a reservoir with production information, the geologic setting, and the state of reservoir depletion. This was an iterative process requiring substantial input from the geological, production and petrophysical engineers. Vital to the process was obtaining accurate production data for each zone in a reservoir, knowledge of the prior completion and stimulation techniques used on a given zone, and knowledge of reservoir drive mechanism and reservoir pressure at the time of completion. The process of reconciling log evaluation results with production data, given knowledge of the completion techniques used and their effectiveness, often revealed opportunities for recompletions in existing wells or drilling new infill wells. In addition, log data quality problems which were previously overlooked and which affect the reservoir model were identified and corrected.

Log Evaluation Uncertainty

A key goal since early 1988 has been to reduce uncertainty in log evaluation results in order to improve reservoir characterization and optimize well completions. Uncertainties in wire-

ine log evaluations in the McAllen Ranch Field primarily result from: highly variable and relatively low formation water salinity (typically less than 20,000 ppm NaCl); difficulties in obtaining representative formation water samples and determining formation water resistivity through log techniques; low permeability reservoirs which result in pay zones having high irreducible water saturations and relatively low resistivity contrasts; different vintage wireline logs and difficult logging conditions which have resulted in an inconsistent log data set with common log quality problems; and poorly defined rock properties for a diagentically complex rock.

Minimizing uncertainties in log evaluation results has been accomplished by improving databases of formation water and key rock property information, and by reducing systematic errors in wireline measurements that have occurred due to the severe logging environment and inadequacies of earlier vintage logs run. With the help of field operations personnel, a widespread water sampling program was undertaken throughout the field to improve the database of produced water properties. Care was taken to only sample wells that produce in sufficient quantities such that contamination from condensation water would be minimal. A research program was also initiated to study the geochemistry of the produced water. With the help of drilling operations, a coring program was undertaken to improve the understanding of key log evaluation parameters and rock properties. Core was obtained in a number of wells having representative reservoir intervals. Systematic errors in log data were often identified by making detailed comparison with other wells in a reservoir and by reconciling log evaluation results with production information.

CONCEPT OF COMMINGLING AND REGULATORY APPROVAL

In 1989, faced with gas prices that were continually declining, engineering and management began reviewing ways to improve the overall profitability of the McAllen Ranch drilling program in order to continue to maximize the return on our investment. In addition to reviewing drilling and completion operating practices to minimize costs, the team reviewed ways to accelerate production by getting contributions from behind pipe reserves and to improve ultimate recovery. In the B-area, historical practice had been to complete each of the three sands, S, T, and U, sequentially beginning from the bottom sand (U) and working upward in the wellbore after each individual sand was depleted.

The historical mindset associated with this sequential completion philosophy was that, by completing each sand individually, future operational risks/costs were minimized. This included primarily the capability to refracture treat an interval without considerable expense or risk of losing the wellbore after it had produced for a sufficient enough period that its fracture had deteriorated. Furthermore, by completing each sand individually, reservoir information, such as pressure transient data, could still be obtained and evaluated without the uncertainty associated with multiple interval testing.

After considerable review by the McAllen team, several drawbacks to this philosophy were identified. Referring to the log in Figure 2, although the S, T, and U sands exhibit similar reservoir properties (permeability, pressure, saturations, fluid characteristics), the S sand typically has the highest pay count, usually on the order of 3-4 times as great as the T or U. Unfortunately, the S sand is also the shallowest interval and thus in a sequential completion would be the last to be opened up for production, up to 20 years after the well was drilled (see top portion of Figure 4).

The first drawback of this philosophy is that because the S sand is produced last in the sequence, any present value associated with its reserves is virtually destroyed. This obviously depends on any given price forecast, of course, but our team felt that the price risk associated with forecasts being correct are as high as any other operational considerations. Secondly, the wellbores in McAllen Ranch have been found to have a finite life of somewhere between 20 and 30 years. Major wellbore integrity problems, such as casing damage, occur frequently after 20 years of production. Over 60 percent of wells greater than 20 years old experience at least some degree of casing damage with resultant loss of reserves in a majority of these wells. The cause of these failures are unknown; however, it has been speculated that they may occur due to reservoir compaction. Figure 4 illustrates the "reserves at risk" associated with producing the sands sequentially versus simultaneously. Historically, only about 33 percent of the reserves would be recovered after 20 years with sequential completions leaving the majority of the reserves remaining behind pipe and "at risk" after the 20 year period.

It was at this point (actually at the first McAllen Ranch Field Management Strategy Sessions) that the idea of commingling (versus sequential) completions of the S, T, and U sands was considered. The pros and cons of this philosophy were carefully reviewed. Upon review, the major drawbacks identified included the operational and mechanical aspects of multiple fracture treatments in a single wellbore, the integrity of the fracture treatments over time, and the decreased capability to monitor depletion/fracture integrity in individual sands via pressure transient analysis. The first problem (multiple fractures in a single wellbore) was an operational problem and is addressed elsewhere in this paper. The second and third problems are somewhat related and were the subject of considerable discussion.

Fracture design at McAllen Ranch has advanced considerably over the past ten years including the increased use of higher

trength proppants to preserve fracture integrity over a wider range of stresses. We found that the largest share of refracture treatments were being performed on wells that had been previously treated with sand as a proppant and not the higher strength proppants. In addition, the majority of our pressure transient work on individual sands was being completed in order to evaluate fracture integrity of these sand treatments. Therefore, with the use of higher strength proppants, we concluded that the risk of having to refracture treat was minimized and thus diagnosis of individual treatments would no longer be as frequent. Thus, even though a commingled completion would increase the uncertainty in evaluating fracture integrity via pressure transient analysis, with better fracture design, the need for this type of diagnostic information was minimized.

As the evaluation progressed, it soon became quite obvious the benefits of commingled completions would far outweigh any drawbacks. The first benefit identified was increased ultimate recovery per well. With commingled completions, ultimate recovery is increased/maximized in three ways. Given a constant per well rate as an economic limit, commingled completions provide an improvement via lower abandonment pressures in each individual sand. This improvement is estimated to average 175 MMcf and 17,500 barrels of condensate per well in the B-area. Secondly, with declining as prices, we were faced with completing new wells only in the better S sand in order to meet our return on investment requirements and thus forego recovering any reserves in the marginal T and U sands. The volumes in these lower sands would not be sufficient to justify attempting any downhole recompletion work in the future. Finally, ultimate recovery is maximized by commingling because risk of losing the wellbore after 20 years is minimized considerably. Although difficult to quantify when a wellbore will be lost, it is obvious there are ultimate recovery benefits to getting the maximum amount of production prior to hitting the 20 year mark. This is illustrated in the lower part of Figure 4 where 85 percent of reserves are recovered via commingling as compared with 33 percent in the sequential case. The sequential versus commingled completion techniques are schematically shown in Figure 5.

Aside from ultimate recovery benefits, commingling zones has a substantial effect on the overall return on investment for the wells. These wells went from being marginally profitable or unprofitable with sequential completions to providing an acceptable rate of return with commingled completions. Several McAllen Ranch wells would not have been drilled had we not considered commingling.

Prior to implementing the commingled completion practice, evidence had to be presented before the Texas Railroad mmission in order to get permission to commingle the three ntervals. During the hearing before the Commission on February 23, 1990, we introduced most of the arguments presented above as justification for consolidating the fields. In addition, we presented evidence that crossflow between zones would be minimal due to similar reservoir characteristics and fluid properties. The Commission approved the S, T, U sands field consolidation on March 20, 1990.

COMPLETION AND REMEDIAL WELL WORK

Once regulatory approval was obtained to commingle production from major reservoirs in the B-area, the engineers in the team immediately initiated the work required to move from concept to reality. Efforts were initially concentrated on new wells, which offered the highest potential production increases and associated economic benefits; however, while this work was ongoing, production, reservoir and petrophysical engineers, and Operations field staff worked closely to prioritize remedial opportunities on the remaining wells in the field. These opportunities included both further commingling and conventional remedial work. Facilities engineers remained closely involved during this entire process to ensure adequate surface facilities were in place to handle the substantial production increase realized.

The Asset Management Team concept discussed previously assisted a great deal in maintaining cross-functional cooperation and communication between most groups; however, further work was required in Production Engineering to ensure effective relationships with those groups such as research and outside companies (contractors) who were not "officially" represented on the team. Subsequently, coordinator roles were developed to attempt to eliminate and prevent any "barriers" in these relationships. Since the majority of our South Texas activities were very similar, these individuals supported both the McAllen Ranch effort and activity in other areas. Roles were established to support hydraulic fracturing, including interactions with Research and service companies, and several other major areas including wellhead equipment, electric wireline operations and downhole production equipment. The individuals assigned to these roles served as a clearinghouse and distributed new information to other engineers, coordinated resolution of problems and assisted Purchasing Department in preparing bids and negotiating contracts in their assigned areas. They improved communication with their "contacts" and made the relationships more "efficient" so more Engineering time could be dedicated to profitable well work.

Maintaining an environment that encouraged innovative thinking and supported appropriate "risk taking" was very important. During the past two years, many changes have been made or evaluated in virtually every aspect of Production Engineering activity. The most significant of these changes were in hydraulic fracturing designs where new technical tools supplied by our research organization (geometry models, design

vare, fluids testing, etc.) allowed us to significantly reduce treatment complexity and cost. For example, our design model no longer incorporates the concept that fluid viscosity plays a significant role in creating fracture geometry. This has allowed us to eliminate additives such as methanol and other gel stabilizers, substantially reduce gel loadings and eliminate cross-linker in pad fluids. These and other advancements in this area have allowed us to reduce fracturing costs by an estimated 15-20 percent.

Significant changes were also made in the areas including perforating designs, production equipment selection and inspection (wellheads, tubulars, packers and miscellaneous accessories) and our philosophy regarding the utilization of used and surplus equipment. All of these changes were encouraged and supported by Management who assisted in "selling" the ideas to other "tentative" individuals where necessary. The only restriction put on the staff during this work was that where several changes may be interrelated, particularly in the area of fracture treatment design, they would be "staged". This would ensure that if unforeseen effects occurred, their cause could be more readily isolated. Overall, very few disappointments were realized in contrast to the substantial successes achieved.

Results of the completions and remedial well work at McAllen Ranch have been particularly impressive. During the two year period 1990-91, the field's production rate increased by over 250 percent from approximately 50 to over 130 MMcf/D (see Figure 6). This increase included production from thirteen new wells which were completed during the period. Average initial rate from the new wells was about 7 MMcf/D, compared with the 1-3 MMcf/D which was historically realized. Remedial well work also contributed a significant portion of the increase. The level of this work was increased by one-third from the previous three year period, from approximately $4.5 million/year during 1987-89 to almost $6 million/year during 1990-91, with improved results. In all, a total of 75 individual fracture/refracture treatments were performed in conjunction with these activities.

Completions

New well completions at McAllen Ranch require both high cost equipment and massive hydraulic fracture treatments to produce at economical rates. The wells range in depth from 12,000 - 14,500 ft. with bottom hole pressures and temperatures exceeding 12,000 psi and 350°F in the deeper intervals. In addition, a sufficient quantity of hydrogen sulfide is present in the gas to make stress corrosion cracking of metal a concern. Typically two or more "stacked" pay intervals are encountered in these wells (Figure 2), thus they require multiple fracture treatments to adequately stimulate the reservoirs.

When performing a "commingled" well completion, production equipment is run and the lowermost pay interval is perforated. The interval is then fracture treated followed by an immediate, short flow period to promote fracture closure. A sand plug is then pumped down the tubing across the interval and subsequently tested to ensure integrity during fracture treatment of the next pay zone. The perforate/fracture treat/sand plug sequence is then repeated moving up the hole until all intervals to be commingled are treated. Finally, the wellbore is cleaned out with a high pressure snubbing unit to allow commingled production from all intervals.

Figure 5 represents this process schematically. The majority of wells completed during the past two years have required two to five treatment sequences. Each of these sequences include fracture treatments that utilize 150-300 M lbs of intermediate strength proppant or up to 1 MM lbs per well.

McAllen B-20 was the first well completed in this manner. The well was brought on line immediately following regulatory approval for commingling. Four treatment sequences were required to adequately treat the pay intervals that the well encountered (S, T and U Sands). Following completion operations, the well produced at an initial rate of over 8 MMcf/D. Had the well been completed only in the lowermost interval as per historical practices, a rate of only 1-2 MMcf/D would have been realized. A production plot for this well is included as Figure 7.

Remedial Well Work

As previously stated, remedial well work also contributed significantly to production increase realized at McAllen Ranch. This work consisted primarily of recompletions (including additional commingling opportunities), refracture treatments and wellbore cleanouts.

Results of remedial activity on McAllen B-16 probably best illustrates the substantial impact of commingling. This well was originally completed in only the U Sand during late 1988. An initial production rate in excess of 1 MMcf/D was achieved; however, production had declined to approximately 500 Mcf/D by early 1990. At that time, the well was worked over and production from the S, T and U Sands was commingled. When production was reestablished, a rate of 10 MMcf/D was achieved. Overall, the well produced only 0.5 Bcf in its first two years of production, whereas in the first year after the workover, it produced in excess of 3.0 Bcf. A production plot for this well is included as Figure 8.

Commingling typically offered the most dramatic results; however, other remedial work was also very successful. Figure 9 shows production from Woods Christian 20, a well that was refracture treated during early 1991. This well was

originally treated with sand at relatively low loadings (< 5 ppg) as the high closure stresses encountered in the McAllen Ranch environment resulted in the sand crushing and a subsequent loss of fracture conductivity. The refracture treatment utilized intermediate strength proppant at much higher loadings (8 ppg) to ensure improved long-term productivity.

Wellbore cleanouts were also found to be extremely profitable in many cases. Initially much of this work was performed with snubbing units; however, coiled tubing is now routinely used where the wells have depleted to the point that surface pressures can be controlled. Effective teamwork between Engineering and Operations resulted in proper risk assessment which allowed the use of coiled tubing at these conditions (depths, temperatures, etc.) to be "sold" to Management. Figure 10 shows the results of such a job on well McAllen 57.

INTERACTION WITH FIELD OPERATIONS

Another key ingredient in the overall success to date of the McAllen Ranch Redevelopment Program was the strong working team relationship that developed between Engineering and field Operations personnel. Drilling, production and facilities engineers developed this relationship by visiting the field frequently and when in the office, communicating with appropriate Operations personnel on a daily basis to ensure lines of communication remained open and that the "field" was getting necessary support from the "office". All major changes to historical practices were discussed with Operations and any differences worked out through both education and compromise prior to implementation. This teamwork allowed new ideas and innovative approaches from both groups to be brought to fruition in a timely and effective manner.

In an effort to enhance this teamwork, Operations personnel were also included in the field's formal Asset Management Team where they had an opportunity to interact with the "subsurface" Engineering specialties (Geological, Petrophysical and Reservoir Engineering). Individuals from these specialties were also encouraged to visit the field particularly for such events as formal well reviews. Overall, the interaction between the groups resulted in a better understanding of the problems encountered by each other and allowed the team to develop a very close and effective working relationship.

RESULTS SUMMARY

The McAllen Ranch Asset Management Team was able to meet or beat all its targets, as summarized here:

- Field gas production rate has increased over 250 percent from 50 MMcf/D to over 130 MMcf/D in less than two years. This current production is the highest rate in the field in over 20 years.
- Application of fine-grid 3-D seismic and synergistic subsurface engineering has resulted in a success rate of over 93 percent for drilling of 15 new wells with over 100 Bcf of new gas reserves added.
- Time to drill new wells has been cut in half, with a world record established for cumulative footage drilled with an 8-5-in. bit, and overall drilling costs have been reduced by 25 percent (over $7 million).
- Average new well initial production rates are 7 MMcf/D compared to previous rates of 1-3 MMcf/D
- The previously untested concept of commingling several massive hydraulically fractured intervals in the same wellbore, separated by hundreds of feet, has been successfully applied after obtaining approval from the Texas Railroad Commission.
- Via commingling, behind pipe non-contributing reserves have been reduced to less than 20 percent of the proved developed reserves. This compares to over 40 percent of developed reserves behind pipe prior to 1990.

In recognition of its efforts exemplifying teamwork and results, the McAllen Ranch Field Team was awarded Shell Oil Company's 1991 President's Award for Team Excellence.

CONCLUSIONS

Based on the extraordinary production results and the excellent teamwork exhibited by the various specialties and functions that worked on the McAllen Ranch team, it can be concluded that effective cross-functional team management of a multi-disciplinary team is indeed possible and necessary in complex oil and gas producing operations. We conclude that the management and organizational actions given below were instrumental in the success of this team effort.

- Eliminating organizational barriers and silos along with support of prudent "risk taking" can lead to innovative technical and business results.

- Empowering the staff to reach collective decisions without management intervention and reducing routing supervision can lead to a sense of accomplishment among the team members and actually speed up all aspects of the approval and implementation process.

- Focusing the team members on a common goal can eliminate "provincial" and specialty-specific targets.

- The cross-functional team management concept can be applied to other fields as evidenced by the results achieved at the McAllen Ranch and our other South Texas fields.

ACKNOWLEDGMENTS

We thank the management of SWEPI for its support and permission to publish this paper. We also wish to recognize the efforts of all past and present members of the McAllen Ranch Asset Management Team, and all the employees of the McAllen Production Unit. Additionally, we would like to thank the Shell Oil Company Bellaire Research Center, Production Operations R&D Staff for their support on hydraulic fracturing.

REFERENCES

1. Hill, D. P., Lennon, R. B., and Wright, C. L.: 1991, "Making an Old Gem Sparkle: The Rejuvenation of McAllen Ranch Field, Texas", CGAGS Transactions, V. 41, p. 325-335.

2. Simon, J. M..: "New Standard Set for South Texas Drilling Performance", paper (SPE 24602) presented at 1992 SPE Annual Technical Conference and Exhibition, Washington, D.C., October 4-7.

NOMENCLATURE

ppg - pounds/gallon
ppm - parts/million

SI METRIC CONVERSION FACTORS

in.	x	2.54*	E+00 = cm
ft	x	3.048*	E-01 = m
ft^3	x	2.831 685	E-02 = m^3
gal	x	3.785 412	E-03 = m^3
sq. mile	x	2.589 988	E+00 = km^2
md	x	9.869 233	E-04 = μm^2
lbm	x	4.535 924	E-01 = kg
psi	x	6.894 757	E+00 = kPa
°F		(°F-32)/1.8	= °C

* Conversion factor is exact.

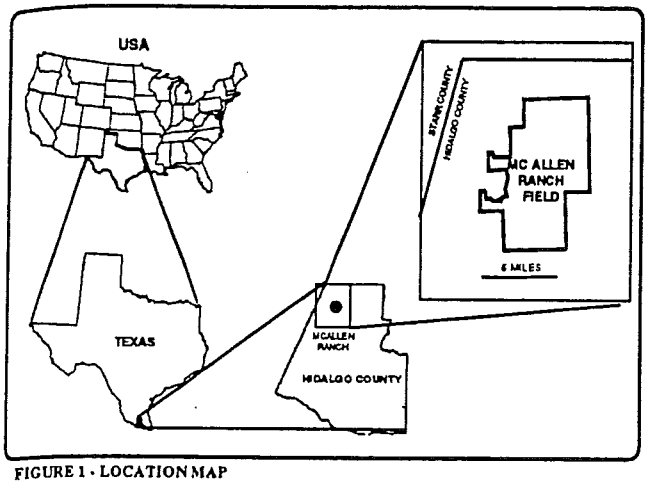

FIGURE 1 - LOCATION MAP

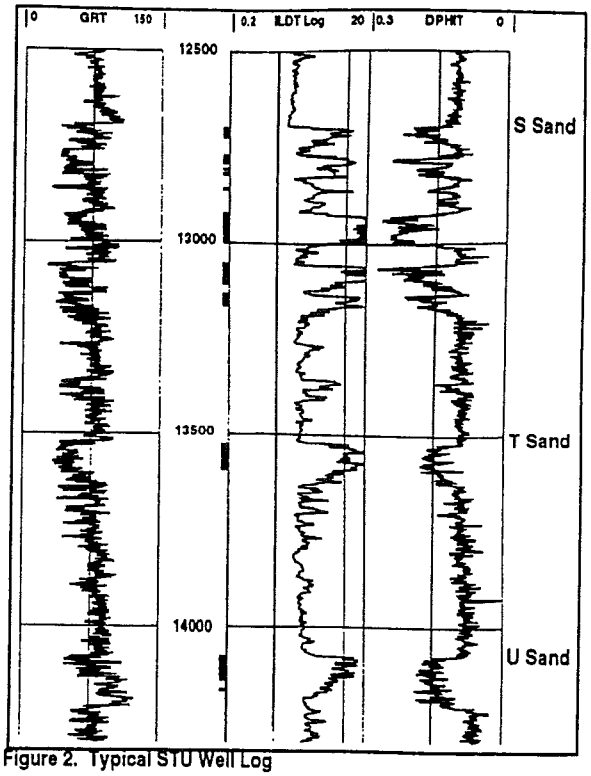

Figure 2. Typical STU Well Log

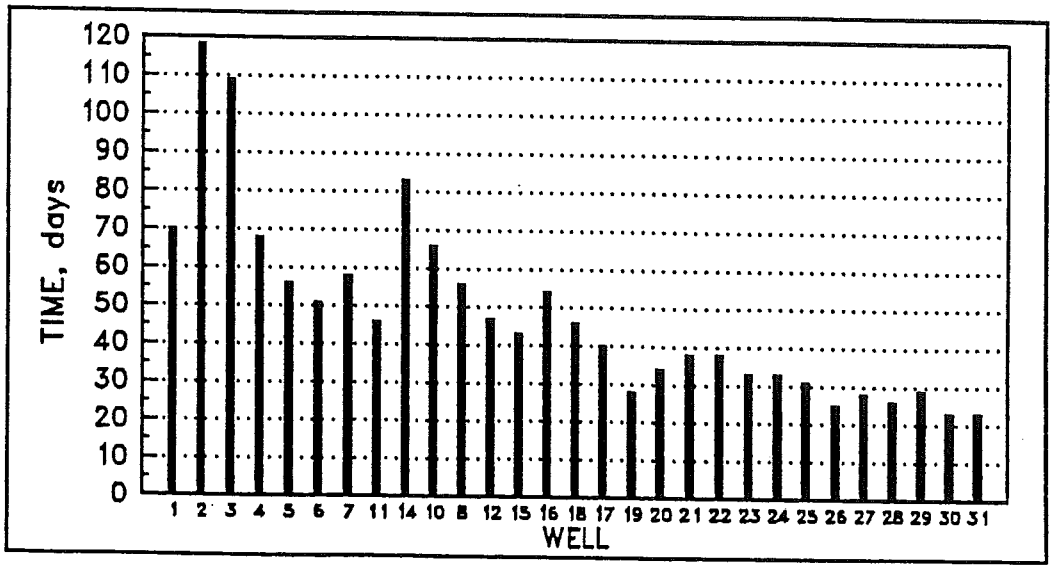

Fig. 3 TIME IN DAYS FROM SPUD TO RIG RELEASE

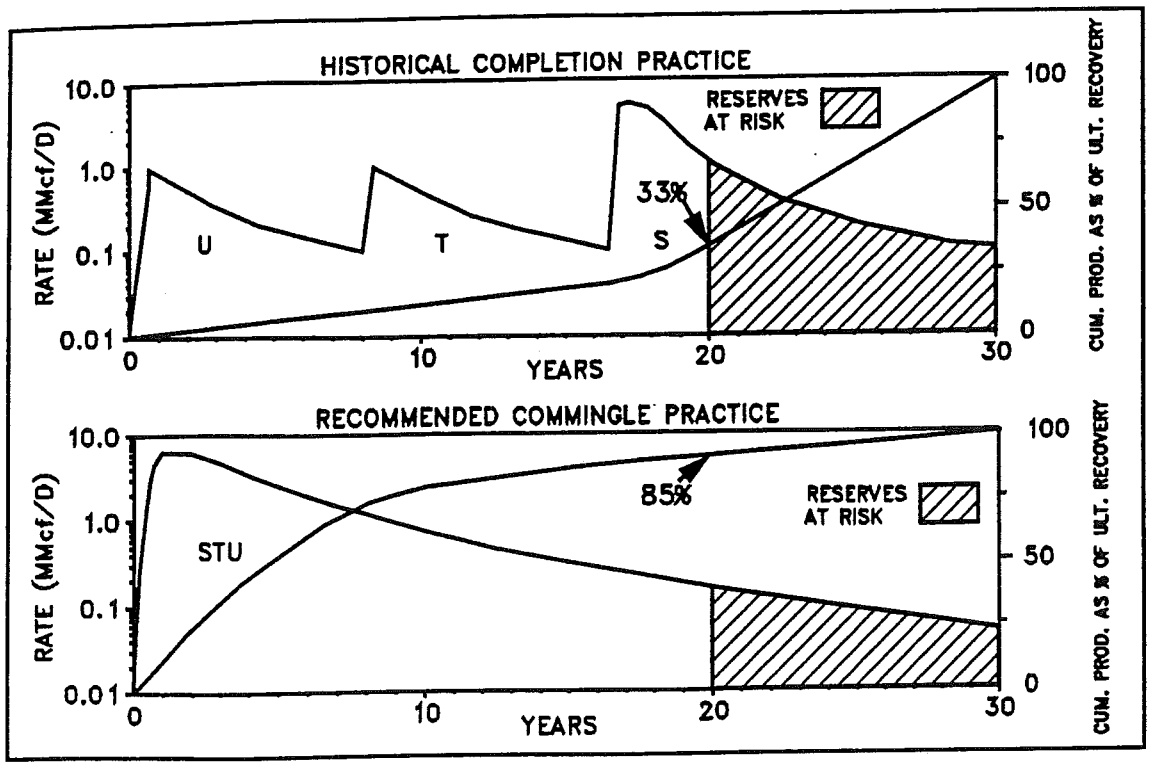

Fig. 4 COMPLETION PRACTICES – WELLBORE LIFE RISK ASSESSMENT

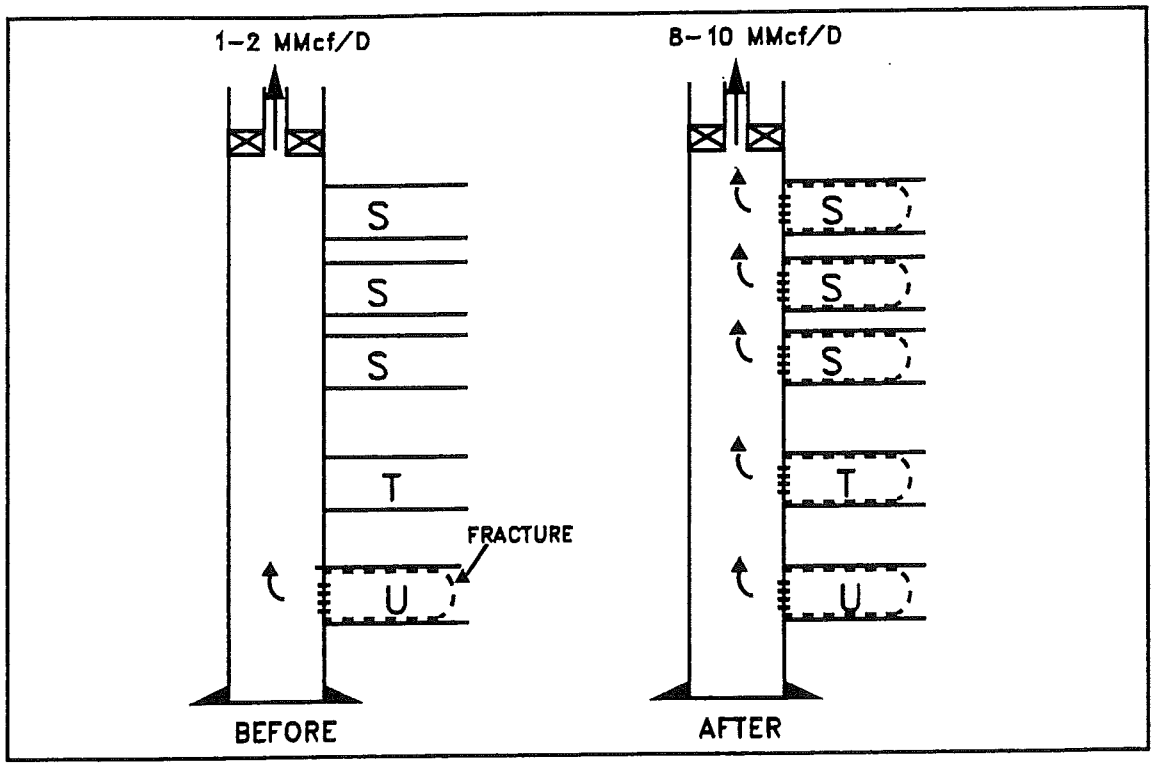

Fig. 5 VICKSBURG 'STU' SAND COMMINGLING

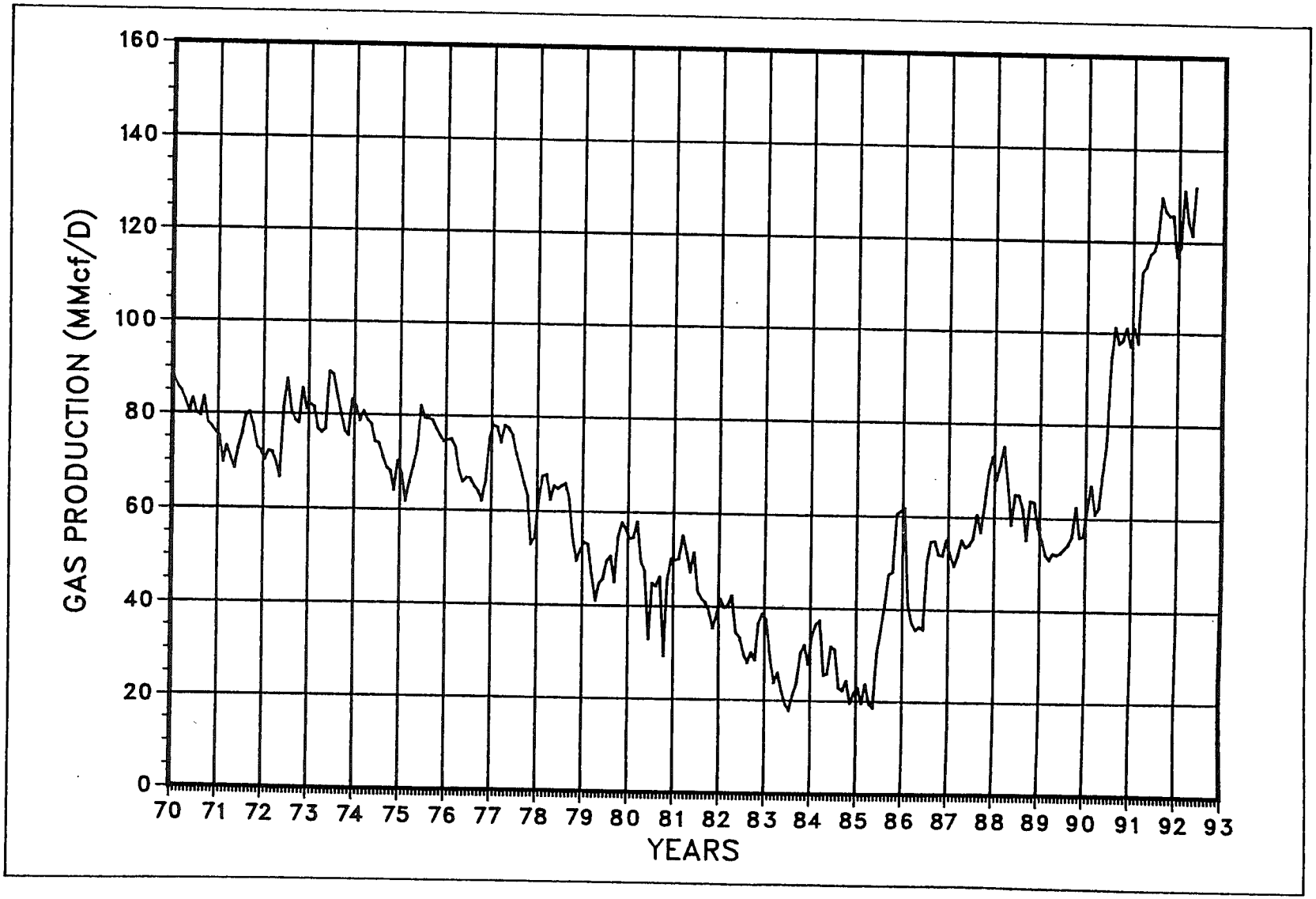

Figure 6 – McAllen Ranch Field Gas Production

FETKOVICH

GOOD LAYERED PAPER

SPE16553/1

THE USE OF DETAILED RESERVOIR DESCRIPTION AND SIMULATION STUDIES IN INVESTIGATING COMPLETION STRATEGIES, CORMORANT - UK NORTH SEA

J.H. Stiles, Esso Exploration and Production U.K.
N.P. Valenti, Exxon Production Research Company

ABSTRACT

A portion of the Cormorant field in the U.K. North Sea is being developed using a subsea production system. All layers in the stratified reservoir section are being waterflooded concurrently by perforating the entire interval in both producers and injectors. The permeability contrast among the layers is such that there is potential for severe imbalance in the movement of the waterflood fronts, resulting in large volumes of early water production from high permeability layers and incomplete displacement of oil from less permeable layers. With the high cost of expanding platform facilities or performing workovers on subsea wells to re-distribute production and/or injection, there is considerable incentive to optimise the completions in new wells.

This paper describes studies undertaken by Esso Exploration and Production U.K. to evaluate various completion strategies for new subsea wells. These studies were done to complement work done by the operator, Shell U.K. Exploration and Production. The studies included detailed reservoir description work to define the oil-in-place and permeability distribution, followed by simulation of the waterflood for a representative reservoir cross-section. Wellbore, flowline and pipeline hydraulics for the complex production and injection system were included to more accurately model well rates. The results provide general insight into the nature of the displacement when waterflooding a stratified section with a limited number of wells. They also provide specific guidance on: (1) dual vs. single completions, (2) perforating, testing and stimulation sequence and (3) the benefits of partially perforating high permeability sands.

INTRODUCTION

The Cormorant Field (Fig. 1) is located in the U.K. North Sea 95 miles north east of the Shetland Islands in about 500 feet of water. The field (Fig. 2) was discovered in 1972 and is composed of four major fault blocks which cover an area of over 10,000 acres and contain over 1.5 billion barrels of oil. The field is operated by Shell U.K. Exploration and Production on behalf of the Shell-Esso joint venture.

The southern portion of the field is developed from the South Cormorant platform while the northern area is developed from the North Cormorant platform. A sophisticated subsea system is being used to recover the oil in Block I lying between the two platforms. This consists of an

As a result of the incentives to limit water production listed above, an evaluation was made of the potential for improving the initial completions. The objective of the work was to seek ways of reducing severe production and injection imbalances that might result in large volumes of early water production.

FLUID PROPERTIES

Block I is overpressured by more than 700 psi and contains a 37-degree API gravity oil. The 0.7-cp oil results in a favourable mobility ratio. The oil is undersaturated by over 2700 psi, has a gas-oil ratio of 480 SCF/STB and an initial oil formation volume factor of 1.27 RB/STB. Key reservoir fluid properties are included in Table 1.

GEOLOGY

The oil at Cormorant was accumulated in the deltaic sands of the Middle Jurassic Brent Group. The Brent Group in Block I has been divided into five productive formations, as shown in Figure 4. These sands, in order from youngest to oldest, are the Upper Ness, Lower Ness, Etive, Rannoch and Broom. The overall thickness of the section, in the northern part of Block I where the new wells are located, is 200-250 feet with net sand totalling 100-150 feet.

A detailed geologic study of the area formed the basis for reservoir engineering hand calculations and a simulation study that utilised a cross sectional model. Several important conclusions resulted from the work. First, in addition to the Mid-Ness shale, there are laterally continuous shaley sections within and at the base of the Lower Ness and at the base of the Rannoch, that will prevent vertical movement of fluids. There are also shaley intervals within the Upper Ness and Rannoch which, although creating localised restrictions to flow, are judged unlikely to completely restrict vertical flow.

The study confirmed the lateral and vertical continuity of the highly permeable Etive sands and concluded that the sands at the top of the Lower Ness (the Lower Ness 'A') also have excellent lateral continuity and were potential paths for rapid water advance. The stratified nature of the section is supported by open hole formation tester pressures. These pressures showed significant variation throughout the section as a result of production from earlier wells.

The geology of the Brent Group sands at Cormorant is discussed in greater detail in References 2-4. Average rock properties are listed in Figure 4. The permeability profile plotted in Figure 4 shows the significant permeability contrast that exists within the section.

PERMEABILITY DISTRIBUTION

Previous studies of Cormorant have shown that the permeability distribution controls waterflood performance. A good understanding of this is therefore required to correctly manage the reservoir, and considerable effort was devoted to this subject in the study.

three times that indicated from well tests. An example of the comparison made for a tested interval in injector W-2 is shown in Figure 8.

This difference is consistent with the evidence that there are delicate clay structures in the rock within the water zone that are damaged during extraction and drying, thereby enhancing the permeability above in situ levels (Ref. 4-6).

CROSS-SECTIONAL SIMULATION MODEL

To evaluate various completion techniques a two-dimensional cross-sectional simulation model was constructed through the area to be waterflooded by wells P-5 and W-4 (Fig. 9). The line of section of the model is shown in Figure 3. The model is composed of 37 layers with 22 blocks in the dip direction giving a total of 814 grid blocks. The width of the model was selected to approximate the average producer and injector spacing of about 4000 feet in the northern portion of the block. A producer and an injector were included in the model at the locations of P-5 and W-4.

Wellbore and flowline hydraulics provided by Shell, and shown as inserts in Figure 9, were used to define well rates. These curves, which are based on assumptions of average flow rates from all UMC wells, include the hydraulics effects of: (a) the common pipelines from the South Cormorant platform to the UMC, (b) the satellite flowlines from the UMC to P-5 and W-4 and (c) the two strings of 3-1/2" tubing which are installed in UMC wells to allow TFL (Thru Flow Line) techniques to be used for well monitoring and maintenance.

Porosities were assigned based on core data corrected for net overburden pressure. Where core data were not available, log-calculated porosities were used. Irreducible water saturations were defined for the various rock types using Shell's log calculations.

Relative permeabilities were based on waterflood tests conducted at reservoir conditions on core material with natural wettability preserved. Because this information was not yet available for Cormorant, relative permeability data for a nearby field that produces similar oil from the Brent Group sands were used. Comparative tests in other Brent Group reservoirs have indicated that coring fluid, preservation and test procedures can have a very significant effect on relative permeabilities (Ref. 7).

Although the water viscosity initially assigned to the model was that corresponding to initial reservoir conditions, it was necessary to adjust the water viscosity in the grid blocks near the injection well with time to approximate the cooling of the reservoir as a result of injecting cold sea water. The timing and areal extent of water viscosity adjustments were based on previous thermal simulation work. Results of this work indicated that the long-term effect on injectivity is roughly equivalent to using the viscosity of the cold sea water within the radius of investigation of the well. (The thermal front was calculated to extend up to 1500 feet from the injector; the distance varied depending on the permeability of each zone and adjacent beds.)

The effects of making the various corrections and adjustment to the core data and modelling cold sea water injection are shown in Table 2.

J.H. STILES
N.P. VALENTI

DUAL COMPLETIONS

One alternative technique to improve the relative velocities of the flood fronts in the individual layers is to control the distribution of fluids through use of dual completions. This would allow injection into part of the section to be restricted. Effective segregation of flow requires that a packer be set in the wellbore opposite a reasonably thick, laterally extensive shale. (Although UMC wells are equipped with two strings of 3-1/2" tubing, this is to allow TFL application, and the wells are not routinely equipped with a second packer to segregate flow between the strings.) Shales with continuity over the northern part of the block were identified in the geological study and are shown in Figure 4.

Two aspects were considered in evaluating the benefits of selective completions. The first concerns the balance between oil-in-place and kh. The distribution of oil-in-place and kh, shown in Table 3, indicates that dual completing P-5 across a shale within or at the base of the Lower Ness would do little to improve this imbalance. The Lower Ness 'A' would still be flooded preferentially in the upper tubing string whereas the Etive would be flooded preferentially in the lower tubing string. Simulation results showed little improvement in waterflood performance with segregated tubing strings using this approach.

Greater improvement could be achieved by placing the packer at the Mid-Ness shale, but the second consideration, the effect on production and injection rate, had to be addressed. Maximum rate is achieved with non-selective production or injection through both strings of 3-1/2" tubing. Dedicating each string to a part of the reservoir interval can result in a significant rate reduction. The combined injection rate for selective completions above and below the Mid-Ness shale in W-4 was calculated using the hydraulics curves and found to be just over 7 kbwpd, versus almost 9 kbwpd for a non-selective completion. Thus, selective completions give a reduction in rate of about 17 percent. Such an injection rate reduction results, in turn, in a reduced oil rate from P-5 due to lack of pressure support. Selective injection has the added risk of the injection rate being much lower than expected due to inaccuracies in estimating permeabilities for the various layers, with an expensive workover being required to alter the completion configuration should the actual injection rate be unacceptable.

ALSO SKINS AND LAYER PRESSURE

* It was concluded that there is little incentive for selective production and/or injection in P-5 and W-4 because the high permeability layers are not appropriately grouped. Having the high permeability sands grouped either at the top or bottom of the reservoir section would offer the best opportunity for improving overall waterflood performance through use of selective completions. Such a situation is not normally encountered at Cormorant due to the depositional sequence.

PARTIAL PERFORATION

Another alternative considered was to alter the production or injection distribution by only partially perforating the wells, in essence by effectively reducing the permeability-thickness of the high permeability sands at the wellbore. Such a techniques, which has been used successfully in North Cormorant platform wells, would avoid the problems of selective injection as discussed above.

Etive in this analysis due to it being well developed and judged to be in good vertical communication with the Etive. The fourth column in the table shows that 44 percent of the injection would go into the Lower Ness 'A' if all intervals were fully perforated. The second column indicates that this sand contains only about 8 percent of the oil-in-place. The kh product and fraction of total well kh are higher in W-3 than in W-4, located to the north, because of a combination of higher permeability and increased sand thickness. As a result, only three feet of the 20-foot thick interval in the Lower Ness 'A' was perforated. This was calculated to reduce the injection rate into that interval by about 45 percent and the initial injection rate for the total well by less than 10 percent.

Additionally, perforation of the high permeability Lower Ness 'A' and Etive sands was only done after the intervals with poorer permeabilities were perforated, tested and stimulated. The distribution actually achieved was measured by running a flowmeter and results are shown in the last column in Table 5. Although the actual distribution does not mirror the oil-in-place exactly, it represents an improvement over that which would have resulted had all layers been fully perforated.

CONCLUSIONS

It is concluded from our work that there is potential to improve the efficiency of the waterflood in the UMC area of Block I at Cormorant through detailed reservoir description and simulation studies. Integration and reconciliation of data from numerous sources are required in doing this. Specific conclusions of the work are:

1. A good understanding of the permeability distribution is critical. Full use should be made of core analysis results, and techniques should be developed to more accurately predict permeabilities in uncored wells. Routine core data have to be corrected to in situ conditions and reconciled with well test results. There was good agreement between corrected core data and well test in the oil-zone, but a large adjustment was needed for core data from the water zone.

2. Wellbore, flowline and pipeline hydraulics and the effects of injecting cold sea water need to be included in the simulation of the waterflood in order to correctly determine the effects of various completion alternatives on field performance.

3. With high permeability sands being distributed throughout the reservoir section rather than being grouped together, there was little justification for dually completing the well, using an additional packer, to improve the production and/or injection distribution.

4. Potential was identified to improve waterflood performance by partially perforating the high permeability sands. The improvement is in the form of increased oil recovery at the terminal watercut, reduced water production and reduced water injection. This is accomplished with only a slight reduction in the initial production and/or injection rates.

5. A large proportion of the final oil recovery is from intervals with lower permeabilities, and recoveries from such sands could be jeopardised if they are damaged at the wellbore. Therefore these

TABLE 1

RESERVOIR CHARACTERISTICS

DEPTH, ft. ss	8750
Pi, psi	4860
TR, F	215
OIL GRAVITY, API	37
GAS-OIL RATIO, SCF/STB	480
BUBBLE POINT, psi	2100
Boi, RB/STB	1.27
μ_{oi}, cp	0.72
OIL-IN-PLACE, MSTB	400

TABLE 2

EFFECTS OF CORE ANALYSIS AND VISCOSITY ADJUSTMENTS

BASIS	Injectivity Index B/D·PSI	Injection Rate KBD
Routine Core Analysis	146	20
Special Core Analysis Correction	89	19
Effect of Cold Water Injection	19	15
Well Test Reconciliation	6	9

TABLE 3

OIL-IN-PLACE AND KH DISTRIBUTION IN WELL P-5

INTERVAL	KH in Well P-5 md-ft	KH in Well P-5 % of Total	Oil-In-Place % of Total	%KH÷%OIP
UPPER NESS	2000	9	26	0.3
LOWER NESS 'A'	3100	14	8	1.8
OTHER LOWER NESS	4700	20	12	1.7
ETIVE	9500	41	20	2.0
RANNOCH	3500	15	31	0.5
BROOM	300	1	3	0.3
TOTAL	23100	100	100	1.0

TABLE 4

PARTIAL PERFORATION STRATEGY

	Initial Rate - KBD: Fully Perforated	Initial Rate - KBD: Partially Perforated	% Reduction
PRODUCER P-5	7.9	[7.1]	10
INJECTOR W-4	[8.9]	5.7	36

STRATEGY FOR BALANCED WATERFLOOD [ ]

TABLE 5

IMPROVED INJECTION DISTRIBUTION - WELL W-3

INTERVAL	% of Oil-In-Place	Perforation Sequence	Injection Distribution - % of Total: Estimated, Fully Perforated	Injection Distribution - % of Total: Actual, Partially Perforated
UPPER NESS	15	1	5	15
LOWER NESS 'A'	10	2	44	6
OTHER LOWER NESS	10	1	4	15
ETIVE/U. RANNOCH	53	2	47	62
LOWER RANNOCH	8	1	0	0
BROOM	4	1	0	2
TOTAL	100	-	100	100

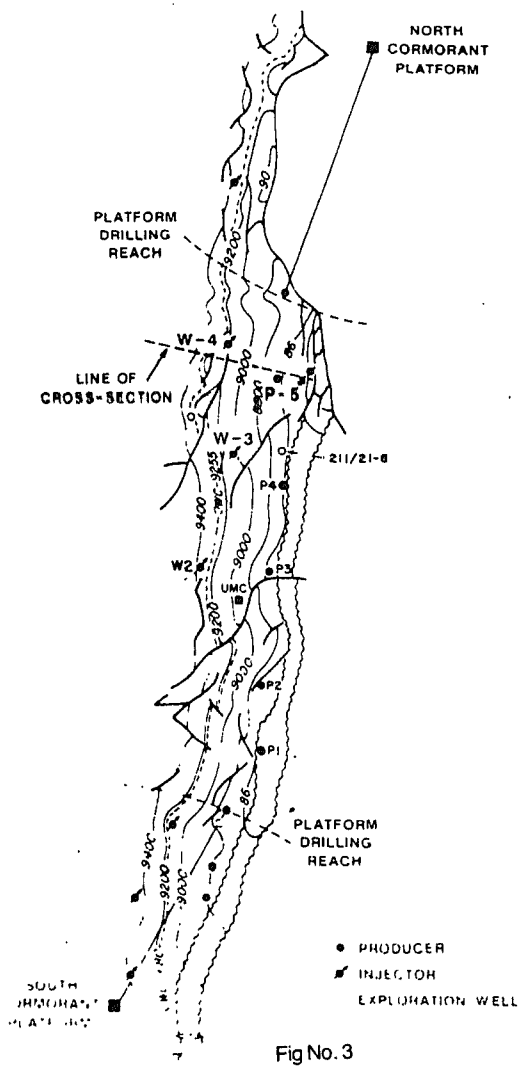

Fig No. 3

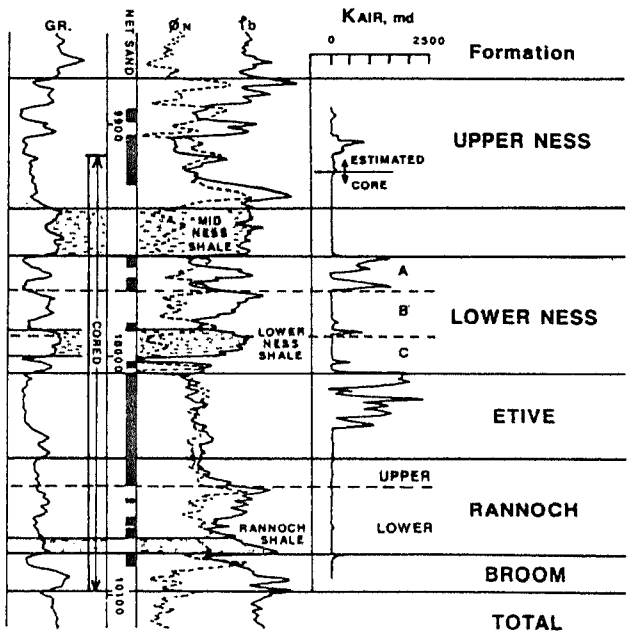

Formation	NET SAND FEET	POROSITY %	PERMEABILITY md
UPPER NESS	25	22	115
LOWER NESS	13	23	125
ETIVE	32	22	145
RANNOCH	25	19	5
BROOM	4	16	20
TOTAL	99	21	95

Fig No. 4

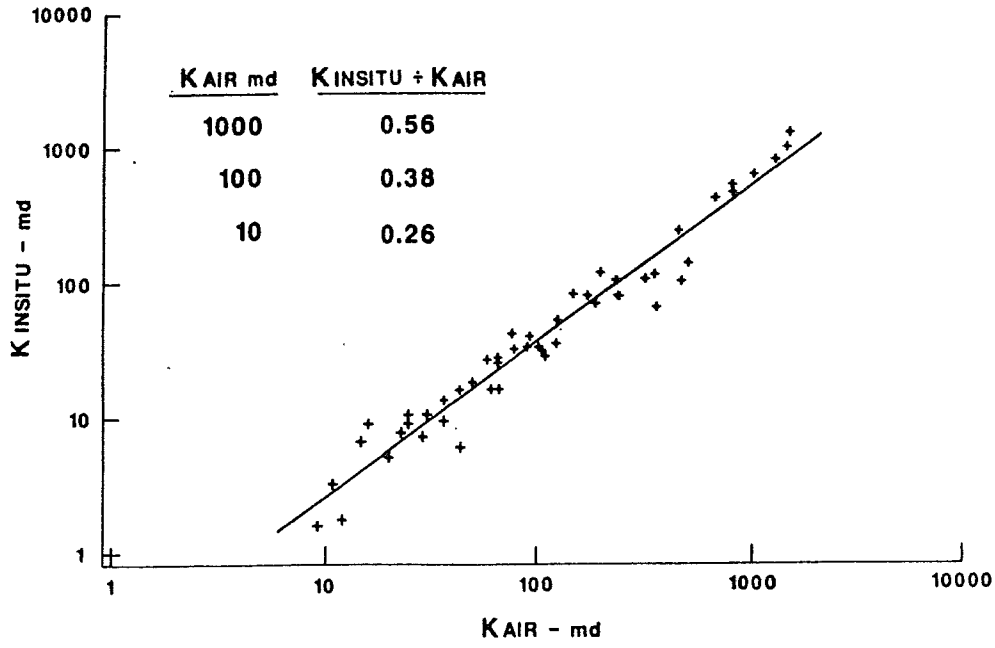

Fig No. 7

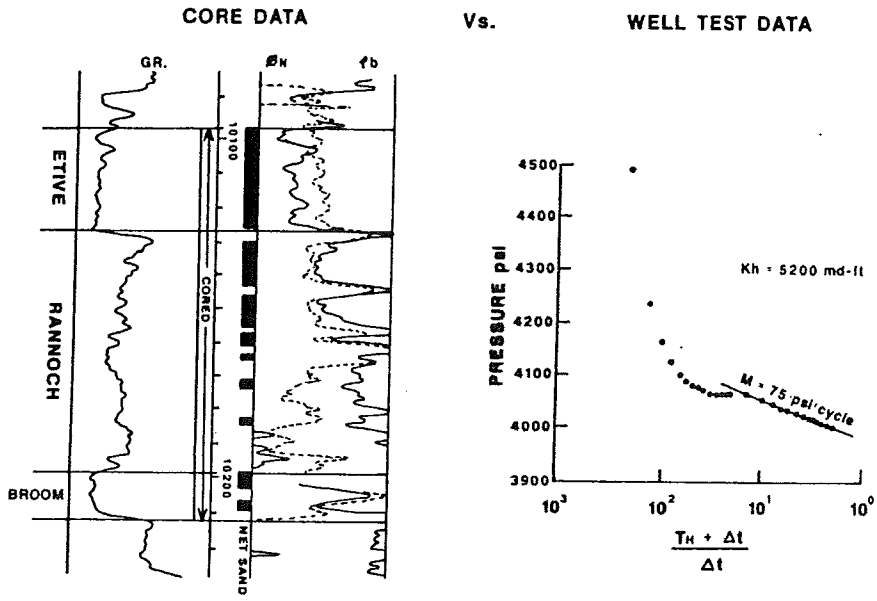

KH_{AIR} = 47,000 md-ft

KH_{INSITU} = 24,000 md-ft →

$\frac{KH_{TEST}}{KH_{INSITU}} = 0.2$

← KH_{TEST} = 5,200 md-ft

Fig No. 8

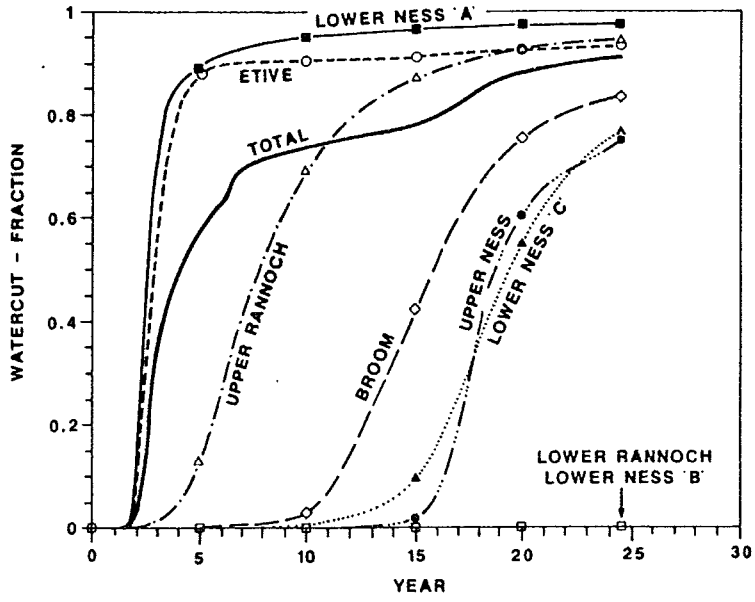

Fig No. 11

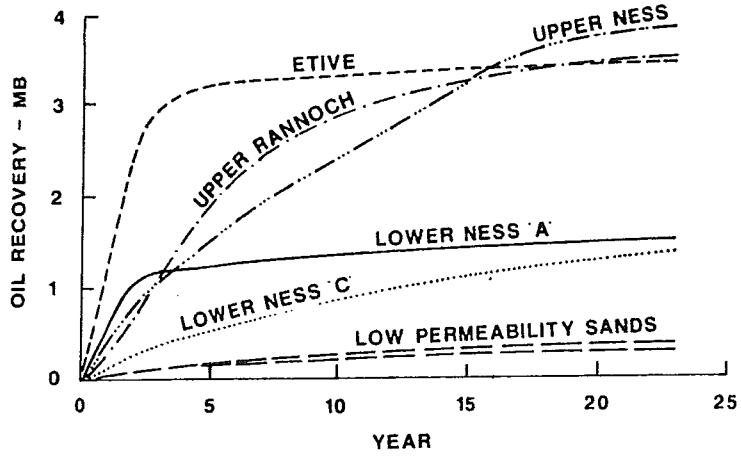

Fig No. 12

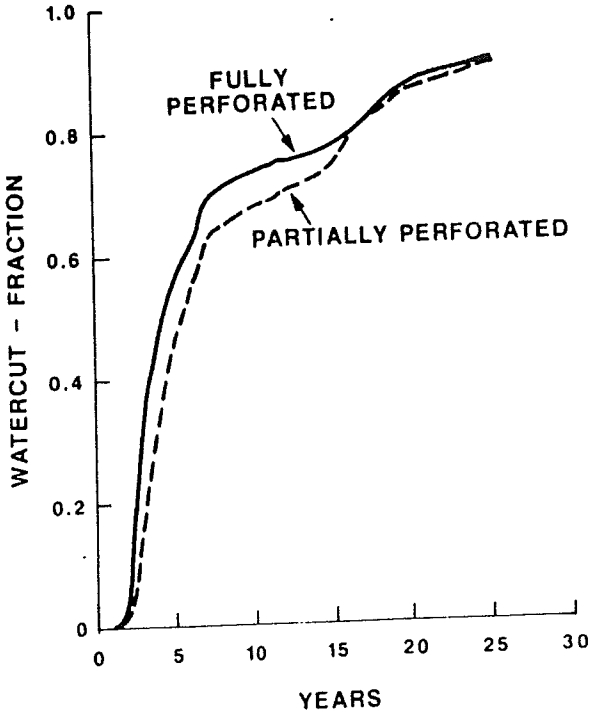

Fig No. 14

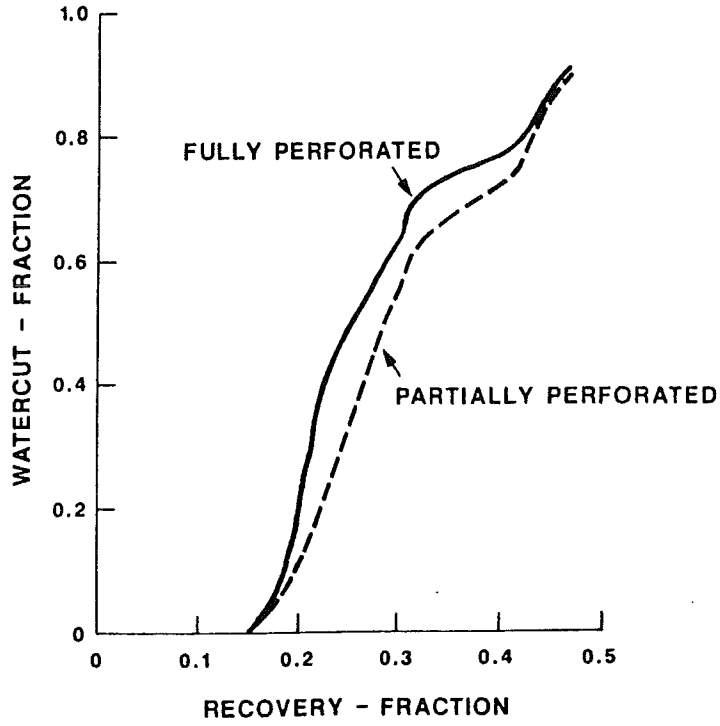

Fig No. 15